國立臺灣大學醫學院免疫學研究所博士論文

Graduate Institute of Immunology

College of Medicine

National Taiwan University

Doctoral dissertation
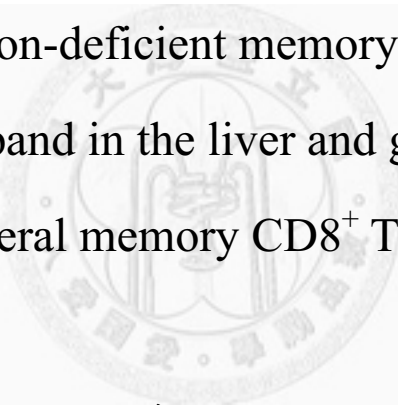
缺乏作用的記憶型 CD8 T 淋巴球在肝臟中增殖

並形成週邊記憶型 CD8 T 淋巴球

Effector function-deficient memory CD8$^+$ T cells

clonally expand in the liver and give rise to

peripheral memory CD8$^+$ T cells

蘇 裕 家

Yu-Chia Su

指導教授: 孔祥智 博士

Adviser: John T. Kung Ph.D

中華民國 99 年 11 月

November, 2010

致謝

當再一次回到學校攻讀免疫學博士班時，心中是又興奮又忐忑不安。

興奮在可以再次充實自己的實力，但對於免疫學這一個和我原本所學實驗動物獸醫學的領域，似乎有點遙遠，又難免心中忐忑。

但在這一個求學的過程，必須說我很幸運地有許多師長與朋友的指導與幫忙，才能讓我最終可以渡過這一切。

謝謝孔老師給我一個沒有後顧之憂的優渥研究環境，也謝謝老師在一次一次的討論之中，給我深入而全面的分析。 孔老師不僅給我做學問上的指導，也一直身教告訴我：如何用正確與正面的態度面對困難的挑戰，以及用堅持自己相信的理想，義無反顧的向前行，這些都是我以往不曾深刻體驗的人生態度。

謝謝我的論文指導老師們：胡承波老師、伍安怡老師、果伽蘭老師及司徒惠康老師，在每次的討論之中給我忠肯而有趣的建議，讓我對於自己的研究能帶著信心堅持下去。

感謝林雅敏學姐在我論文中最重要的部分，用超強的流式細胞儀和神乎奇技的技術，像大海撈針一般，拿到質精量多的細胞，才有後續的實驗。

謝謝李淑萍學姐永遠把顯微鏡維持在最佳的狀態，並用豐富的經驗，讓我突破許多難關，才會有這些漂亮的結果。

當然也要謝謝這些年來，N609 實驗室、突變鼠實驗室與動物房裏的任何一個夥伴，芬苓學姐、宜婷、美鈴、張綿小姐……每一張曾在實驗室出現的面容，我都深深的感謝大家這些年的幫助與包容，也永遠記得跟各位一起度過的日子。

最後謝謝我的家人，在這些年忍受我任性的堅持這條路，讓他們增加了許多負擔。一切的一切，只有感謝。

<div align="right">

蘇裕家

2010, 12, 22

</div>

中文摘要

未觸碰到抗原的 CD8$^+$ T 細胞 (naïve CD8$^+$ T cells) 在體外 (*in vitro*) 同時接受 T 細胞受器 (T cell receptor) 與第四介白素 (interleukin-4) 的活化後，可以在抗原相容 (histocompatible) 小鼠體內，長期存活成為記憶型 CD8$^+$ T 細胞 (memory CD8$^+$ T cells)。 在含有這些記憶型 CD8$^+$ T 細胞移植的小鼠，有一獨特亞群的記憶型 CD8$^+$ T 細胞在肝臟中 (T$_{LM}$) 被發現。 但在缺乏第十五介白素甲型受體 (interleukin-15 receptor α) 的小鼠肝臟中，這些 T$_{LM}$ 細胞明顯減少。T$_{LM}$ 細胞表現 CD62L^{low}CCR7$^-$ 相似於作用記憶型 CD8$^+$ T 細胞 (effector memory CD8$^+$ T cells; T$_{EM}$)，但丙型干擾素 (IFN-γ) 的誘發能力、細胞毒殺功能 (cytotoxicity) 及 T 細胞受器刺激所誘發的細胞增生則明顯比 T$_{EM}$ 細胞低落。利用 CFSE 試劑 (carboxyfluorescein diacetate succinimidyl ester) 檢測 T$_{EM}$ 細胞在體內 (*in vivo*) 的恆定性增生 (homeostatic proliferation)，發現 T$_{LM}$ 細胞的增生需依賴肝臟所表現的第十五介白素甲型受體。 免疫螢光染色 (immunofluorescent staining) 的結果發現 T$_{LM}$ 細胞形成的細胞簇 (cell cluster) 大量散布在野生型 (wildtype) 小鼠肝臟，但在缺乏第十五介白素甲型受體的肝臟不存在。 利用同時刺激 T 細胞受體與第四介白素受體，在體外活化表現 Vβ5$^+$ 與 Vβ8$^+$ T 細胞受體的 CD8$^+$ T 細胞後，移植等量的 Vβ5$^+$ 與 Vβ8$^+$ T 細胞受體 CD8$^+$ T 細胞到抗原相容小鼠，在肝臟所形成的每一個 CD8$^+$ T 細胞簇僅表現單一的 Vβ5$^+$ 與 Vβ8$^+$ T 細胞受體，由此證實肝臟中 CD8$^+$ T 細胞簇是由單一的 T$_{LM}$ 細胞無性增生所形成。 當小鼠耐受李斯特菌 (*Listeria monocytogenes*) 感染後，其肝臟亦可觀察到由單一的 T$_{LM}$ 細胞無性增生所形成的細胞簇。 T$_{LM}$ 細胞簇局限在肝血竇 (sinusoid) 之外，與肝臟星狀細胞 (hepatic stellate cells) 相接近，且與表現第十五介白素及第十五介白素甲型受體的樹突樣構造 (dendrite-like processes) 並存。 CD62L^{low} T$_{LM}$ 細胞自肝臟中純化後再被移植到未受刺激的小鼠中，會轉移到脾臟與淋巴節中並增加 CD62L 表現如核心記憶型 CD8$^+$ T 細胞 (central memory CD8$^+$ cells; T$_{CM}$)。 不同於以往，

我們的這個發現指出肝臟對刺激記憶型 CD8$^+$ T 細胞的生長與維持其恆定扮演重要的腳色。 一般認為肝生檢 (biopsy) 樣本中出現局部淋巴球增生即為病理現象，但我們的發現結果揭示了記憶型 CD8$^+$ T 細胞在肝臟無性增生是正常生理現象而非病理特徵。

ABSTRACT

Upon adoptive transfer into congenic histocompatible hosts, naïve $CD8^+$ T cells stimulated *ex vivo* by TCR in the presence of IL-4 persist in the hosts and become long-lived memory cells. A unique subset of memory $CD8^+$ T cells resides in the liver (T_{LM}) and this subset is highly reduced in the IL-15Rα-knockout (ko) liver. T_{LM} cells are similar to effector memory (T_{EM}) cells in that they are both $CD62L^{low}CCR7^-$, but are unlike T_{EM} cells in that they express reduced IFN-γ inducibility, cytolytic activity and TCR-induced proliferation. CFSE dilution assay results indicate that T_{LM} cells undergo IL-15Rα-dependent proliferation. Immunofluorescent staining revealed that the T_{LM} cells form a large number of cell clusters in the liver of WT but not IL-15Rα-ko mice. T_{LM} cells form clusters through clonal expansion because adoptive transfer of an admixture of TCR+ IL-4-activated $Vβ8^+$ and $Vβ5^+$ $CD8^+$ T cells results in clusters composed exclusively of $Vβ5^+$ or $Vβ8^+$ cells. Clonal expansion of $CD8^+$ T cells is also found in the liver of *Listeria monocytogenes*-immune mice. T_{LM} cell clusters in the liver are located around the sinusoid, closely associate with hepatic stellate cells, and are in close association with $IL-15^+$ and $IL-15Rα^+$ dendrite-like processes. Sorted $CD62L^{low}$ T_{LM} cells can migrate to other organs after re-transfer and display increased CD62L expression and become phenotypically similar to central memory (T_{CM}) cells. Our

results bring to light a previously unappreciated role of the liver in the growth and

maintenance of memory CD8$^+$ T cells.   These results also indicate that clonal growth

of memory CD8$^+$ T cells in the liver is a normal physiological process and that

caution should be exercised in interpreting focal lymphoid growth in clinical liver

biopsy specimens as pathology and not normal physiology.

Contents

ii

List of Figures

Introduction

Antigen-specific CD8^{+} T cells are activated when they encounter pathogenic microorganisms that have been appropriately processed and presented by professional antigen-presenting cells. These activated CD8^{+} T cells undergo massive expansion and perform cytotoxic killing of cells that have been infected by pathogens. After pathogen clearance, approximately 5 to 10% of antigen-specific memory T cells become long-lived memory cells. Memory CD8^{+} T cells express rapid cytotoxic functions and more efficiently control subsequent infections they had encountered previously.

1.   Memory CD8^{+} T cell subsets

Antigen-specific memory T cells have been classified as CD62L^{hi}CCR7^{+} central memory T (T_{CM}) cells and CD62L^{low}CCR7^{−} effector memory T (T_{EM}) cells. T_{CM} cells home to lymphoid organs, and T_{EM} cells migrate to non-lymphoid organs. T_{EM} cells express effector functions and provide rapid and prompt response to infection (1). T_{CM} cells have a greater capacity than T_{EM} cells to be maintained *in vivo* through homeostatic proliferation (2). Generation of these different subsets of memory CD8^{+} T cells is influenced by many factors. First, Wherry and co-workers proposed a linear differentiation pathway of memory CD8^{+} T cell subsets (2). In this model, naïve CD8^{+} T cells differentiate first into T_{EM} effectors followed by their subsequent conversion into T_{CM} cells. In contrast, T_{CM} cells have been shown to convert into T_{EM} cells (3).

2

Second, some studies have shown that the generation and differentiation of the different subsets of memory CD8^{+} T cells can be determined by the local cytokine environment or antigen-specific T cell frequency (4-6). Third, anatomical locations have been shown to regulate the memory differentiation program (7, 8). These apparent controversial reports bring out two issues. First, the CD62L and CCR7 markers commonly used to define memory CD8^{+} T cell subsets are likely insufficient to define all memory subsets in a comprehensive manner. Second, a unifying pathway for memory CD8^{+} T cell development has not emerged. Using Ag+IL-4 to activate naïve CD8^{+} T cells, I have found a large number of these cells in the liver in the form of cell clusters after their adoptive transfer into histocompatible hosts. The purpose of this thesis is to characterize this subset of liver memory CD8^{+} T cells in the context of mechanism of generation, function, and memory CD8^{+} T cell development pathway.

2. Role of IL-4 in the generation of memory CD8^{+} T cells

IL-4 is critical for Th2 cell generation; it also inhibits the inflammatory response of CD8^{+} T cells (9). IL-4 plays an important role in the induction of protective *Leishmania*-specific CD8^{+} T cells and in the development and magnitude of CD8^{+} T cell response to *Plasmodium* infection (10, 11). Work in our laboratory has shown that naïve CD8^{+} T cells activated *in vitro* by TCR-signaling and IL-4 can efficiently turn into

CTL memory cells when transferred to congenic histocompatible hosts (12, 13). According to these studies, IL-4 promotes the generation of memory CD8^{+} T cells, especially in parasite immunization.   It is possible that IL-4 directs the development of a functionally distinct subset of memory CD8^{+} T cell subset.

3. Role of IL-15 and IL-15Rα in the homeostasis of memory CD8^{+} T cells

Homeostasis of memory CD8^{+} T cells is dependent on both IL-15 and IL-7 (14, 15). While IL-7 is required for the survival of memory CD8^{+} T cells, IL-15 is required for the homeostatic proliferation of memory CD8^{+} T cells (16, 17).   Memory phenotype CD8^{+} T cells are deficient in both IL-15-knockout (ko) and IL-15Rα-ko mice (18, 19). Survival of LCMV-induced memory CD8^{+} T cells is poor (17), and proliferation of memory CD8^{+} T cells in IL-15-ko mice is significantly reduced (20).   In addition, IL-15 transgenic (tg) mice have increased memory CD8^{+} T cells (21).   IL-15Rα expression on CD8^{+} T cells is not required for homeostasis of memory CD8^{+} T cells (22), but IL-15Rα expression on neighboring cells can mediate homeostatic expansion of memory CD8^{+} T cells through trans-presentation of IL-15 (23, 24).

4. Role of lymphoid and non-lymphoid organs in the homeostasis of CTL memory

IL-15 (25) and IL-15Rα (26) are expressed in many non-lymphoid organs, which may

4

all be important for homeostasis of memory CD8^{+} T cells.   IL-15 expression is similar

in several non-lymphoid organs (25), but IL-15Rα expression is the most abundant in

the liver (26).   Because memory CD8^{+} T cells can persist in the absence of secondary

lymphoid organs (27, 28), organs other than secondary lymphoid organs must play an

important role in the maintenance of memory CD8^{+} T cells.   Bone marrow (BM) has

been demonstrated to be a site for homeostatic proliferation of memory CD8^{+} T cells

(20, 29, 30), a process that is dependent on IL-15 and IL-15Rα (17, 31).   Indeed,

IL-15Rα^{+} cells in the BM have been shown to maintain the homeostasis of memory

CD8^{+} T cells (31).   Whether the expression of IL-15 and IL-15Rα in non-lymphoid

organs (25, 26) contributes to the homeostasis of memory CD8^{+} T cells is however

largely unknown.   High level IL-15Rα expression in the liver has been reported and its

role in memory CD8^{+} T cell generation/maintenance is of high interest for further

investigation.

5. Immunoregulation of hepatic stellate cells (HSC) in the liver

In the past decade, HSC-related literature has increased dramatically, highlighting

significant progress on the roles played by HSC in liver biology and pathology (32).

Morphological characteristics of HSC include vitamin A-containing cytoplasmic lipid

droplets and long dendrite-like processes.   HSCs reside in the space of Disse, the space

between hepatocytes and anti-luminal side of sinusoidal endothelial cells. Porcine and rat HSC are prominent in the periportal zones (32-34). Physiological functions of HSC are of long-standing interest, although they are difficult to study because their isolation requires lengthy procedures and that many of their *in vivo* functions are not likely revealed by studying isolated HSCs *ex vivo*. HSCs can develop into bile ducts and secret hepatocyte mitogens (35, 36). During liver injury, HSCs develop into the myofibroblasts, cells responsible for fibrosis of the injured liver. HSC also possesses immuno-regulatory functions. IL-15-producing hepatic HSC has been shown to enhance homeostatic proliferation of liver NKT cells (37). In addition, HSC secretes proinflammatory molecules such as MCP-1, RANTES, and neutrophil-attracting chemokines and performs antigen presenting cell functions (37-39). HSC is the major depot of vitamin A which is converted to retinoic acid, an active form of vitamin A (40, 41). Vitamin A enhances IL-2R expression on T cells and plays critical immuno-regulatory roles (42, 43). Moreover, retinoic acid receptor γ-ko mice have a defective memory $CD8^+$ T cell response to *Lm*-infection, and that $CD8^+$ T cells from retinoid X receptor-ko mice are proliferation-deficient and prone to apoptosis (44, 45). Taken together, HSC is a candidate cell that contributes to memory $CD8^+$ T cell maintenance in the liver.

6. *Listeria monocytogenes*-induced memory CD8^{+} T cells

Listeria monocytogenes (*Lm*) is a gram-positive, intracellular pathogen that induces a strong CTL memory response in the mouse (46). *Lm* lyses the phagosomes of the host cells using a virulence factor, listerolysin O (LLO), replicates in the cytosol of macrophages and hepatocytes, and spreads from cell to cell (47, 48). *Lm* causes severe inflammation in the spleen and liver during a systemic infection. Experimental infection of mice with *Lm* has served as a model for analyzing Th1 immune response. *In vivo* neutralization of IL-4 enhances *Lm* clearance in B6 mice (49). However, IL-4 produced by CD4^{+} NKT cells during the early stage of *Lm* infection can regulate the migration of macrophages and influence the activation of CTLs and the generation of CTL memory (50, 51). As *Lm* infection of the mouse is a widely used experimental system to study the memory CD8^{+} T cell response to pathogens, I have adopted it to study memory CD8^{+} T cell generation and maintenance in the liver.

Materials and Methods

1. *Mice.*

2C TCR tg mice (52, 53) were bred onto C57BL/10ScN (B10) and C57BL/6J (B6) in our laboratory. 2C CD8^{+} T cells recognize the SIYRYYGL (SL8) peptide in the context of H-2K^b. B6.*TL* and B10.*TL* are B6 and B10 *Thy1^{a}CD8^a* congenic strains, respectively. IL-15Rα-ko mice were purchased from The Jackson Laboratory and backcrossed onto B6 background in our laboratory. These mice were bred in the animal facility of Institute of Molecular Biology under specific pathogen-free conditions. All animals used were 6 to 12 weeks of age and sex-matched. All experimental procedures were performed in accordance to active protocols approved by the IACUC of Academia Sinica.
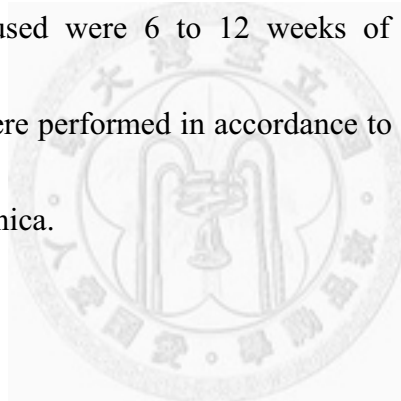
2. *Splenic CD8⁺ T cells isolation.*

A. reagents

1× PBS

NaCl (1.06400; Merck)	137 mM
KCl (1.04936; Merck)	2.7 mM
Na_2PO_4 (1.06580; Merck)	4.3 mM
KH_2PO_4 (1.04873; Merck)	1.4mM

1M HEPES pH7.3

HEPES (1.10110; Merck)	238.3 gm/L

1×Hanks' balanced salt (HBSS)

HBSS (H6136; Sigma-Aldrich)	1 package/L
1M HEPES pH7.3	20 ml/L

HBSS+5% fetal bovine serum (FBS)

FBS (10437-028; GIBCO; heat inactivated at 56°C, 1 h)	50 ml/L

ACK (RBC lysis buffer)

NH_4Cl (1.01145; Merck)	0.83%
$KHCO_3$ (P9144; Sigma-Aldrich)	0.1%

Antibodies

Antigen	Clone	Conjugation	References

10

2C TCR	1B2	FITC (F)	(54)
CD8	53-6.7	Cy5, PE	(55)
CD62L	Mel-14	F	(56)
CD44	IM7	Cy5	(57)
TCR Vβ5	MR9-4	F	(58)
TCR Vβ8	F23.1	Cy5	(59)
CD8	3.155	Purified	(60)
Mouse κ light chain	187.1	Purified	(61)
Mouse μ heave chain	Bet-2	Purified	(62)

B. Procedures

All splenic CD8^{+} T cells were enriched from the spleen by panning (63).   To check

purity, enriched 2C CD8^{+} T cells were stained with F-anti-2C TCR & Cy5-anti-CD8.

To check the naïve phenotype, CD8^{+} T cells were stained with F-anti-CD62L &

Cy5-anti-CD44.   Samples were analyzed using the FACSCalibur (Becton Dickinson).

The purity of CD8^{+} cells was always >95% and ~70% CD8^{+} cells were

CD62L^{hi}CD44^{low} naïve phenotype.   In certain experiments, B10 CD8^{+} T cells were

stained with F-anti-TCR Vβ5, Cy5-anti-TCR Vβ8, and PE-anti-CD8.   TCR Vβ5^{+} or

Vβ8^{+} CD8^{+} T cells were then sorted out by FACSVantage (Becton Dickinson).

3. *In vitro generation of long-term survival CD8⁺ T cells.*

A. Reagents

7.5% NaHCO₃

NaHCO$_3$ (1.06329; Merck)	7.5 gm/ 100 ml

1000× β-mercaptoethanol (2-ME; 55 mM)

β-mercaptoethanol (M3148; Sigma)	0.195 ml 2-ME/50 ml PBS

Mishell-Dutton (MD) medium +5 % FBS

MEM (41500-034; GIBCO)	1 package/L
7.5% NaHCO$_3$	30 ml/L
1M HEPES pH7.3	50 ml/L
100× Penicillin + Streptomycin (P3539; Sigma-Aldrich)	10 ml/L
1000× 2-ME	1 ml/L
FBS (SH30071.03; HyClone)	50 ml/L

Recombinant IL-2 (Biogen)

Recombinant IL-4 (214-14; PeproTech)

Peptide

SIYRYYGL (SL8; AnaSpec)

Antibodies

Antigen	Clone	Conjugation	References
CD3	500A.A2	Purified	(64)
CD28	57.31	Purified	(65)

B. Procedures

The *in vitro* generation of memory CD8^{+} T cells has been described previously (13). LPS-activated, irradiated (750-rad) T-depleted B6 splenocytes were used as APCs (66). Splenic 2C TCR tg CD8^{+} T cells (1×10^5 cells/ml) were activated with APCs (5×10^5 cells/ml) and SL8 peptide (0.5 μg/ml) for 3 days.   Exogenous rIL-2 (5000 U/ml = 1.14 ng/ml = 16.7 BRMPU/ml) and mIL-4 (5000 U/ml = 2.5 ng/ml) were added to the culture medium.   Activated CD8^{+} T cells were washed and rested in fresh medium (2×10^6 cells/10 ml) with rIL-2 (1.14 ng/ml) for 2 days.   The number of adoptively transferred donor CD8^{+} T cells into B10.*TL* mice was 8×10^6 cells per recipient, except where specifically indicated.   WT Vβ5^{+} and Vβ8^{+}CD8^{+} T cells were activated *in vitro* by anti-CD3/CD28 presented by LPS-activated B blasts (66).

4. *Analysis of donor cells in PBL.*

A. Reagents

ACK (RBC lysis buffer)

HBSS+5% FBS

Antibodies

Antigen	Clone	Conjugation	References
CD8	53-6.7	Cy5	(55)
Thy-1.2	30H12	F	(55)

B. Procedures

Orbital blood was collected and treated with ACK buffer. The peripheral blood lymphocyte (PBL) was obtained and suspended in HBSS+5% FBS. The PBL was stained with F-anti-Thy-1.2 and Cy5-anti-CD8 for FACS analysis. The donor CD8$^+$ T cells were traced in the PBL at indicated time points. The frequencies of the donor CD8$^+$ cells to total CD8$^+$ T cells were determined and shown.

5. *Isolation of lymphocytes from the liver.*

A. Reagents

PBS

ACK (RBC lysis buffer)

HBSS+5% FBS

2% Collagenase IV stock

   Collagenase IV (C5138; Sigma)   2 gm/ 100 ml

0.2% DNase I stock

   DNase I (1 284 932, Roche)   0.2 gm/ 100 ml

Digestion buffer in HBSS+5% FBS

   2% collagenase IV stock   1 ml/ 100 ml

   0.2% DNase I stock   1 ml/ 100 ml

24 % Histodenz in HBSS+5% FBS

   Histodenz (D2158; Sigma)   2.4 gm/ 7.6 ml

B. Procedures

The isolation procedure for intra-hepatic lymphocytes (IHL) is a modified version of a previously published procedure (67). The portal vein was perfused with 3 ml ice-cold PBS and 5 ml digestion buffer (HBSS+5% FBS containing collagenase IV,

0.02%, and DNase I, 0.002%). The perfused livers were obtained and gently

homogenized with Cell strainer (BD Falcon). The slurry from a single liver was

digested in 10 ml digestion buffer (37°C, 45 min, 120 rpm). Intrahepatic lymphoid

cells were enriched by gradient centrifugation (24% Histodenz, 4°C, 20 min, 1580g).

6. *Single cell suspensions obtained from lymphoid organs.*

A. Reagents

    HBSS

    ACK (RBC lysis buffer)

    HBSS+5% FBS

B. Procedures

The spleen, mesenteric lymph nodes (LN) and BM were excised. Then the spleen and LN were gently teared apart with forceps in HBSS. The resulting cells were treated with ACK buffer and distributed in HBSS+5% FBS for staining. BM was obtained as previously described (20). Two femurs were flushed with 5 ml ice-cold HBSS+5% FBS. The resulting cells were treated with ACK buffer and distributed in HBSS+5% FBS for analysis.

7. *CFSE dilution assay.*

A. Reagents

PBS

ACK (RBC lysis buffer)

HBSS+5% FBS

1 mM Carboxyfluorescein succinimidyl ester (CFSE)

CFSE (V12883; Molecular Probes)	1 vial
DMSO	90 µl

10 µM CFSE in PBS

1 mM CFSE	1 µl/ 10 ml PBS

Antibodies

Antigen	Clone	Conjugation	References
CD8	53-6.7	A680	(55)
2C TCR	1B2	Cy5	(54)
Thy-1.2	30H12	PE	(55)
CD8	3.155	Purified	(60)
Mouse κ light chain	187.1	Purified	(61)
Mouse µ heave chain	Bet-2	Purified	(62)

B. Procedures

Total splenic CD8$^+$ T cells (Thy-1.2$^+$ donor + Thy-1.2$^-$ host CD8$^+$ T cells) from the first set of adoptive hosts were enriched by panning on day 7 post-adoptive transfer and labeled with CFSE (2 μM, 37°C, 15 min). Total CD8$^+$ T cells containing 5×10^5 donor CD8$^+$ T cells were re-transferred into a second set of B10.*TL* hosts. On day 28 post-retransfer, both donor and B10.*TL* CD8$^+$ T cells were obtained from the spleen and liver. Cells were stained with PE-anti-Thy-1.2, Cy5-anti-2C TCR and A680-anti-CD8 mAbs to identify Ag+IL-4-activated donor CD8$^+$ T cells. CFSE intensity of the donor cell was analyzed by FACS.
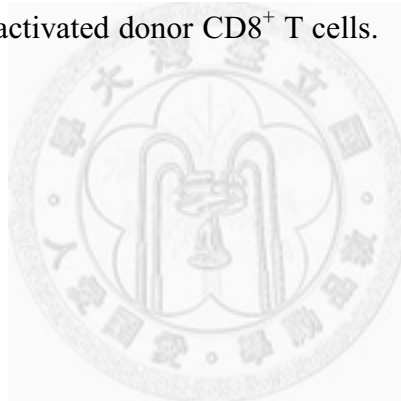
8. Histological, immunofluorescent and immunohistochemistry staining.

A. Reagents

PBS

O.C.T. compound (4583; Tissue-Tek)

1 mM Hoechst 33342

    Hoechst 33342 (Polyscience)   642 μg/ 1 ml

0.2 μM Hoechst 33342

    1 mM Hoechst 33342   1 μl/ 500 μl

Mayer's haematoxylin (MHS16; Sigma-Aldrich)

Glycerol (1.04093; Merck)

ImmPACT DAB kit (SK-4105; Vector lab)

Malinol (MUTO)

Antibodies

Antigen	Clone	Conjugation	References
Thy-1.2	30H12	A488, Cy5	(55)
CD8	53-6.7	PE	(55)
TCR Vβ5	MR9-4	A488	(58)
TCR Vβ8	F23.1	A647	(59)
IL-15	Goat IgG	Purified	BAF447; R&D

IL-15Rα	Goat IgG	Purified	Sc-1524; Santa Cruz
GFAP	Mouse IgG2b	A647	556330, BD Pharmingen
Pan cytokeratin	Mouse IgG	A546	C2563, Sigma
Rat IgG (H+L)	Goat IgG	HRP	112-035-167; Jackson Immunoresearch Lab
Goat IgG (H+L)	Donkey IgG	HRP	705-036-147; Jackson Immunoresearch Lab

B. Procedures

The histological examination for H&E staining was performed according to standard procedures. The tissues for IF and IHC staining were embedded with O.C.T. compound and frozen immediately. Tissues were then cut into 5-8 µm thick sections. The sections were fixed with acetone (4°C, 10 min). Fixed sections were stained with indicated fluorescent dyes-conjugated antibodies (4°C, 8h). Fluorochrome- conjugated monoclonal antibodies used include: AlexaFluor488 (A488)-1B2 anti-2C TCR, A488- and PE-conjugated anti-Thy-1.2, A488-anti-Vβ5, PE-anti-CD8, A647-anti-Vβ8, A647-anti-GFAP, A546-anti-pan cytokeratin. The cell nuclei were counterstained with 0.2 µM Hoechst 33342. The slides were mounted with mounting medium (Glycerol:PBS vol. ratio = 1:1) and observed by confocal microscopy (LSM 510,

ZEISS).

For IHC staining, fixed samples were stained with indicated antibodies (4°C, 16h). Purified antibodies used include: anti-CD8 (clone 53-6.7), anti-Thy-1.2 (clone 30H12), anti-IL-15, and anti-IL-15Rα. Then the sections were stained with HRP-conjugated anti-rat Ig (4°C, 6h). DAB precipitation was performed by ImmPACT DAB kit. The cell nuclei were counterstained with Mayer's haematoxylin (Room temperature, 1 min). The slides were dehydrated and mounted with Malinol. The images were collected by AxioImager microscope Z1 with Axiovision software (ZEISS).

A cluster is defined as 6 or more CD8$^+$ T cells in close proximity to each other. The number of donor cell clusters was determined by scanning a defined volume (area of observation determined by ImageJ software × section thickness of 5 μm). The number of the cluster count was converted to a volume of 1 mm^3. The average liver volume of 1560 mm^3 was derived from the volume determined from 5 mice between 8 to 12 weeks of age. The total number of CD8$^+$ T cell clusters for the entire liver was estimated by multiplying the number of clusters per mm^3 by the average liver volume. The average number of donor cells of 11.3 per cluster was determined by counting Thy-1.2$^+$ cells in 31 randomly chosen clusters. The total number of CD8$^+$ T cells for the entire liver was estimated by the number of clusters per liver multiplied by 11.3.

9. RNA extraction and reverse transcription.

A. Reagents

RNA nanoprep$^®$ kit (Stratagene)

RNasin (Promega)

0.35 μg/ml Oligo-dT (Amersham Pharmacia)

1.25 mM dNTP (R725; Invitrogen)

0.1 M DTT (P2325; Invitrogen)

M-MLV reverse transcriptase (28025-013; Invitrogen)

5× Reverse transcriptase buffer (18057-018; Invitrogen)

B. Procedures

The DNA-free RNA from the tissue was extracted by the Absolutely RNA nanoprep$^®$ kit. The RNA (2 μg/ 7 μl) was incubated with 0.5 μl RNasin, and 2 μl oligo-dT (65°C, 5 min) and then reverse-transcribed using 1 μl M-MLV reverse transcriptase, 2 μl DTT, 4 μl 5× RT buffer, and 5 μl dNTP (37°C, 90 min).

10. Quantitative real-time polymerase chain reaction

A. Reagents

Supertherm Taq polymerase 250U (JMR-801; Violet Bioscience)

10× PCR buffer with 15mM MgCl$_2$ (JMR-420; Violet Bioscience)

2.5 mM dNTP

LightCycler® FastStart DNA MasterPLUS SYBR Green I (12 239 264 001, Roche)

Primer sets for real-time PCR

  IL-15-4F (5'- tggaagcccatcgccatagc-3')

  IL-15-4R (5'- ggagacctacactgacacag-3')

  IL-15Ra-F (5'- attgagcatgctgacatccg-3')

  IL-15Ra-R (5'- tctgatgcacttgaggctgg-3')

  GAPDH F109 (5'- ttgcagtggcaaagtggag-3')

  GAPDH R355 (5'- agacaaaatggtgaaggtc-3')

B. Procedures

  Gene expression levels of IL-15, IL-15Rα and GAPDH were analyzed by real-time

quantitative PCR (LightCycler; Roche Diagnostic Systems).　Sample cDNA was added

to FastStart DNA MasterPLUS SYBR Green I mixture and subjected to PCR

amplification (45 cycles at 95°C for 10 s, at 58°C for 5 s, and at 72°C for 11 s).

Expression of GAPDH was used as the housekeeping gene control.

11. *Electron microscopy*

A. Reagents

Paraformaldehyde, 16% aqueous solution (Electron Microscopy Science)

Glutaraldehyde, 8% aqueous solution (Electron Microscopy Science)

OsO_4 (Electron Microscopy Science)

B. Procedures

The liver was perfused with 5 ml 4% paraformaldehyde in PBS *via* the portal vein. The perfused liver was removed and fixed for an additional 4h. The fixed liver was cut into ~1 mm^3 cubes. The liver slices were post-fixed with 2.5% glutaraldehyde and 4% paraformaldehyde in PBS (4°C, overnight) and then 1% OsO_4 (Room temperature, 2h). The slices were dehydrated and embedded in spurr. Sections of spurr-embedded specimens were cut with a diamond knife by ULTRACUT (Reichert-Jung) and examined by electron microscopy (Tecnai G2 spirit TWIN).

12. Listeria monocytogenes immunization of mice

A. Reagents

Listeria monocytogenes 5334

Brain heart infusion broth (Difco^{TM}, BD)

B. Procedures

Listeria monocytogenes (Lm) 5334 is a clinical isolate from National Taiwan University Hospital and grown to middle log-phase in brain-heart infusion broth.   The *Lm* stocks were preserved by 20% glycerol and stored in -70°C, ready for use.   B6 mice were inoculated intravenously with a non-lethal dose (6×10^3 CFU) of *Lm* and organs were harvested on day 60 post infection.   The inoculating size of each infection was confirmed by serial dilution.

13. Statistical analysis

The student's *t* test was applied for statistical analysis. A *p* value of less than 0.05 was considered statistically significant. Frequency of co-localization of $CD8^+$ T cell clusters and HSC was compared to frequency of the random collected images containing HSC by one-tailed Fisher Exact Probability Test (68). A p-value of less than 0.05 was considered statistically significant.

Results

IL-15Rα is required for the maintenance of Ag+IL-4-activated memory CD8$^+$ T cells

In our laboratory, it has been shown that naive 2C CD8$^+$ T cells activated *ex vivo* by antigen in the presence of IL-4 turn into long-lived, functional memory cells after adoptive transfer into congenic histocompatible hosts (13). I examined whether IL-15Rα was required for the homeostasis of Ag+IL-4-activated memory CD8$^+$ T cells. Using the Ag+IL-4-stimulated memory CD8$^+$ T cell generation system, the ratio of donor CD8$^+$ T cells to total CD8$^+$ T cells in the PBL of WT and IL-15Rα-ko host mice was determined (Figure 1). In IL-15Rα-ko host mice, the ratio of donor CD8$^+$ T cells to total CD8$^+$ T cells decreased dramatically from 3% to 0.5% in 40 days post-adoptive transfer. By contrast, the ratio of donor CD8$^+$ T cells was maintained relatively constant at ~3% in WT hosts for the nearly 5 mo observation period. The homeostasis of Ag+IL-4-activated memory CD8$^+$ T cells is therefore dependent on host IL-15Rα expression.

Large numbers of donor Ag+IL-4-activated CD8$^+$ T cells are found in the WT liver, but not in the IL-15Rα-ko liver

Using the Ag+IL-4-mediated high efficiency memory CD8$^+$ T cell generation system, I next examined the distribution of donor memory CD8$^+$ T cells in different host tissues/organs (Figure 2). The donor to total (donor + host) CD8$^+$ T cell ratios showed

that donor CD8^{+} T cells were most frequently found in the liver, followed by BM, spleen, and LN. To distinguish memory CD8^{+} T cells of the liver from central memory (CD62L^{hi} T_{CM}) and effector memory (CD62L^{low} T_{EM}) T cells (69), I named this population "liver memory T (T_{LM})" cells. Since host IL-15Rα was required for the maintenance of memory CD8^{+} T cells, the presence of donor cells is expected to dramatically decrease in the organs with deficient IL-15Rα expression. Total cell numbers of donor cells in the spleen, LN, liver and BM of WT and IL-15Rα-ko hosts were estimated on day 28 post-adoptive transfer (Figure 3). Absolute counts of donor CD8^{+} T cells were the highest for the spleen, then liver, followed by BM and lastly the LN. Liver was only second to the spleen which harbored the highest absolute numbers of donor CD8^{+} T cells. The liver is either a homing organ favored by a population of memory CD8^{+} T cells or that the liver is a site of memory CD8^{+} T cell growth and renewal. The absolute numbers of donor cells strikingly lower in all IL-15Rα-ko organs examined. The total donor cell numbers in the WT livers were 9.9 times of those seen in IL-15Rα-ko livers. On the other hand, total donor cell numbers in the WT spleens, LNs and BM were 1.9 to 3.1 times of those in IL-15Rα-ko host organs. Thus, the liver may transpresent IL-15 signals to memory CD8^{+} T cells to effect their survival and/or expansion.

T_{LM} cells undergo homeostatic proliferation in the liver and are unlike T_{CM} and T_{EM}

cells

To confirm that the liver memory CD8$^+$ T cells are T_{EM} cells, CD62L expression of the

Ag+IL-4-activated donor CD8$^+$ T cells in different organs was first analyzed (Figure 4).

The results showed that similar to T_{EM} cells, more than 90% of liver memory T cells

expressed low levels of CD62L.   The effector function of T_{LM} cells was further studied.

CD62L^{low}Thy-1.2$^+$ T_{LM} cells were sorted out and stimulated by plate-bound anti-CD3-

and anti-CD28 mAbs.   Proliferation of T_{LM} cells was 10% and 5% of the proliferation

of T_{EM} and T_{CM} cells, respectively (Figure 5).   Hence, T_{LM} cells, unlike T_{CM} or T_{EM}

cells, proliferate poorly upon TCR-stimulation. T_{BM} cells (memory CD8$^+$ T cells in

the BM) were also relatively proliferation-deficient, but were slightly better than T_{LM}

cells.

The CTL activity and interferon-γ (IFN-γ) production by liver memory T cells were

then compared to those of T_{CM} and T_{EM} cells (Figure 6 & Figure 7). T_{LM} and T_{BM} cells

were less effective in killing H-2L^d-bearing P815 targets.   Furthermore, T_{LM} cells

produced less IFN-γ than T_{EM} and T_{CM} cells upon TCR stimulation (mean fluorescence

intensity: 62 vs 152).   The isolation procedures of IHL did not damage the CD8$^+$ T

cells (Figure 8).

More Ag+IL-4-activated memory CD8$^+$ T cells enter the cell cycle in the liver

To assess the extent to which the abundant memory CD8$^+$ T cells found in the liver arose from homeostatic proliferation, I analyzed the cellular division history of memory CD8$^+$ T cells using the CFSE dilution assay. Ag+IL-4-activated donor CD8$^+$ T cells obtained from the spleen on day 7 post-adoptive transfer were labeled with CFSE and subsequently re-transferred to a second host mouse. CFSE fluorescence patterns of donor cells in various host organs were examined on day 28 after re-transfer. The majority of donor T$_{LM}$ and T$_{BM}$ cells had divided 2 to 4 times, while those in the spleen and LN only 1 to 2 times (Figure 9). The observed cell division is IL-15Rα-dependent as no division was observed in the IL-15Rα-ko hosts. These results suggest that the liver, like BM, provides a better environment than peripheral lymphoid organs for memory CD8$^+$ T cell homeostatic proliferation.

Formation of T$_{LM}$ clusters in the liver

To access the anatomical niche that contributes to T$_{LM}$ expansion, livers were harvested from the mice that had received Ag+IL-4-activated 2C CD8$^+$ T cells on day 7 post-adoptive transfer. H&E-stained liver sections revealed cell clusters composed of cells characteristic for lymphocytes and the clusters were surrounded by hepatocytes and sinusoid endothelial cells (Figure 10). Neutrophils were occasionally found in

some cell clusters, and no hepatocytes were found within the confines of these cell

clusters. To determine the origin of T_{LM} clusters, liver cryosections of recipient mice

were subjected to Thy-1.2 immunofluorescent staining. As can be seen in Figure 11,

cell clusters are composed of Thy-1.2$^+$ CD8$^+$ T cells. As host T cells are all Thy-1.1$^+$

and do not express Thy-1.2, these results clearly show that T_{LM} clusters are of donor cell

origin.

Next, I investigated the distribution of T_{LM} cell clusters in the liver. The liver

cryosections were subjected to anti-CD8 immunohistochemical staining on day 60 after

transfer (Figure 12A). The number and size of CD8$^+$ T cell clusters found near the

portal triad (within 100 μm), central vein (within 100 μm), and the midzonal region

(outside portal triad and central vein regions) were tabulated. T_{LM} clusters were

preferentially distributed in the midzonal region (16.0±2.1 / mm^3) and near the portal

triad (9.8±1.0 / mm^3), rather than in regions near the central vein (2.6±1.2 / mm^3), and

the sizes of cell clusters in each region showed no significant difference (Figure 12B).

Since the frequency of T_{LM} cell clusters in the midzonal region was the highest,

followed by portal triad and central vein regions, the formation of the T_{LM} cell clusters

is not correlated with the direction of blood flow, which travels from portal triad to

midzonal and then central vein regions. The distribution of the T_{LM} cell clusters

appears to coincide with HSC presence (33, 34), suggesting a possible role of HSC is in

T_{LM} clusters formation.

Since the generation of T_{LM} clusters was dependent on IL-15Rα (Figure 3), I then compared the number of cell clusters in liver sections of IL-15Rα-ko and WT hosts. Fifty-four liver sections of IL-15Rα-ko mice were examined, and not a single cell cluster was found, whereas of the 9 liver sections of WT mice examined, 8 clusters were identified (Figure 13A).   Based on the fact that one cluster consists, on average, of 11.3 cells, I estimated that the entire liver of a WT mouse contained about 5×10^5 (4.7×10^4 clusters / liver $\times11.3$) donor cells (Figure 13B), an estimate that is consistent with the actual number of donor cells that could be physically recovered (Figure 2 & 3), indicating that the majority of memory CD8$^+$ T cells exist in the liver in the form of clusters.   In contrast to the WT mouse liver, less than 9.2×10^3 (8.1×10^2 clusters / liver $\times11.3$) donor cells were recovered from the liver of an IL-15Rα-ko recipient (Figure 13B).   These results together indicate that host IL-15Rα expression is required for T_{LM} cluster formation in the liver.

I next studied whether T_{LM} cell clusters cause pathology by analyzing serum ALT and AST of recipient mice and by *in situ* TUNEL staining of liver cryosections. T_{LM} cell clusters did not cause hepatocyte damage (Figure 14A), nor did cells within T_{LM} clusters undergo apoptosis (Figure 14B).

T_{LM} cells undergo clonal expansion in the liver

To investigate how T_{LM} cell clusters were formed, Vβ5$^+$ and Vβ8$^+$ CD8$^+$ T cells were

purified by sorting and mixed in equal proportions after *in vitro*

anti-CD3+IL-4-stimulation. FACS analysis of the donor Vβ5$^+$ and Vβ8$^+$ T cells

showed that the percentages of these two populations were almost the same in the

spleen and liver on both day 7 and day 60 after transfer (Figure 15), indicating that both

Vβ5$^+$ and Vβ8$^+$ T cells expanded equally well. Confocal microscopic results showed

that of the 13 T_{LM} cell clusters examined, 6 (46%) contained exclusively Vβ5$^+$ cells, and

the other 6 (46%) exclusively Vβ8$^+$ cells on day 7 after transfer (Figure 16). Similarly

on day 60 after transfer, 50% contained exclusively Vβ5$^+$ and 50% exclusively Vβ8$^+$

cells (Figure 17). Since individual T_{LM} cell clusters are made up from cells with single

TCR usages, T_{LM} cell clusters are the results of clonal expansion of single cells *in situ*.

Clonal nature of T_{LM} clusters in the liver of Listeria monocytogenes-immune mice

To further strengthen the finding of clonal expansion of T_{LM} cells in the liver, WT mice

were subjected to sublethal *Listeria monocytogenes* (*Lm*) immunization. Because

single cell suspension recovered from the liver of *Lm*-immune hosts contained CD8$^+$ T

cells that were 64% Vβ8$^+$ (Figure 18), there was biased expansion of T cells belonging

to the Vβ8 family, a finding consistent with previously published results (70). If liver

CD8^{+} T cells were generated elsewhere and homed to micro-niches that support the survival of clusters of memory CD8^{+} T cells, each individual CD8^{+} T cell cluster would be expected to contain roughly 60% Vβ8^{+} cells. Instead, of the 12 T_{LM} clusters identified, 6 contained either no or very few Vβ8^{+} cells. For the other 6 clusters, Vβ8^{+} cells were readily detectable and constituted 80% to 100% of Thy-1.2^{+}CD8^{+} cells in the clusters. The non-random nature of nearly all or no Vβ8^{+} T cell presence in all 12 clusters examined indicates that these clusters are clonal descendents of single cells and are similar to the Ag+IL-4-stimulated memory CD8^{+} T cells. I also randomly examined a total of 40 liver sections from three aged-matched naïve control mice for the presence of T_{LM} clusters. Only one Vβ8^{−} cluster was found. *Lm*-immune and aged-matched naïve livers were also examined for the presence of CD8^{+} T_{LM} clusters by CD8 immunohistochemistry staining (Figure 19). The entire liver of a *Lm*-immune mouse contained an estimated 5.7×10^3 T_{LM} clusters, which was 17-fold higher than that of naïve livers (3.2×10^2 clusters). Most CD8^{+} T cell clusters seen in the liver of *Lm*-immune mice must therefore have been formed as a result of *Lm* infection.

Dendrite-like IL-15Rα^{+} processes are involved in the T_{LM} cell cluster

Based on the IL-15 transpresentation model, I examined the expressions of IL-15 and IL-15Rα in T_{LM} cell clusters. Immunohistochemical staining of serial liver sections

revealed that all 13 T_{LM} clusters contained cells that expressed IL-15 and IL-15Rα in their dendrite-like processes (Figure 20), suggesting that these cells may be involved in the formation of CD8$^+$ T_{LM} cell clusters. To confirm that the presence of IL-15$^+$ and IL-15Rα^+ dendrite-like processes is unique to T_{LM} cell clusters, I compared fields with T_{LM} cell clusters to those without. Of 13 randomly selected fields without T_{LM} clusters, 8 contained IL-15$^+$ (62%) and 4 IL-15Rα^+ (31%) dendrite-like processes. A significant increase in IL-15$^+$ and IL-15Rα^+ dendrite-like processes was observed in the fields with T_{LM} clusters (fields with CD8$^+$ T cell clusters vs. non-cluster, IL-15$^+$: 100% vs. 62%, p=0.02; IL-15Rα^+: 100% vs. 31%, p=0.0002). Our finding of close physical association of IL-15$^+$ and IL-15Rα^+ dendrite-like processes with CD8$^+$ T_{LM} clusters suggests significant roles in facilitating CD8$^+$ T_{LM} cluster formation by these IL-15$^+$ and IL-15Rα^+ dendrite-like processes.

As IL-15Rα expression on memory CD8$^+$ T cells is not required for their survival (22), along with my results showing dendrite-like patterns of IL-15Rα^+ signals associated with T_{LM} clusters (Figure 20C), T_{LM} cluster formation in the liver is likely to be mediated through IL-15 transpresentation rather than direct IL-15 action through IL-15R expression on CD8$^+$ memory cells.

T_{LM} cell clusters are closely associated with HSC

Next, I examined the spatial relationship between T_{LM} clusters and HSC.

Immunofluorescent staining of liver sections were stained with 1B2 mAb, anti-GFAP,

and anti-pan cytokeratin antibodies to detect donor 2C CD8$^+$ T cells, HSC and

hepatocytes, respectively (Figure 21A & 21B). The presence of HSC was detected in

11 out of 11 T_{LM} clusters, but only in 7 of 11 non-cluster fields, in the liver sections

obtained from day 7 adoptive transfer hosts (11/11 vs. 7/11; p=0.045). Similarly, the

presence of HSC was detected in all 14 T_{LM} clusters, but only in 9 of 14 non-cluster

fields (p=0.02), in liver sections obtained from day 69 adoptive transfer hosts (Figure

21C). In addition, unlike the GFAP$^+$ HSC in the 1B2$^+$ clusters, the GFAP$^+$ HSC in the

non-cluster fields showed close contact with hepatocytes. Our findings indicate that

HSC may play an essential role for the formation and maintenance of T_{LM} cell clusters.

Neutrophils with characteristic segmental nuclei and autofluorescence (71) were

seen in some CD8$^+$ T_{LM} clusters. In liver sections on day 7 and day 69 post-adoptive

transfer, 6 of 11 and 10 of 14 T_{LM} clusters contained neutrophils. No neutrophils were

found in 14 random fields away from T_{LM} clusters, and statistical analysis revealed

highly significant differences for neutrophils for areas associated and away from T_{LM}

clusters (day 7, p=0.006; day 69, p<0.001).

Electron microscopic examination further revealed structural details of the spatial

relationship between the T_{LM} clusters and closely associated non-T cells (Figure 22).

Clearly, three T cells with the characteristics of scanty cytoplasm are in close contact

with the HSC, which had two clearly visible and characteristic lipid droplets.   Notably,

the dendrite-like cytoplasmic processes of the HSC are in close contact with each of the

three T cells.   Further analysis revealed that HSC had significantly higher IL-15 and

IL-15Rα mRNA levels than that of total liver (Figures 23).   Thus, it is possible that

HSC can transpresent IL-15 signals for the formation of T_{LM} cell clusters.   These

observations together indicate that IL-15/IL-15Rα expressing HSC by being in close

contact with T cells may provide the cytokine microenvironment needed for the

homeostatic proliferation and maintenance of memory CD8$^+$ T cells in the liver.

T_{LM} cells can convert to T_{EM} and T_{CM} cells in the spleen

To address the question of whether T_{LM} cells can home to lymphoid organs, T_{CM}, T_{EM},

and T_{LM} cells were isolated by sorting on day 60 post-adoptive transfer and

re-transferred separately into second recipient mice.   On day 14 after re-transfer, the

distribution of donor cells in the spleen, LN, and liver were determined (Figure 24).

Donor T_{LM} cells preferentially homed to the liver (1.44%), at rates that were 29- and

144-fold the rates to the spleen (0.05%) and LN (0.01%).   When splenic T_{EM} cells

were re-transferred, 0.16%, 0.02% and 1.09% of donor CD8$^+$ T cells among total CD8$^+$

T cells were found in the spleen, LN, and liver, respectively.   Relative abundance for

transferred T_{EM} cells were 6.8 ($1.09 \div 0.16$) and 55 ($1.09 \div 0.02$) for liver:spleen and liver:LN, respectively.   For transferred T_{CM} cells, 0.73%, 0.33% and 1.29% of donor $CD8^+$ T cells among total $CD8^+$ T cells were found in the spleen, LN, and liver, respectively; and the relative abundance for transferred T_{CM} cells were 1.8 ($1.29 \div 0.73$) and 3.9 ($1.29 \div 0.33$) for liver:spleen and liver:LN, respectively.

In addition, while >65% of donor T_{LM} and T_{EM} cells that homed to the spleen and LN were $CD62L^{hi}$, only 19.8% of donor T_{LM} cells that homed to the liver were $CD62L^{hi}$ (Figure 25).   By contrast, >90% of donor T_{CM} cells that homed to the spleen and LN remained $CD62L^{hi}$ but only 58.6% that homed to the liver were $CD62L^{hi}$.   Based on the results of the migration patterns and changes of CD62L expression, it appears that all T_{CM}, T_{EM}, and T_{LM} cells are interconvertable after re-transfer and that the anatomical locations from which donor cells are found is a key determining factor in memory $CD8^+$ T cell marker expression and possibly their immune function.

Discussion

Role of HSC in the formation of memory CD8^{+} T cell clusters

The primary finding in my research is that memory CD8^{+} T cells expand clonally to form cell clusters in the liver of normal but not IL-15Rα-ko mice. These memory CD8^{+} T cell clusters are in close contact with the IL-15Rα^{+} and IL-15^{+} dendrite-like processes. Kupffer cells (KC), HSC and hepatocytes are all known to produce IL-15 (37, 72, 73). KCs and HSCs reside in the sinusoid and the space of Disse, respectively. Thus, the existence of memory CD8^{+} T cell clusters in the sinusoid may indicate that KC participates in the clonal expansion of memory CD8^{+} T cells. On the other hand, if memory CD8^{+} T cells form clusters in the space of Disse, HSC and/or hepatocytes may be involved in the clonal expansion of memory CD8^{+} T cells. Through my preliminary EM work, I found one T_{LM} cluster in an anatomical location characteristic of the space of Disse. In addition, CD8^{+} T_{LM} clusters reside outside of the sinusoid lumen and are closely in contact with GFAP^{+} HSCs. This implies that HSC may play a role in clonal expansion of memory CD8^{+} T cells. It is noted that HSCs express high levels of IL-15 and IL-15Rα. Thus, IL-15Rα^{+} HSC is expected to transpresent IL-15 to memory CD8^{+} T cells in the liver and thus play significant roles in the expansion and maintenance of memory CD8^{+} T_{LM} clusters. The HSC may secret chemokines to attract the homing of memory CD8^{+} T cells. The HSC may also secrete collagens to help form a scaffold that is required for clonal expansion of memory CD8^{+} T cells to

take place. Additional studies of HSC-induced proliferation of memory CD8^{+} T cells

are required to obtain a better picture of the *in situ* proliferation of memory CD8^{+} T

cells in the liver. One such study is to express IL-15Rα under the control of the

GFAP-promoter in IL-15Rα-ko mice. Here, IL-15Rα expression on HSC alone, can

directly address its role in the homeostasis of memory CD8^{+} T cells. Neutrophils are

also found within T_{LM} cell clusters, but the role of the neutrophils, if any, is unclear.

Neutrophils have been shown to be attracted by chemokines produced by transformed

HSC (38). They may stimulate HSCs to secrete collagen or other substances (74) that

are required for clonal expansion of memory CD8^{+} T cells. Other cell types, including

sinusoid endothelial cells and hepatocytes that are closely associated with T_{LM} clusters

may also be involved in the clonal expansion of memory CD8^{+} T cells. HepG2 cells

and immortalized human hepatocytes have been shown to express IL-15 and IL-15Rα

and contribute to the *in vitro* proliferation of memory CD8^{+} T cells (75). It is therefore

possible that hepatocytes are also actively engaged in the homeostasis of memory CD8^{+}

T cells. The precise nature of the niche that promotes memory T_{LM} cluster formation,

whether involving HSC, or HSC in conjunction with hepatocytes and endothelial cells,

requires further experimentation.

The anatomical niches for formation of memory CD8^{+} T cell clusters

There were 4.7×10^4 and 5.7×10^3 T_{LM} clusters per liver, respectively, for host mice that had received Ag+IL-4-activated CD8$^+$ T cells (8×10^6/mouse) or that had been *Lm*-immunized. These numbers are significantly higher than the background T_{LM} clusters in the naïve B6 mice (3.2×10^2). However, the number of memory CD8$^+$ T_{LM} clusters in the liver resulting from adoptive transfer of 8×10^6 Ag+IL-4-stimulated naïve CD8$^+$ T cells appears to have reached a plateau as adoptive transfer of more donor CD8$^+$ T cells did not result in further increases of T_{LM} clusters. It indicates that the anatomical niches for the formation of memory CD8$^+$ T cells in the liver are limiting. The number of T_{LM}-permissive niches is much less than the number of HSCs. Thus, other factors and/or cells should be essential in the formation of the memory CD8$^+$ T_{LM} clusters. Homing of memory CD8$^+$ T cells to the space of Disse is presumably chemokine-dependent. I measured mRNA expression of several chemokine receptors of the Ag+IL-4-activated CD8$^+$ T cells. The CXCR6 expression of the Ag+IL-4-activated CD8$^+$ T cells is 6-fold higher than CD8$^+$ T cells activated without IL-4 (data not shown). CXCL16, the ligand for CXCR6, has been shown to induce NKT cell crawling in the sinusoid and is expressed on the sinusoid endothelial cell (76). The sinusoid endothelial cell also expresses ICAM-1 that may mediate adhesion between memory CD8$^+$ T cells and sinusoid endothelial cells. Thus, the sinusoid endothelial cells may play a role for recruitment of memory CD8$^+$ T cells into the space

of Disse. Although T_{LM} clusters did not reside in the sinusoid lumen, KC may play an indirect role in the clonal expansion of memory CD8$^+$ T cells. I found that T_{CM} or T_{EM} cells converted to T_{LM} cells in the liver, and lost their effector function. KC has been shown to dampen the effector function of CD8$^+$ T cells through the production of IL-10 (77, 78). The genetic program that leads to depressed effector function may also cause T_{LM} cells to enter a state uniquely suited for homeostatic expansion. Taken together, multiple requirements are likely required before a micro-anatomical niche becomes permissible for T_{LM} clonal expansion.

Are T_{LM} cells a new subset of memory CD8$^+$ T cells?

Low CD62L expression has been used to define T_{EM} cells. However, the CD62L^{low} T_{LM} cells are different from T_{EM} cells because they express lower TCR-induced proliferation, IFN-γ production, and cytotoxic function. Thus, T_{LM} cells are not identical to spleen T_{EM} cells. A question raised here is whether T_{LM} cells belong to a new subset of memory CD8$^+$ T cells or that their depressed functional properties result from the unique micro-environment of the liver. My results have shown that all three T_{CM}, T_{EM} and T_{LM} donor cells can migrate to other organs and that the "low" IFN-γ functionality of T_{LM} cells can be converted to "high" when they migrate to the spleen. Accordingly, T_{LM} cells appear not to represent a distinct lineage of memory CD8$^+$ T

cells distinct from the T_{EM} and T_{CM} cells.   Because IL-15 stimulation modulates the

cytotoxic functions of memory CD8$^+$ T cells by induction of the NKR expression (79),

and that the liver environment induces the clonal expansion of memory CD8$^+$ T cells in

an IL-15-IL-15R-dependent fashion, it is possible that the liver environment can

modulate the functional properties of CD8$^+$ T_{LM} cells.   Since the CD62L^{low} T_{LM} cells

are not identical to T_{EM} cells, the traditional classification of central and effector

memory CD8$^+$ T cells based on CD62L and CCR7 expression is not adequate in

defining all subsets of memory CD8$^+$ T cells.   Thus, new markers are required for the

comprehensive classification of all subsets of memory CD8$^+$ T cells.

The relationship among the T_{CM}, T_{EM} and T_{LM} cells

After CD62L^{low} T_{LM} cells are purified and adoptively transferred into histocompatible

congenic hosts, they can convert to CD62L^{hi} memory CD8$^+$ T cells in the spleen and LN

but remain CD62L^{low} in the liver.   Liver memory CD8$^+$ T cells may remain CD62L^{low}

as long as they stay in the liver, but when they migrate out of the liver to enter

peripheral lymphoid tissues, they convert to the CD62L^{hi} phenotype.

After spleen CD62L^{hi} T_{CM} cells are purified and adoptively transferred into

histocompatible congenic hosts, donor CD8$^+$ T cells can migrate into the liver, and at

least 40% of donor cells that home to the liver can convert to CD62L^{low}.   This result is

inconsistent with the $T_{EM} \rightarrow T_{CM}$ pathway, and is more compatible with the $T_{CM} \rightarrow T_{EM}$ pathway. Alternatively, all T_{CM} cells may be CD62L^{hi}, but not all CD62L^{hi} cells are T_{CM} cells. If so, some CD62L^{hi} memory CD8$^+$ T cells can be T_{EM} cells and are thus able to migrate into the liver. The other possible explanation is that the liver environment is directly responsible for the decreased CD62L^{low} expression, either by preventing the transcription of the CD62L gene or by causing CD62L shedding.

Memory CD8$^+$ T cells divide once every 2 weeks (80), so a small population of memory CD8$^+$ T cells enter the cell cycle at any given time. Loss of CD62L expression has been shown for T cells engaged in cell cycle progression (81). Therefore, T_{CM} cells undergoing proliferation would lose their CD62L expression and be classified as T_{EM} cells. In addition, the issue of how long it takes before the memory CD8$^+$ T cell regain the high CD62L expression after cell division stops is unknown and is worthy of further exploration.

Although memory CD8$^+$ T cells can be efficiently generated in our *in vitro* culture system, these *in vitro* Ag+IL-4-generated memory CD8$^+$ T cells may not reflect the heterogeneity of memory CD8$^+$ T cells generated *in vivo* in response to natural viral of bacterial infections. Using mice that had been infected by *Listeria monocytogenes*, the formation of clonally expanded CD8$^+$ T_{LM} cell clusters in the liver was also found. The clonal nature of T_{LM} clusters therefore applies to *in vitro*- as well as *in*

vivo-generated memory CD8$^+$ T cells.

Cytokine-mediated homeostatic expansion and TCR-induced expansion and cytotoxicity may be mutually exclusive genetic programs

The CD62L^{low} T$_{LM}$ cells are proliferation-deficient, express low IFN-γ and cytotoxic functions upon TCR-stimulation. Spleen T$_{EM}$ cells, in contrast, express potent effector functions upon TCR stimulation. Since T$_{LM}$ cells undergo IL-15-dependent homeostatic expansion, but do not proliferate in response to TCR-stimulation, it is possible that TCR-induced and IL-15R-induced cell proliferation programs are mutually exclusive. It is also possible that effector functions of memory CD8$^+$ T cells are inhibited by the liver microenvironment as KC, for example, may inhibit the effector functions of memory CD8$^+$ T cells through the production of IL-10 (77, 78).

Redundant roles of the liver and BM in memory CD8$^+$ T cell homeostasis

BM has been reported as a preferred organ for homeostasis of memory CD8$^+$ T cells (20). My findings indicate that the liver can play a similar role as the BM in the homeostatic expansion of memory CD8$^+$ T cells. Liver is the largest organ of our body and the high level of IL-15Rα expression has the potential for IL-15 trans-presentation to mediate homeostatic expansion of memory CD8$^+$ T cells (26). Liver sinusoid
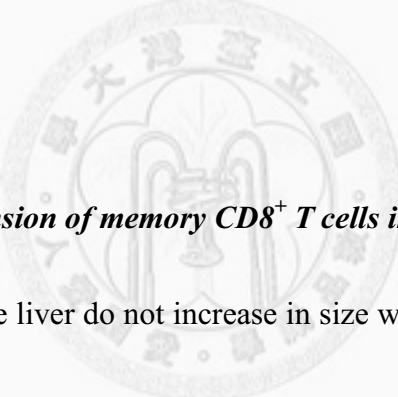
endothelial cells express CXCL16 (76), which can attract CXCR6$^+$ T$_{EM}$ and T$_{CM}$ cells to home to the liver and undergo homeostatic proliferation there.   In contrast, BM attracts T$_{CM}$ cells and may only induce proliferation of the T$_{CM}$ cells (20, 29).   In addition, liver is exposed to exogenous antigens from the gut (gut-liver axis) or circulation, and may help bystander memory CD8$^+$ T cell proliferation (82, 83).   This indicates that the liver may play other immune functions in addition to homeostatic maintenance of memory CD8$^+$ T cells.   On the other hand, the apparent redundancy of both the liver and the BM in mediating homeostatic maintenance of CD8$^+$ memory T cells may also be explained by the highly important nature of memory CD8$^+$ T cell maintenance and that redundancy provides a survival advantage.   Thus, if either the liver or the BM is temporarily damaged, homeostatic maintenance of CD8$^+$ memory T cells can still be carried out in the other undamaged organ.   Alternatively, the liver and BM may maintain functionally distinct subsets of memory CD8$^+$ T cells.

Subset-specific T cell growth and survival fate in the liver

T$_{LM}$ cells proliferated but did not undergo apoptosis in the liver.   Therefore, the liver plays a role in the maintenance of memory CD8$^+$ T cells.   This is contrary to the commonly held view of the liver as the graveyard for activated CD8$^+$ T cells (67, 84-85).   My finding is consistent with previous reports showing the presence of memory CD8$^+$ T

cells in the liver (1, 2, 86-88). Since memory CD8$^+$ T cells express more

anti-apoptotic Bcl-2 than effector T cells (89), memory CD8$^+$ T cells may resist

liver-induced apoptosis better than normal effector T cells (90). The survival and

proliferation of memory CD8$^+$ T cells in the liver provide exciting research directions

that will allow us to bring out the cellular and molecular mechanisms of how the liver

contributes to the homeostasis of memory CD8$^+$ T cells. Also, my findings provide

further proof that the homeostasis of memory CD8$^+$ T cells can be maintained in

non-lymphoid organs.

***A model of the clonal expansion of memory CD8$^+$ T cells in the liver***

CD8$^+$ T$_{LM}$ cell clusters in the liver do not increase in size with age (data not shown) and

display no signs of apoptosis. Thus, I propose that the T$_{LM}$ cells exit the liver to enter

peripheral circulation after *in situ* clonal expansion has reached a level beyond which

the T$_{LM}$-permissible niches can support. Although my data do not directly prove this

point, T$_{LM}$ cells can survive well in the liver, spleen, and LN after their adoptive transfer

into histocompatible hosts. Collectively, Ag+IL-4-stimulated memory CD8$^+$ T cells

may circulate between lymphoid and non-lymphoid organs. I propose that the memory

CD8$^+$ cell clusters form in the following steps (Figure 26). First, the memory CD8$^+$ T

cells migrate into the parenchyma, most likely the space of Disse, where single memory

CD8$^+$ T cells interact with HSC. HSC then trans-presents IL-15 signals to memory CD8$^+$ T cells. The memory CD8$^+$ T cells expand clonally and form T$_{LM}$ clusters in the liver. When the size of the cell clusters becomes large and the memory CD8$^+$ T cells cannot receive the IL-15 signals from the HSC, the cells of the T$_{LM}$ clusters stop proliferation and leave the liver to enter peripheral circulation. Because constituent cells of any given T$_{LM}$ cluster all express a single TCR Vβ, interpreting memory CD8$^+$ T cells in the liver must follow a "one in, all out" rule.

Conclusions

Two major findings are reported in my thesis. First, activation by Ag+IL-4 induces a previously unappreciated subset of memory CD8$^+$ T cells with weak effector functions, yet with strong homeostatic proliferation ability. Second, the clonal nature of CD8$^+$ T$_{LM}$ clusters indicates that finding a T$_{LM}$-permissive liver niche by a single CD8$^+$ memory T cell is a rate-limiting event and that it is unlikely that two single memory CD8$^+$ T cells can find the same niche. In addition, once a T$_{LM}$ cluster has formed, it no longer allows entry of other memory CD8$^+$ T cells, although this may be simply caused by the rare nature of a single memory CD8$^+$ T cells finding a T$_{LM}$-permissive niche. Since there is no evidence of apoptosis for either CD8$^+$ T cells or for nearby hepatocytes, the CD8$^+$ T cells formed by clonal expansion most likely traffic out of the liver and

contribute to the pool of long-lived, circulating memory CD8$^+$ T cells. In addition, IL-15Rα$^+$ HSC showed intimate association with T$_{LM}$ clusters may therefore play critical roles in the initiation and/or maintenance of memory CD8$^+$ T cell homeostatic expansion in the liver. This newly uncovered role of the liver in the maintenance of memory CD8$^+$ T cells may benefit future vaccine development against infectious agents or liver cancers as well as basic research on the cellular and molecular mechanisms of memory CD8$^+$ T cell generation and maintenance. Lastly, caution should be exercised in interpreting clinical finding of focal lymphocyte infiltration in patient liver biopsies, as focal lymphocyte growth may represent normal physiology and not necessarily pathology.
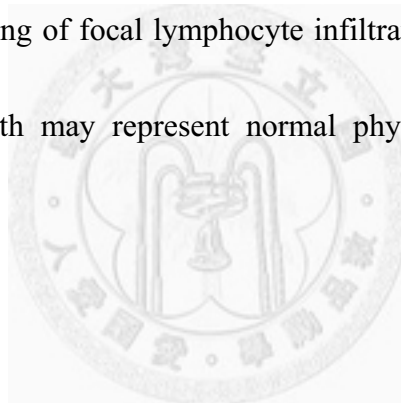
References

1. Masopust, D., V. Vezys, A. L. Marzo, and L. Lefrancois. 2001. Preferential localization of effector memory cells in nonlymphoid tissue. *Science* 291:2413-2417.

2. Wherry, E. J., V. Teichgraber, T. C. Becker, D. Masopust, S. M. Kaech, R. Antia, U. H. von Andrian, and R. Ahmed. 2003. Lineage relationship and protective immunity of memory CD8 T cell subsets. *Nat Immunol* 4:225-234.

3. Marzo, A. L., H. Yagita, and L. Lefrancois. 2007. Cutting edge: migration to nonlymphoid tissues results in functional conversion of central to effector memory CD8 T cells. *J Immunol* 179:36-40.

4. Manjunath, N., P. Shankar, J. Wan, W. Weninger, M. A. Crowley, K. Hieshima, T. A. Springer, X. Fan, H. Shen, J. Lieberman, and U. H. von Andrian. 2001. Effector differentiation is not prerequisite for generation of memory cytotoxic T lymphocytes. *J Clin Invest* 108:871-878.

5. Marzo, A. L., K. D. Klonowski, A. Le Bon, P. Borrow, D. F. Tough, and L. Lefrancois. 2005. Initial T cell frequency dictates memory CD8+ T cell lineage commitment. *Nat Immunol* 6:793-799.

6. Obar, J. J., K. M. Khanna, and L. Lefrancois. 2008. Endogenous naive CD8+ T cell precursor frequency regulates primary and memory responses to infection.

Immunity 28:859-869.

7. Masopust, D., V. Vezys, E. J. Wherry, D. L. Barber, and R. Ahmed. 2006. Cutting edge: gut microenvironment promotes differentiation of a unique memory CD8 T cell population. *J Immunol* 176:2079-2083.

8. Kedzierska, K., J. Stambas, M. R. Jenkins, R. Keating, S. J. Turner, and P. C. Doherty. 2007. Location rather than CD62L phenotype is critical in the early establishment of influenza-specific CD8+ T cell memory. *Proc Natl Acad Sci U S A* 104:9782-9787.

9. Swain, S. L., A. D. Weinberg, M. English, and G. Huston. 1990. IL-4 directs the development of Th2-like helper effectors. *J Immunol* 145:3796-3806.

10. Morrot, A., J. C. Hafalla, I. A. Cockburn, L. H. Carvalho, and F. Zavala. 2005. IL-4 receptor expression on CD8+ T cells is required for the development of protective memory responses against liver stages of malaria parasites. *J Exp Med* 202:551-560.

11. Stager, S., J. Alexander, A. C. Kirby, M. Botto, N. V. Rooijen, D. F. Smith, F. Brombacher, and P. M. Kaye. 2003. Natural antibodies and complement are endogenous adjuvants for vaccine-induced CD8+ T-cell responses. *Nat Med* 9:1287-1292.

12. Chang, M. L., Y. T. Chen, Y. C. Su, and J. T. Kung. 2003. Cytotoxic T lymphocytes

generated by short-term in vitro TCR stimulation in the presence of IL-4 are therapeutically effective against B16 melanoma. *J Biomed Sci* 10:644-650.

13. Huang, L. R., F. L. Chen, Y. T. Chen, Y. M. Lin, and J. T. Kung. 2000. Potent induction of long-term CD8+ T cell memory by short-term IL-4 exposure during T cell receptor stimulation. *Proc Natl Acad Sci U S A* 97:3406-3411.

14. Kaech, S. M., J. T. Tan, E. J. Wherry, B. T. Konieczny, C. D. Surh, and R. Ahmed. 2003. Selective expression of the interleukin 7 receptor identifies effector CD8 T cells that give rise to long-lived memory cells. *Nat Immunol* 4:1191-1198.

15. Ku, C. C., M. Murakami, A. Sakamoto, J. Kappler, and P. Marrack. 2000. Control of homeostasis of CD8+ memory T cells by opposing cytokines. *Science* 288:675-678.

16. Carrio, R., C. E. Rolle, and T. R. Malek. 2007. Non-redundant role for IL-7R signaling for the survival of CD8+ memory T cells. *Eur J Immunol* 37:3078-3088.

17. Becker, T. C., E. J. Wherry, D. Boone, K. Murali-Krishna, R. Antia, A. Ma, and R. Ahmed. 2002. Interleukin 15 is required for proliferative renewal of virus-specific memory CD8 T cells. *J Exp Med* 195:1541-1548.

18. Lodolce, J. P., D. L. Boone, S. Chai, R. E. Swain, T. Dassopoulos, S. Trettin, and A. Ma. 1998. IL-15 receptor maintains lymphoid homeostasis by supporting lymphocyte homing and proliferation. *Immunity* 9:669-676.

19. Kennedy, M. K., M. Glaccum, S. N. Brown, E. A. Butz, J. L. Viney, M. Embers, N. Matsuki, K. Charrier, L. Sedger, C. R. Willis, K. Brasel, P. J. Morrissey, K. Stocking, J. C. Schuh, S. Joyce, and J. J. Peschon. 2000. Reversible defects in natural killer and memory CD8 T cell lineages in interleukin 15-deficient mice. *J Exp Med* 191:771-780.

20. Becker, T. C., S. M. Coley, E. J. Wherry, and R. Ahmed. 2005. Bone marrow is a preferred site for homeostatic proliferation of memory CD8 T cells. *J Immunol* 174:1269-1273.

21. Yajima, T., H. Nishimura, R. Ishimitsu, T. Watase, D. H. Busch, E. G. Pamer, H. Kuwano, and Y. Yoshikai. 2002. Overexpression of IL-15 in vivo increases antigen-driven memory CD8+ T cells following a microbe exposure. *J Immunol* 168:1198-1203.

22. Burkett, P. R., R. Koka, M. Chien, S. Chai, F. Chan, A. Ma, and D. L. Boone. 2003. IL-15R alpha expression on CD8+ T cells is dispensable for T cell memory. *Proc Natl Acad Sci U S A* 100:4724-4729.

23. Schluns, K. S., T. Stoklasek, and L. Lefrancois. 2005. The roles of interleukin-15 receptor alpha: Trans-presentation, receptor component, or both? *Int J Biochem Cell Biol* 37:1567-1571.

24. Dubois, S., J. Mariner, T. A. Waldmann, and Y. Tagaya. 2002. IL-15Ralpha

recycles and presents IL-15 In trans to neighboring cells. *Immunity* 17:537-547.

25. Grabstein, K. H., J. Eisenman, K. Shanebeck, C. Rauch, S. Srinivasan, V. Fung, C. Beers, J. Richardson, M. A. Schoenborn, M. Ahdieh, and et al. 1994. Cloning of a T cell growth factor that interacts with the beta chain of the interleukin-2 receptor. *Science* 264:965-968.

26. Giri, J. G., S. Kumaki, M. Ahdieh, D. J. Friend, A. Loomis, K. Shanebeck, R. DuBose, D. Cosman, L. S. Park, and D. M. Anderson. 1995. Identification and cloning of a novel IL-15 binding protein that is structurally related to the alpha chain of the IL-2 receptor. *Embo J* 14:3654-3663.

27. Moyron-Quiroz, J. E., J. Rangel-Moreno, L. Hartson, K. Kusser, M. P. Tighe, K. D. Klonowski, L. Lefrancois, L. S. Cauley, A. G. Harmsen, F. E. Lund, and T. D. Randall. 2006. Persistence and responsiveness of immunologic memory in the absence of secondary lymphoid organs. *Immunity* 25:643-654.

28. Obhrai, J. S., M. H. Oberbarnscheidt, T. W. Hand, L. Diggs, G. Chalasani, and F. G. Lakkis. 2006. Effector T cell differentiation and memory T cell maintenance outside secondary lymphoid organs. *J Immunol* 176:4051-4058.

29. Mazo, I. B., M. Honczarenko, H. Leung, L. L. Cavanagh, R. Bonasio, W. Weninger, K. Engelke, L. Xia, R. P. McEver, P. A. Koni, L. E. Silberstein, and U. H. von Andrian. 2005. Bone marrow is a major reservoir and site of recruitment for central

memory CD8+ T cells. *Immunity* 22:259-270.

30. Parretta, E., G. Cassese, P. Barba, A. Santoni, J. Guardiola, and F. Di Rosa. 2005. CD8 cell division maintaining cytotoxic memory occurs predominantly in the bone marrow. *J Immunol* 174:7654-7664.

31. Schluns, K. S., K. D. Klonowski, and L. Lefrancois. 2004. Transregulation of memory CD8 T-cell proliferation by IL-15Ralpha+ bone marrow-derived cells. *Blood* 103:988-994.

32. Friedman, S. L. 2008. Hepatic stellate cells: protean, multifunctional, and enigmatic cells of the liver. *Physiol Rev* 88:125-172.

33. Azais-Braesco, V., M. L. Hautekeete, I. Dodeman, and A. Geerts. 1997. Morphology of liver stellate cells and liver vitamin A content in 3,4,3',4'-tetrachlorobiphenyl-treated rats. *Journal of hepatology* 27:545-553.

34. Wake, K., and T. Sato. 1993. Intralobular heterogeneity of perisinusoidal stellate cells in porcine liver. *Cell Tissue Res* 273:227-237.

35. Libbrecht, L., D. Cassiman, V. Desmet, and T. Roskams. 2002. The correlation between portal myofibroblasts and development of intrahepatic bile ducts and arterial branches in human liver. *Liver* 22:252-258.

36. Skrtic, S., K. Wallenius, K. Sjogren, O.G. Isaksson, C. Ohlsson, and J.O. Jansson. 2001. Possible roles of insulin-like growth factor in regulation of physiological and

pathophysiological liver growth. *Hormone research* 55 Suppl 1:1-6.

37. Winau, F., G. Hegasy, R. Weiskirchen, S. Weber, C. Cassan, P. A. Sieling, R. L. Modlin, R. S. Liblau, A. M. Gressner, and S. H. Kaufmann. 2007. Ito cells are liver-resident antigen-presenting cells for activating T cell responses. *Immunity* 26:117-129.

38. Sprenger, H., A. Kaufmann, H. Garn, B. Lahme, D. Gemsa, and A. M. Gressner. 1997. Induction of neutrophil-attracting chemokines in transforming rat hepatic stellate cells. *Gastroenterology* 113:277-285.

39. Schwabe, R. F., R. Bataller, and D. A. Brenner. 2003. Human hepatic stellate cells express CCR5 and RANTES to induce proliferation and migration. *American journal of physiology* 285:G949-958.

40. Geerts, A. 2001. History, heterogeneity, developmental biology, and functions of quiescent hepatic stellate cells. *Semin Liver Dis* 21:311-335.

41. Blomhoff, R., M.H. Green, J.B. Green, T. Berg, and K.R. Norum. 1991. Vitamin A metabolism: new perspectives on absorption, transport, and storage. *Physiological reviews* 71:951-990.

42. Stephensen, C. B. 2001. Vitamin A, infection, and immune function. *Annual review of nutrition* 21:167-192.

43. Ballow, M., S. Xiang, S. J. Greenberg, L. Brodsky, C. Allen, and G. Rich. 1997.

Retinoic acid-induced modulation of IL-2 mRNA production and IL-2 receptor expression on T cells. *Int Arch Allergy Immunol* 113:167-169.

44. Dzhagalov, I., P. Chambon, and Y. W. He. 2007. Regulation of CD8+ T lymphocyte effector function and macrophage inflammatory cytokine production by retinoic acid receptor gamma. *J Immunol* 178:2113-2121.

45. Stephensen, C. B., A. D. Borowsky, and K. C. Lloyd. 2007. Disruption of Rxra gene in thymocytes and T lymphocytes modestly alters lymphocyte frequencies, proliferation, survival and T helper type 1/type 2 balance. *Immunology* 121:484-498.

46. Harty, J. T., L. L. Lenz, and M. J. Bevan. 1996. Primary and secondary immune responses to Listeria monocytogenes. *Curr Opin Immunol* 8:526-530.

47. Portnoy, D. A., T. Chakraborty, W. Goebel, and P. Cossart. 1992. Molecular determinants of Listeria monocytogenes pathogenesis. *Infect Immun* 60:1263-1267.

48. Cossart, P., M.F. Vicente, J. Mengaud, F. Baquero, J.C. Perez-Diaz, and P. Berche. 1989. Listeriolysin O is essential for virulence of Listeria monocytogenes: direct evidence obtained by gene complementation. Infect Immun 57:3629-3636.

49. Teixeira, H. C., and S. H. Kaufmann. 1994. Role of NK1.1+ cells in experimental listeriosis. NK1+ cells are early IFN-gamma producers but impair resistance to Listeria monocytogenes infection. *J Immunol* 152:1873-1882.

50. Flesch, I. E., A. Wandersee, and S. H. Kaufmann. 1997. IL-4 secretion by CD4+ NK1+ T cells induces monocyte chemoattractant protein-1 in early listeriosis. *J Immunol* 159:7-10.

51. Ueda, N., H. Kuki, D. Kamimura, S. Sawa, K. Seino, T. Tashiro, K. Fushuku, M. Taniguchi, T. Hirano, and M. Murakami. 2006. CD1d-restricted NKT cell activation enhanced homeostatic proliferation of CD8+ T cells in a manner dependent on IL-4. Int Immunol 18:1397-1404.

52. Sha, W. C., C. A. Nelson, R. D. Newberry, D. M. Kranz, J. H. Russell, and D. Y. Loh. 1988. Selective expression of an antigen receptor on CD8-bearing T lymphocytes in transgenic mice. *Nature* 335:271-274.

53. Chen, F.L., and J.T. Kung. 1996. Deficient CD4+ T cell proliferation in the class 1 MHC-restricted 2C TCR-transgenic mouse. J Immunol 156:2036-2044.

54. Kranz, D.M., D.H. Sherman, M.V. Sitkovsky, M.S. Pasternack, and H.N. Eisen. 1984. Immunoprecipitation of cell surface structures of cloned cytotoxic T lymphocytes by clone-specific antisera. Proc Natl Acad Sci U S A 81:573-577.

55. Ledbetter, J. A., and L. A. Herzenberg. 1979. Xenogeneic monoclonal antibodies to mouse lymphoid differentiation antigens. *Immunol Rev* 47:63-90.

56. Gallatin, W. M., I. L. Weissman, and E. C. Butcher. 1983. A cell-surface molecule involved in organ-specific homing of lymphocytes. *Nature* 304:30-34.

57. Trowbridge, I. S., J. Lesley, R. Schulte, R. Hyman, and J. Trotter. 1982. Biochemical characterization and cellular distribution of a polymorphic, murine cell-surface glycoprotein expressed on lymphoid tissues. *Immunogenetics* 15:299-312.

58. Bill, J., O. Kanagawa, J. Linten, Y. Utsunomiya, and E. Palmer. 1990. Class I and class II MHC gene products differentially affect the fate of V beta 5 bearing thymocytes. *J Mol Cell Immunol* 4:269-279; discussion 279-280.

59. Staerz, U. D., H. G. Rammensee, J. D. Benedetto, and M. J. Bevan. 1985. Characterization of a murine monoclonal antibody specific for an allotypic determinant on T cell antigen receptor. *J Immunol* 134:3994-4000.

60. Sarmiento, M., A. L. Glasebrook, and F. W. Fitch. 1980. IgG or IgM monoclonal antibodies reactive with different determinants on the molecular complex bearing Lyt 2 antigen block T cell-mediated cytolysis in the absence of complement. *J Immunol* 125:2665-2672.

61. Yelton, D. E., C. Desaymard, and M. D. Scharff. 1981. Use of monoclonal anti-mouse immunoglobulin to detect mouse antibodies. *Hybridoma* 1:5-11.

62. Kung, J. T., S. O. Sharrow, D. G. Sieckmann, R. Lieberman, and W. E. Paul. 1981. A mouse IgM allotypic determinant (Igh-6.5) recognized by a monoclonal rat antibody. *J Immunol* 127:873-876.

63. Fichtner, A. T., S. Anderson, M. G. Mage, S. O. Sharrow, C. A. Thomas, 3rd, and J. T. Kung. 1987. Subpopulations of mouse Lyt-2+ T cells defined by the expression of an Ly-6-linked antigen, B4B2. *J Immunol* 138:2024-2033.

64. Havran, W. L., M. Poenie, J. Kimura, R. Tsien, A. Weiss, and J. P. Allison. 1987. Expression and function of the CD3-antigen receptor on murine CD4+8+ thymocytes. *Nature* 330:170-173.

65. Gross, J. A., E. Callas, and J. P. Allison. 1992. Identification and distribution of the costimulatory receptor CD28 in the mouse. *J Immunol* 149:380-388.

66. Chen, Y. T., and J. T. Kung. 2005. CD1d-independent developmental acquisition of prompt IL-4 gene inducibility in thymus CD161(NK1)-CD44lowCD4+CD8- T cells is associated with complementarity determining region 3-diverse and biased Vbeta2/Vbeta7/Vbeta8/Valpha3.2 T cell receptor usage. *J Immunol* 175:6537-6550.

67. Mehal, W.Z., F. Azzaroli, and I.N. Crispe. 2001. Immunology of the healthy liver: old questions and new insights. Gastroenterology 120:250-260.

68. Fisher, R. 1922. On the Interpretation of χ2 from Contingency Tables, and the Calculation of P. *Journal of the Royal Statistical Society* 85:87-94.

69. Sallusto, F., D. Lenig, R. Forster, M. Lipp, and A. Lanzavecchia. 1999. Two subsets of memory T lymphocytes with distinct homing potentials and effector

functions. *Nature* 401:708-712.

70. Huleatt, J. W., I. Pilip, K. Kerksiek, and E. G. Pamer. 2001. Intestinal and splenic T cell responses to enteric Listeria monocytogenes infection: distinct repertoires of responding CD8 T lymphocytes. *J Immunol* 166:4065-4073.

71. Heintzelman, D. L., R. Lotan, and R. R. Richards-Kortum. 2000. Characterization of the autofluorescence of polymorphonuclear leukocytes, mononuclear leukocytes and cervical epithelial cancer cells for improved spectroscopic discrimination of inflammation from dysplasia. *Photochemistry and photobiology* 71:327-332.

72. Golden-Mason, L., A. M. Kelly, D. G. Doherty, O. Traynor, G. McEntee, J. Kelly, J. E. Hegarty, and C. O'Farrelly. 2004. Hepatic interleuklin 15 (IL-15) expression: implications for local NK/NKT cell homeostasis and development. *Clinical and experimental immunology* 138:94-101.

73. Suzuki, A., S. McCall, S. S. Choi, J. K. Sicklick, J. Huang, Y. Qi, M. Zdanowicz, T. Camp, Y. X. Li, and A. M. Diehl. 2006. Interleukin-15 increases hepatic regenerative activity. *Journal of hepatology* 45:410-418.

74. Casini, A., E. Ceni, R. Salzano, P. Biondi, M. Parola, A. Galli, M. Foschi, A. Caligiuri, M. Pinzani, and C. Surrenti. 1997. Neutrophil-derived superoxide anion induces lipid peroxidation and stimulates collagen synthesis in human hepatic stellate cells: role of nitric oxide. *Hepatology* 25:361-367.

75. Correia, M. P., E. M. Cardoso, C. F. Pereira, R. Neves, M. Uhrberg, and F. A. Arosa. 2009. Hepatocytes and IL-15: a favorable microenvironment for T cell survival and CD8+ T cell differentiation. *J Immunol* 182:6149-6159.

76. Geissmann, F., T. O. Cameron, S. Sidobre, N. Manlongat, M. Kronenberg, M. J. Briskin, M. L. Dustin, and D. R. Littman. 2005. Intravascular immune surveillance by CXCR6+ NKT cells patrolling liver sinusoids. *PLoS biology* 3:e113.

77. Knolle, P., J. Schlaak, A. Uhrig, P. Kempf, K. H. Meyer zum Buschenfelde, and G. Gerken. 1995. Human Kupffer cells secrete IL-10 in response to lipopolysaccharide (LPS) challenge. *Journal of hepatology* 22:226-229.

78. Brooks, D. G., M. J. Trifilo, K. H. Edelmann, L. Teyton, D. B. McGavern, and M. B. Oldstone. 2006. Interleukin-10 determines viral clearance or persistence in vivo. *Nat Med* 12:1301-1309.

79. Correia, M. P., A. V. Costa, M. Uhrberg, E. M. Cardoso, and F. A. Arosa. 2010. IL-15 induces CD8+ T cells to acquire functional NK receptors capable of modulating cytotoxicity and cytokine secretion. *Immunobiology*.

80. Tough, D. F., S. Sun, X. Zhang, and J. Sprent. 2000. Stimulation of memory T cells by cytokines. *Vaccine* 18:1642-1648.

81. Jung, T. M., W. M. Gallatin, I. L. Weissman, and M. O. Dailey. 1988. Down-regulation of homing receptors after T cell activation. *J Immunol*

141:4110-4117.

82. Tough, D. F., P. Borrow, and J. Sprent. 1996. Induction of bystander T cell proliferation by viruses and type I interferon in vivo. *Science* 272:1947-1950.

83. Tough, D. F., S. Sun, and J. Sprent. 1997. T cell stimulation in vivo by lipopolysaccharide (LPS). *J Exp Med* 185:2089-2094.

84. Crispe, I. N., T. Dao, K. Klugewitz, W. Z. Mehal, and D. P. Metz. 2000. The liver as a site of T-cell apoptosis: graveyard, or killing field? *Immunol Rev* 174:47-62.

85. Huang, L., K. Sye, and I. N. Crispe. 1994. Proliferation and apoptosis of B220+CD4-CD8-TCR alpha beta intermediate T cells in the liver of normal adult mice: implication for lpr pathogenesis. *Int Immunol* 6:533-540.

86. Unsoeld, H., S. Krautwald, D. Voehringer, U. Kunzendorf, and H. Pircher. 2002. Cutting edge: CCR7+ and CCR7- memory T cells do not differ in immediate effector cell function. *J Immunol* 169:638-641.

87. Dikopoulos, N., I. Jomantaite, R. Schirmbeck, and J. Reimann. 2003. Specific, functional effector/memory CD8+ T cells are found in the liver post-vaccination. *Journal of hepatology* 39:910-917.

88. Marshall, D. R., S. J. Turner, G. T. Belz, S. Wingo, S. Andreansky, M. Y. Sangster, J. M. Riberdy, T. Liu, M. Tan, and P. C. Doherty. 2001. Measuring the diaspora for virus-specific CD8+ T cells. *Proc Natl Acad Sci U S A* 98:6313-6318.

89. Grayson, J. M., A. J. Zajac, J. D. Altman, and R. Ahmed. 2000. Cutting edge: increased expression of Bcl-2 in antigen-specific memory CD8+ T cells. *J Immunol* 164:3950-3954.

90. Wang, X. Z., S. E. Stepp, M. A. Brehm, H. D. Chen, L. K. Selin, and R. M. Welsh. 2003. Virus-specific CD8 T cells in peripheral tissues are more resistant to apoptosis than those in lymphoid organs. *Immunity* 18:631-642.
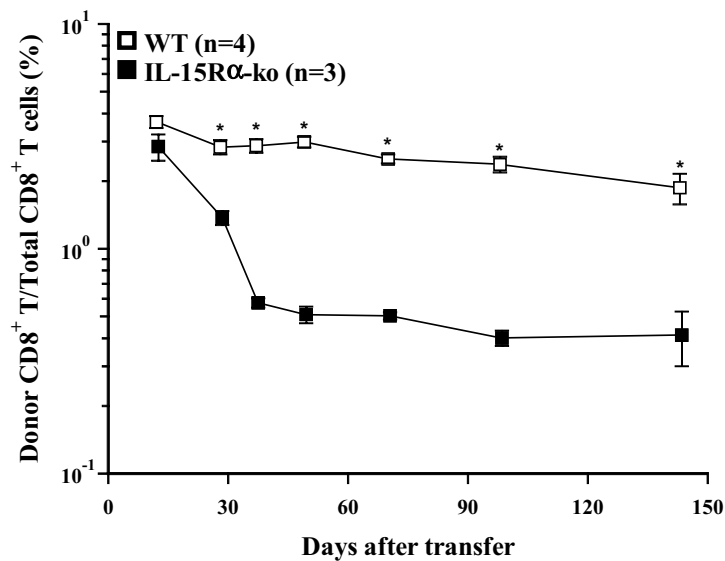
Figures

Figure 1. Long-term survival of Ag+IL-4-activated CD8$^+$ T cells depends on host IL-15Rα expression.   Ag+IL-4-activated 2C CD8$^+$ T cells (4×10^6) were adoptively transferred into each of 4 WT (☐) and 3 IL-15Rα-ko (■) hosts. PBL were obtained at indicated time points and stained with PE-anti-CD8 and Cy5-anti-2C TCR (1B2) mAbs. The ratios (means±SEM) of donor CD8$^+$ T to total CD8$^+$ T cells were determined. *, significant differences between the WT and IL-15Rα-ko groups at each time point (p<0.01). Results of one of two experiments are shown.
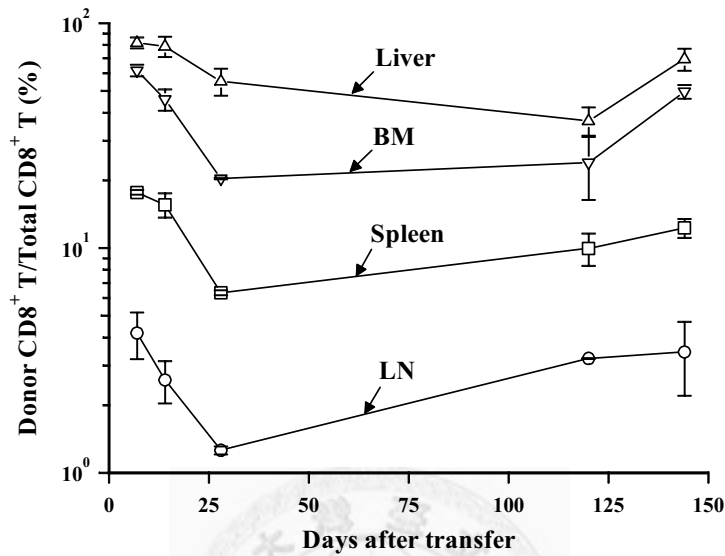
Figure 2. Large numbers of adoptively transferred Ag+IL-4-activated CD8^{+} T cells are found in the liver. Naive CD8^{+}Thy-1.2^{+} T cells from 2C tg mice were stimulated with Ag+IL-4 and adoptively transferred into a group of 10 congenic Thy-1.2^{−} B10.*TL* mice (8x10^{6} cells per host). Single cell suspensions were made from the liver (△), BM (▽), spleen (□), and LN (○) of the recipient mice at indicated time points after transfer, and stained with PE-anti-CD8 and Cy5-anti-Thy-1.2 mAbs. The ratios (means±SEM) of donor CD8^{+} T to total CD8^{+} T cells were determined. For each indicated time points, data from two mice were averaged. Results of one of two experiments are shown.
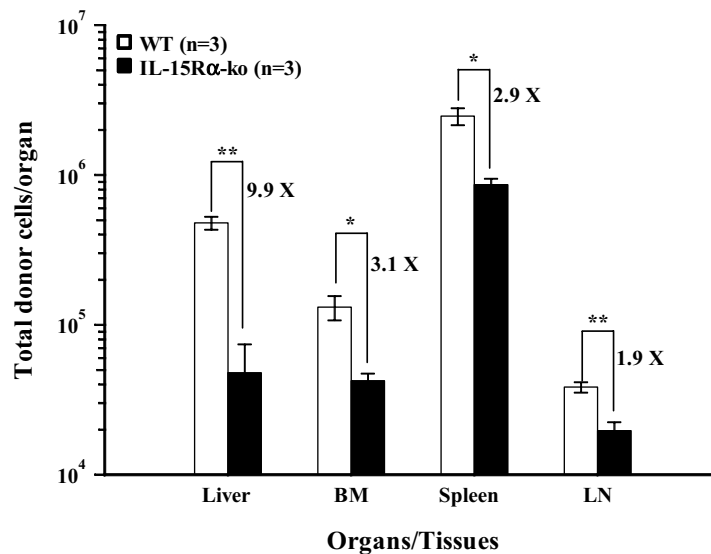
Figure 3. Deficient survival of Ag+IL-4-activated CD8$^+$ T cells in IL-15Rα-ko mice. Ag+IL-4-activated 2C CD8$^+$ T cells were adoptively transferred into WT (□) or IL-15Rα-ko (■) recipient mice as Figure 1 (8×10^6 per mouse). Single cell suspensions from the spleen, BM, LN and liver were prepared from host mice on day 28 after adoptive transfer and stained by A680-anti-CD8 and Cy5-anti-2C TCR mAbs. The frequency of donor CD8$^+$ T cells in total CD8$^+$ T cells were then determined. Total cell numbers of donor cells in each organ are estimated and shown. Numbers on the top of bars indicate the ratios of total donor cells in WT over IL-15R-ko hosts for indicated organs. There were 3 mice per group. Results of one of two experiments are shown. *, significant differences between the WT and IL-15Rα-ko groups ($p<0.05$). **, very significant differences between the WT and IL-15Rα-ko groups ($p<0.01$).
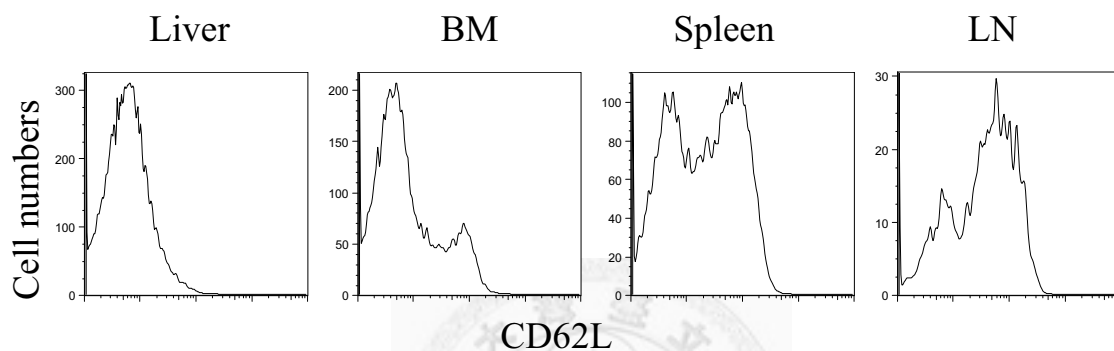
Figure 4. CD62L expression of the Ag+IL-4-activated memory CD8^{+} T cell in different organs. Ag+IL-4-activated 2C memory CD8^{+} T cells were adoptively transferred into B10.*TL* host mice (8×10^6 cells per host). Single cell suspensions from the host spleen, BM, LN, and liver were obtained on day 90 after adoptive transfer and stained with FITC-anti-CD62L, PE-anti-CD8, and Cy5-anti-2C TCR mAbs. CD62L expression of 2C CD8^{+} T cells are shown in histograms. Results of one of more than three experiments are shown.
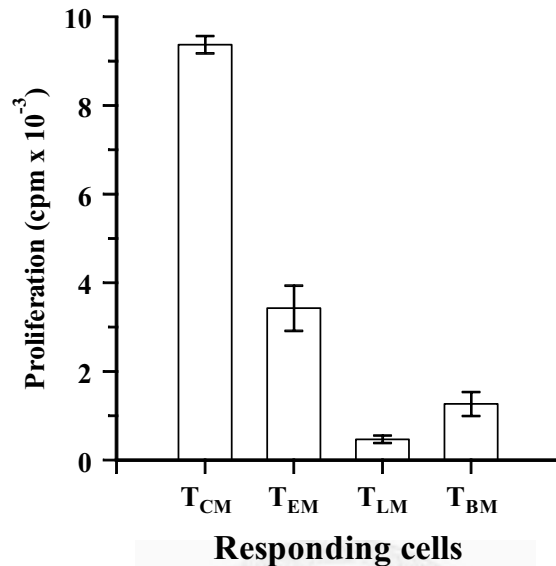
Figure 5. TCR-induced proliferation of T_{LM} cells is highly deficient and is lower than the proliferation responses of T_{CM} and T_{EM} cells. 2C memory CD8+ T cells (1.6×10^7) generated by Ag+IL-4-activation were adoptively transferred into B6.*TL* recipients. Single cell suspensions from indicated host organs were obtained on day 70 after adoptive transfer and stained with FITC-anti-CD62L, Cy5-anti-Thy-1.2, and TR-anti-CD8 mAbs. The indicated subsets of donor memory 2C CD8+ T cells were sorted out and activated in duplicates by plate-bound anti-CD3+anti-CD28 mAbs for 24 h and their proliferative ability was assessed by a 6-h thymidine pulse. Results of one of two experiments are shown. T_{EM}, spleen CD62L^low^Thy-1.2+CD8+ cells; T_{CM}, spleen CD62L^hi^Thy-1.2+CD8+ cells; T_{LM}, liver CD62L^low^Thy-1.2+CD8+ cells; T_{BM}, BM CD62L^low^Thy-1.2+CD8+ cells.
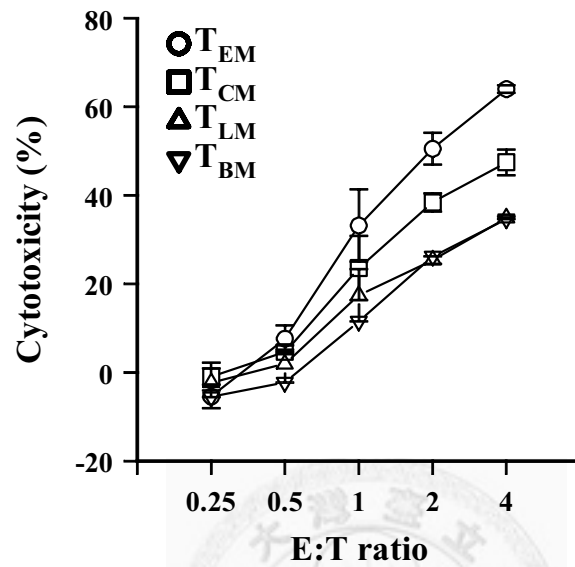
Figure 6. **Cytolytic ability of T$_{LM}$ cells is lower than T$_{CM}$ and T$_{EM}$ cells.** 2C memory CD8$^+$ T cells (1.6×10^7) generated by Ag+IL-4-activation were adoptively transferred into B6.*TL* recipients. Single cell suspensions from indicated host organs were obtained on day 70 after adoptive transfer and stained with FITC-anti-CD62L, Cy5-anti-Thy-1.2, and TR-anti-CD8 mAbs. The indicated subsets of donor memory 2C CD8$^+$ T cells were sorted out and their CTL activity was assayed in duplicates at different effector-to-target cell ratios, using L^d-bearing P815 cells as targets. Results of one of two experiments are shown.
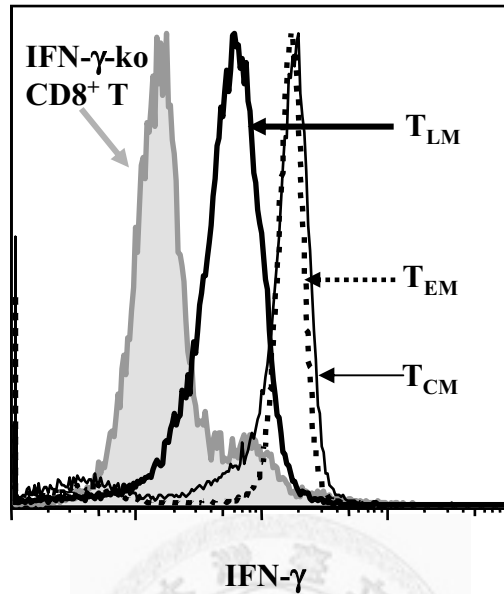
Figure 7. **T_{LM} cells express lower IFN-γ than T_{CM} and T_{EM} cells after TCR-stimulation.** 2C memory CD8^{+} T cells (1.6×10^{7}) generated by Ag+IL-4-activation were adoptively transferred into B6.*TL* recipients. Single cell suspensions were prepared from the liver, and spleen and different subsets of Thy-1.2^{+}CD8^{+} T cells were sorted out on day 60 after the adoptive transfer. Naïve spleen CD8^{+} T cells (CD8^{+}CD44^{low}) were sorted out from IFN-γ-ko mice were used as a negative control. CD8^{+} T cells were activated by plate-bound anti-CD3+anti-CD28 mAbs for 9 h, and subjected to intracellular staining with Cy5-anti-IFN-γ mAb. Intracellular IFN-γ signals of naïve splenic IFN-γ-ko CD8^{+} T cells (grey shallow), T_{LM} (thick line), T_{CM} (thin line), and T_{EM} (dashed line) are shown. Results of one of two experiments are shown.
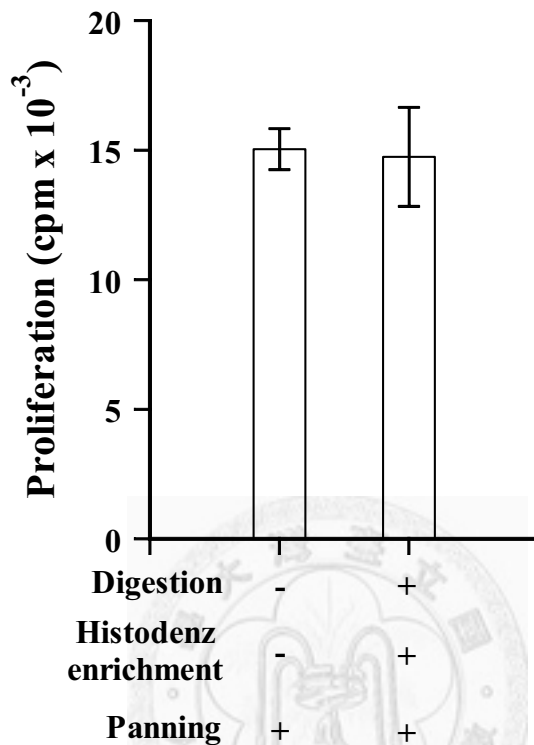
Figure 8. CD8^{+} T cells are not damaged by the isolation procedure of intrahepatic lymphocytes. Spleen cells obtained from B6 mice were obtained through a routine isolation procedure or through the procedure (collagenase digestion, Histodenz centrifugation) used to isolate liver lymphocytes. CD8^{+} T cells were then enriched by panning of total or collagenase-treated, Histodenz-enriched spleen cells. Enriched spleen CD8^{+} T cell subsets were activated in wells coated with 10 μg/ml anti-CD3+anti-CD28 for 24 h as described in *Materials and Methods*. No significant differences were found between different treated spleen CD8^{+} T cells.
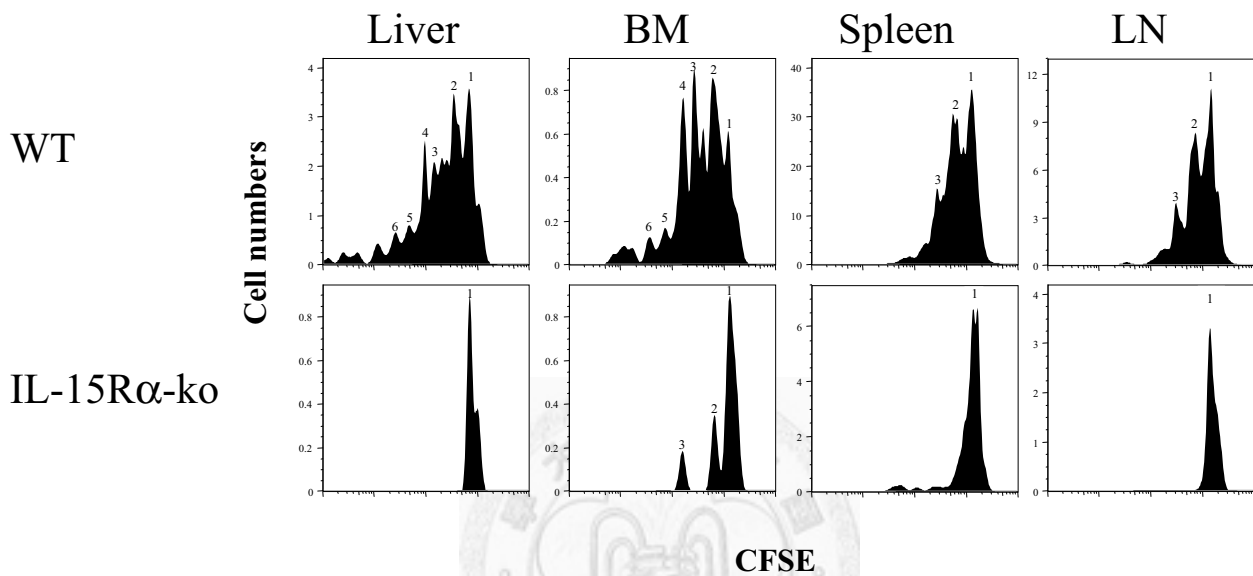
Figure 9. Host IL-15Rα expression is required for the proliferation of Ag+IL-4-activated memory CD8⁺ T cells. Ag+IL-4-activated 2C CD8⁺ T cells were adoptively transferred into B6.*TL* host mice (8×10⁶/mouse). On day 7 after transfer, spleen CD8⁺ T cells were enriched, labeled with CFSE and then adoptively transferred to a second host mouse. On day 28 after re-transfer, single cell suspensions of the indicated organs from the WT and IL-15Rα-ko hosts were stained with PE-anti-CD8, and Cy5-anti-2C TCR (1B2) mAbs. Number of cell divisions are shown on the top of the histogram. Results of one of two experiments are shown.
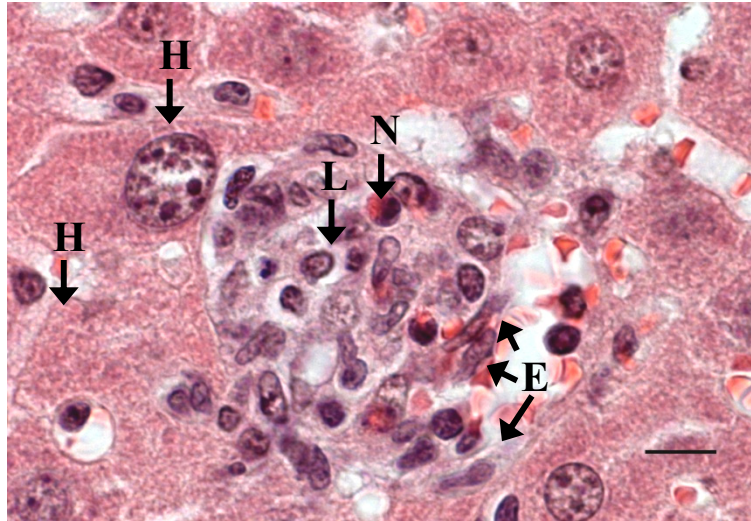
Figure 10. Ag+IL-4-activated CD8$^+$ T cells form clusters in the liver: H&E stain.
Ag+IL-4-activated 2C CD8$^+$ T cells (Thy-1.2$^+$; 8×10^6) were adoptively transferred into
B10.*TL* recipients. Livers were harvested from the recipients on day 7 after transfer and
subjected to H&E staining. One representative cell cluster is shown (scale bar, 10 µm).
The cell cluster is composed of active mononuclear lymphoid cells (L) and neutrophils (N)
and surrounded by hepatocytes (H) and sinusoid endothelial cells (E). Three host mice per
group were included in each experiment. One of more than two experiments are shown.
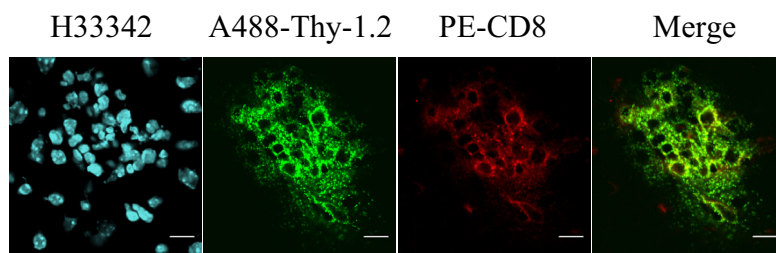
| H33342 | A488-Thy-1.2 | PE-CD8 | Merge |

Figure 11. Ag+IL-4-activated CD8^{+} T cells form clusters in the liver: immunofluorescent stain. Ag+IL-4-activated 2C CD8^{+} T cells (Thy-1.2^{+}; 8×10^6) were adoptively transferred into B10.*TL* recipients. Livers were harvested from the recipients on day 7 after transfer. Cryosections were stained with A488-anti-Thy-1.2 and PE-anti-CD8 mAbs (scale bar, 10 µm). Three host mice per group were included in each experiment. One of more than two experiments is shown.
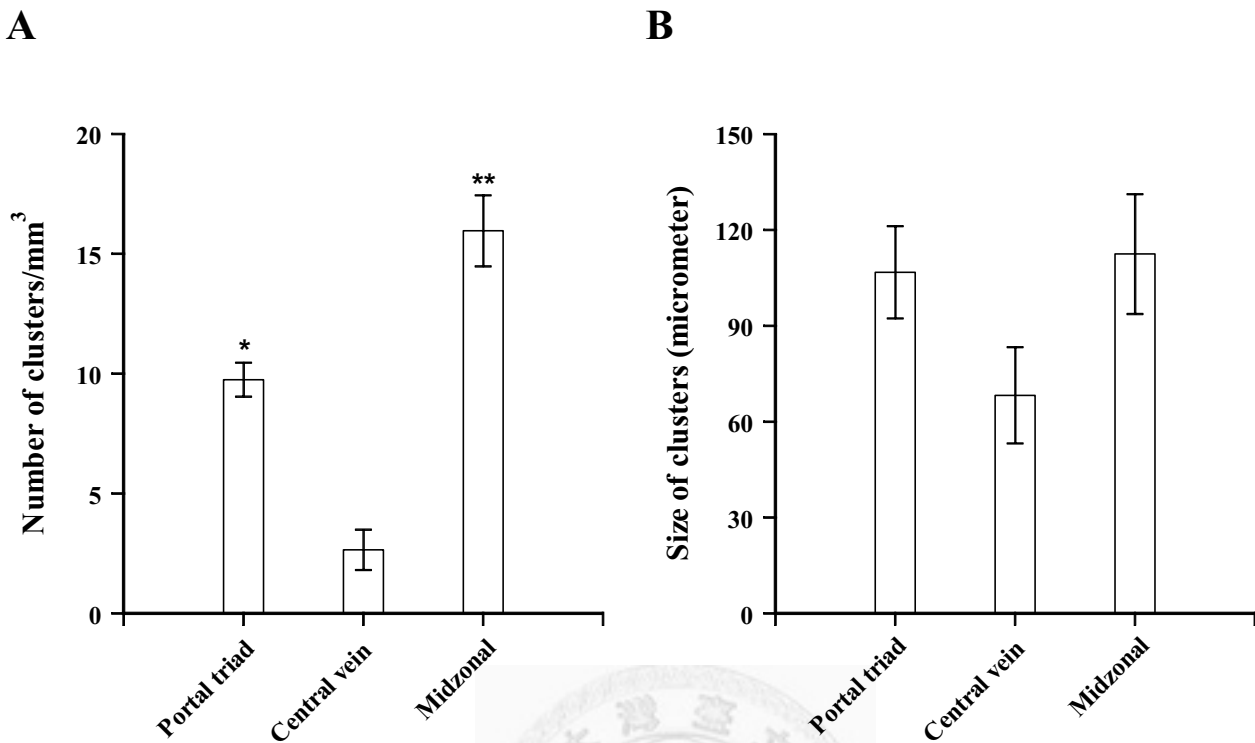
Figure 12. The distribution and size of the memory CD8+ T cell clusters. Ag+IL-4-activated 2C CD8+ T cells (8x10^6) were adoptively transferred into B6 hosts. On day 60 after adoptive transfer, host liver sections were subjected to CD8 immunohistochemical staining. The frequency of the cell clusters and the number of donor cells in the cell clusters were analyzed as described in the *Materials and Methods*. The size (means±SEM) of the cell cluster was determined by averaging of long axis & short axis. The frequency (A) and size (B) of CD8+ T cell clusters located in portal triad, central vein, and midzonal regions are shown in bar plots (means±SEM). *, significant difference between the centrilobular and portal groups (p=0.013). **,significant difference between the centrilobular and midozonal groups (p=0.008). The values shown were derived from triplicates.
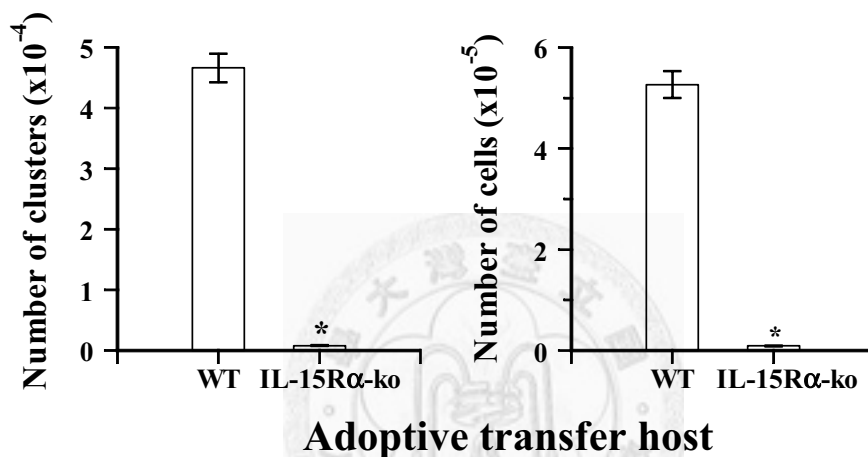
A

B

Adoptive transfer host
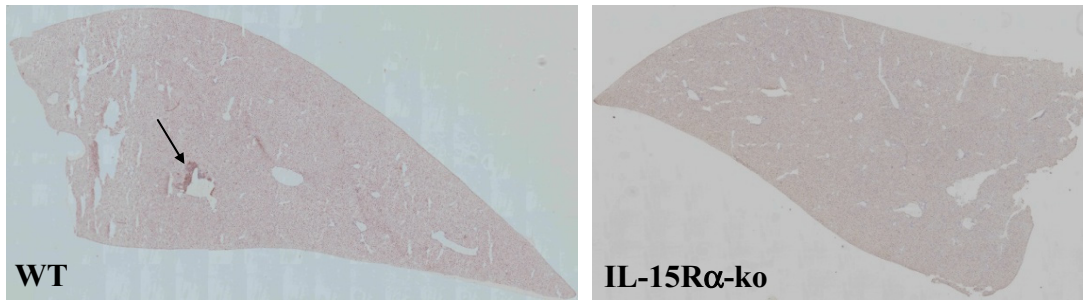
Figure 13. Ag+IL-4-activated CD8$^+$ T cells do not form cell clusters in the IL-15Rα-ko liver. Ag+IL-4-activated 2C CD8$^+$ T cells were adoptively transferred into WT (B6) and IL-15Rα-ko hosts (8×10^6). On day 120 after adoptive transfer, host liver sections were stained with rat anti-CD8 mAb, followed by HRP-anti-rat IgG. DAB was used for color development. A. CD8$^+$ T cell clusters (marked by an arrow) were found in WT host liver sections. B. The frequency of the cell cluster and the donor cell numbers in the cell clusters were analyzed as described in the *Materials and Methods*. *, no cell cluster was found in any of the IL-15Rα-ko livers examined. The average volume of the IL-15Rα-ko livers examined was 1.92 mm^3/liver $\times$ 3 livers. The data shown were derived from the averages of 3 WT and 3 IL-15Rα-ko hosts.

A

B
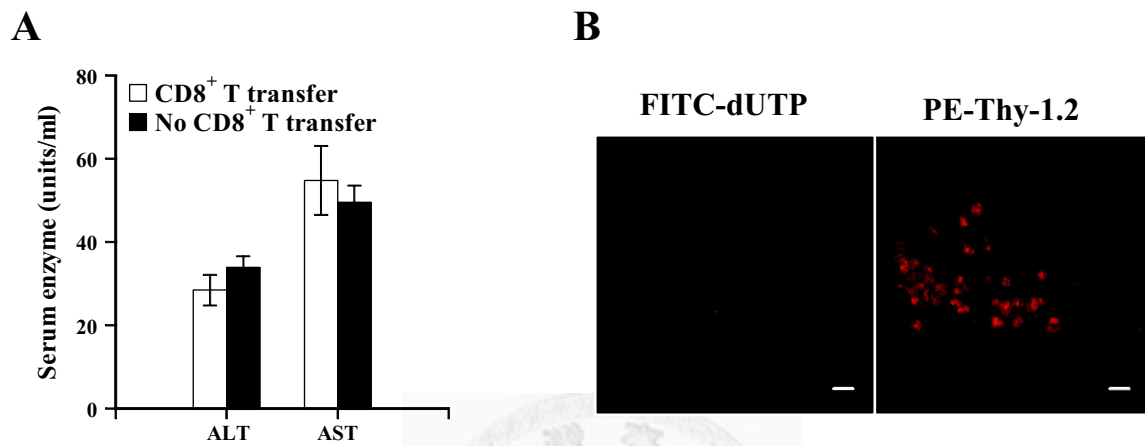
Figure 14. **Ag+IL-4-activated memory CD8⁺ T cells do not damage or undergo apoptosis in the liver.** A. Serum aspartate aminotransferase (AST) and alanine aminotransferase (ALT) were determined from groups of 5 host mice that received adoptive transfer 7 days previously (8×10^6; open symbols) and control mice (no adoptive transfer, solid symbols). B. On day 14 after adoptive transfer, host liver sections were stained by PE-anti-Thy-1.2 (red) and FITC-dUTP (green) to detect donor and apoptotic cells, respectively (scale bar, 10 µm).

A. day 7

B. day 60

Spleen

Liver

Vβ5+=47.1%
Vβ8+=52.3%

Vβ5+=47.3%
Vβ8+=47.2%

Spleen

Liver

Vβ5+=37.6%
Vβ8+=56.6%

Vβ5+=33.6%
Vβ8+=50.9%

Vβ8 (y-axis), Vβ5 (x-axis)
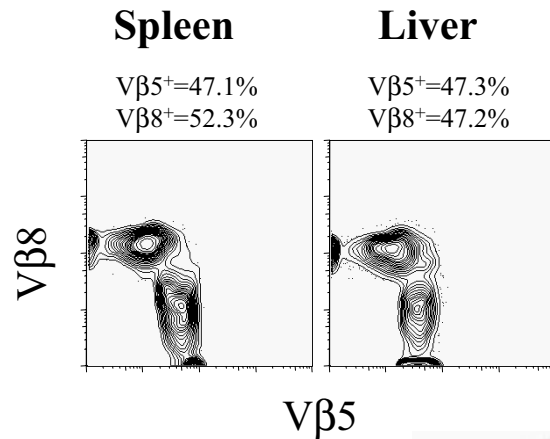
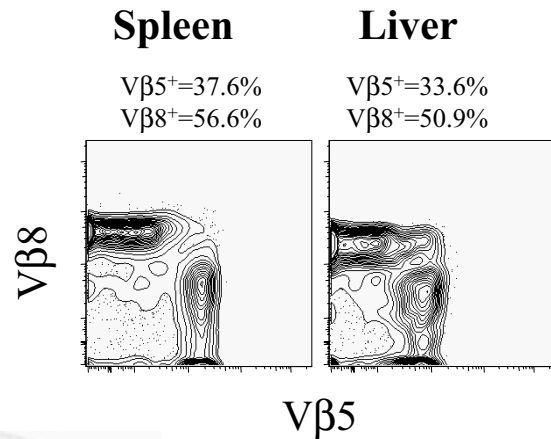**Figure 15. Vβ5+ and Vβ8+ CD8+ T cells activated by TCR+IL-4 are equally able to undergo homeostatic expansion.** TCR Vβ5+ and Vβ8+ B10 CD8+ T cells were activated *in vitro* by anti-CD3/CD28 presented by LPS-activated B blasts and exogenous IL-4. Equal numbers (4x10^6 each) of the TCR+IL-4-activated Vβ5+ and Vβ8+ CD8+ T cells were mixed and adoptively transferred into B10.*TL* host mice. The hosts were sacrificed on day 7 (A) and day 60 (B) after adoptive transfer. Single cell suspension from spleens and livers were stained with A488-anti-TCR Vβ5, PE-anti-Thy-1.2, A647-anti-TCR Vβ8, and A680-anti-CD8 mAbs. The contours show the TCR usages by the Thy-1.2+CD8+ donor cells and the percentages of specific Vβ usage in total donor CD8+ T cells are also shown. All experimental groups were performed in duplicates. Results of one of two experiments are shown.

A

	PE-Thy-1.2	A488-Vβ5	A647-Vβ8	Merge
#1				
#2				

B

Vβ8

	−	+
+	6	1
−	0	6
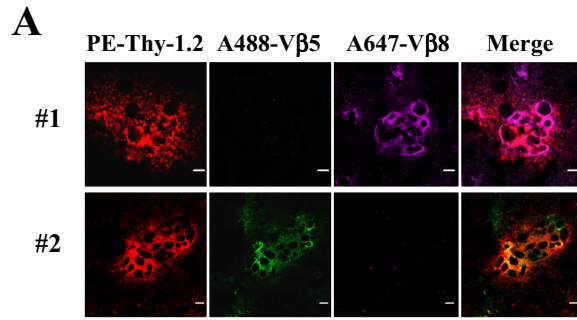
Vβ5

Figure 16. Clonal expansion of adoptively transferred TCR+IL-4-activated CD8+ T cells in the liver: day 7 after transfer. Equal numbers (4×10^6 each) of the TCR+IL-4-activated Vβ5+ and Vβ8+ CD8+ T cells were mixed and adoptively transferred into B10.*TL* host mice. A. Host liver sections obtained from 7 days post-adoptive transfer hosts were stained with A488-anti-Vβ5, PE-anti-Thy-1.2 and A647-anti-Vβ8 mAbs. Confocal images of two representative clones (labeled #1 and #2) show either Vβ8+ or Vβ5+ cells, but not mixed cells (scale bar, 5 μm). B. Of the 13 donor clusters found in day 7 adoptive host liver sections, 6 contained Vβ8+, but no Vβ5+ cells, 6 contained Vβ5+, but no Vβ8+ cells, while one contained mixed Vβ8+ and Vβ5+ cells. Results of one of two experiments are shown.

A

B
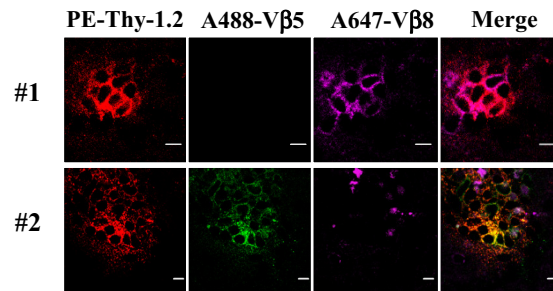
Figure 17. Clonal expansion of adoptively transferred TCR+IL-4-activated CD8^{+} T cells in the liver: day 60 after transfer. Equal numbers (4x10^{6} each) of the TCR+IL-4-activated Vβ5^{+} and Vβ8^{+} CD8^{+} T cells were mixed and adoptively transferred into B10.*TL* host mice.   A. Host liver sections obtained from 60 days post-adoptive transfer hosts were stained with A488-anti-Vβ5, PE-anti-Thy-1.2 and A647-anti-Vβ8 mAbs. Confocal images of two representative clones (labeled #1 and #2) show either Vβ8[+] or Vβ5^{+} cells, but not mixed cells (scale bar, 5 μm). B. Of the 20 donor clusters found in d60 adoptive host liver sections, 10 contained Vβ8[+], but no Vβ5^{+} cells and the other 10 contained Vβ5[+], but no Vβ8^{+} cells. Results of one of two experiments are shown.
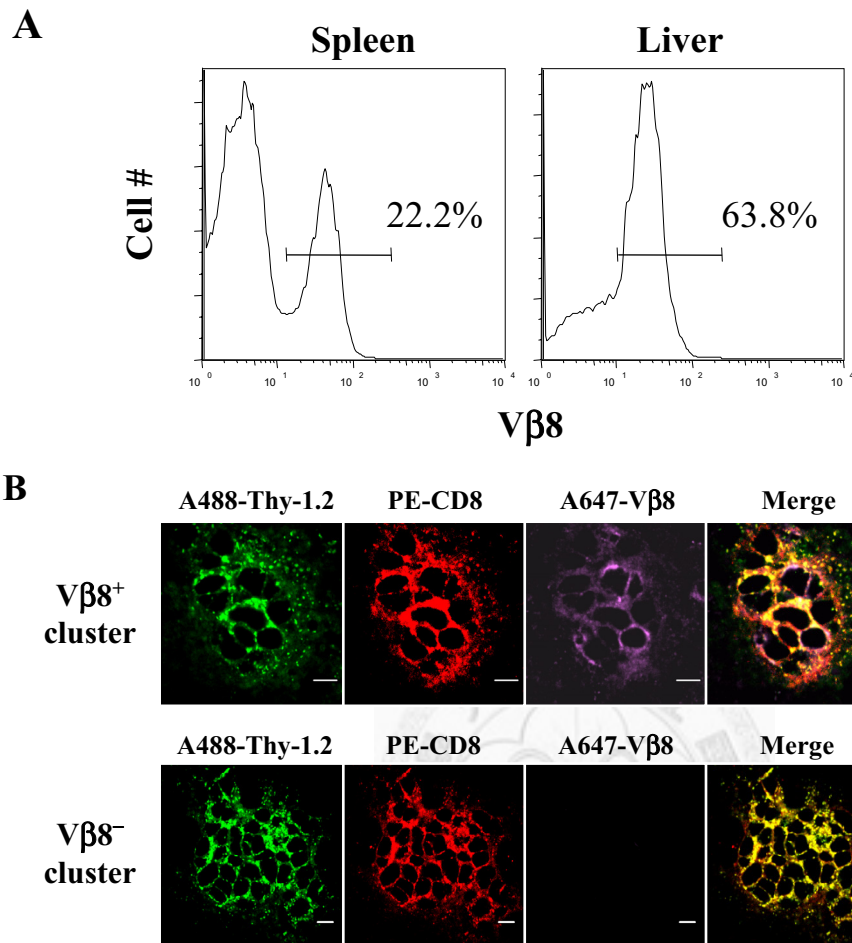
Figure 18. Clonal expansion of CD8+ T cell in the liver of *Listeria monocytogenes (Lm)*-immune mice. B6 mice were intravenously immunized with a sub-lethal dose (6×10^3 CFU) *Listeria monocytogenes (Lm)* 5334, a clinical isolate from the National Taiwan University Hospital. A. Spleen cells and intrahepatic lymphocytes were obtained from *Lm*-immune B6 mice on day 60 post-*Lm* exposure and stained with PE-anti-CD8 and Cy5-anti-Vβ8. Histograms of Vβ8 expression (% positive cells as indicated) are shown. CD8+ T cells among intrahepatic lymphocyte show biased (elevated) usage of Vβ8. B. Liver sections from day 60 post-*Lm* exposure mice were stained with A488-anti-Thy-1.2, PE-anti-CD8, and A647-anti-Vβ8. One representative each of Vβ8+ (top row) and Vβ8− (lower row) clusters are shown (scale bar, 5 μm). Of the total of 12 CD8+ clusters examined, six each were Vβ8+ and Vβ8−.
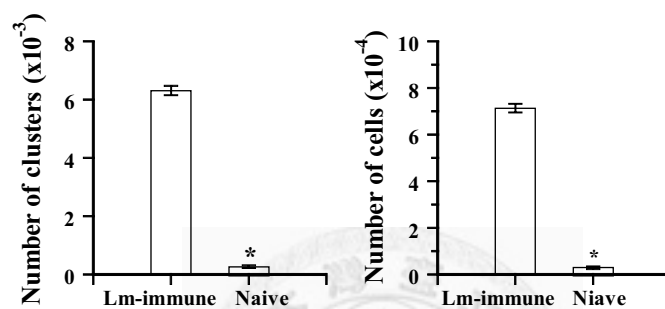
Figure 19. Increased CD8⁺ T cell clusters in the liver of *Lm*-immune than naïve control mice. B6 mice were intravenously immunized with a sub-lethal dose (6×10^3 CFU) *Listeria monocytogenes* (*Lm*) 5334, a clinical isolate from the National Taiwan University Hospital. The frequency of the cell cluster (Left panel) and the donor cell numbers in the cell clusters (Right panel) were analyzed as described in the *Materials and Methods*. *p<0.01. The average volume of the naïve and *Lm*-immune livers examined was 0.7 mm³/liver and 1.3 mm³/liver, respectively. There were 3 mice per experimental group.
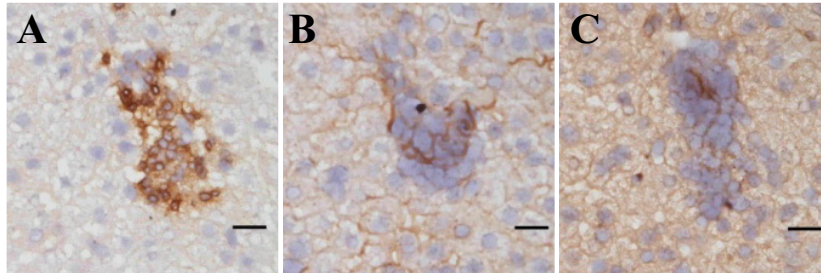
Figure 20. Close physical association of IL-15$^+$ and IL-15R$^+$ dendrite-like processes with CD8$^+$ T$_{LM}$ clusters.   Ag+IL-4-activated 2C CD8$^+$ T cells were adoptively transferred into B6.*TL* recipients (1.6×10^7). Livers were collected from the recipient mice for cryosection on day 7 after transfer, and cut into 8 μm serial sections. The three serial sections were individually stained with rat anti-Thy-1.2 (A), goat anti-mIL-15 (B), and goat anti-mIL-15Rα (C) Abs, and respective secondary antibodies. DAB was used for color development. Serial sections of one representative CD8$^+$ T cell cluster of total 13 cell clusters are shown (scale bar, 20 μm).
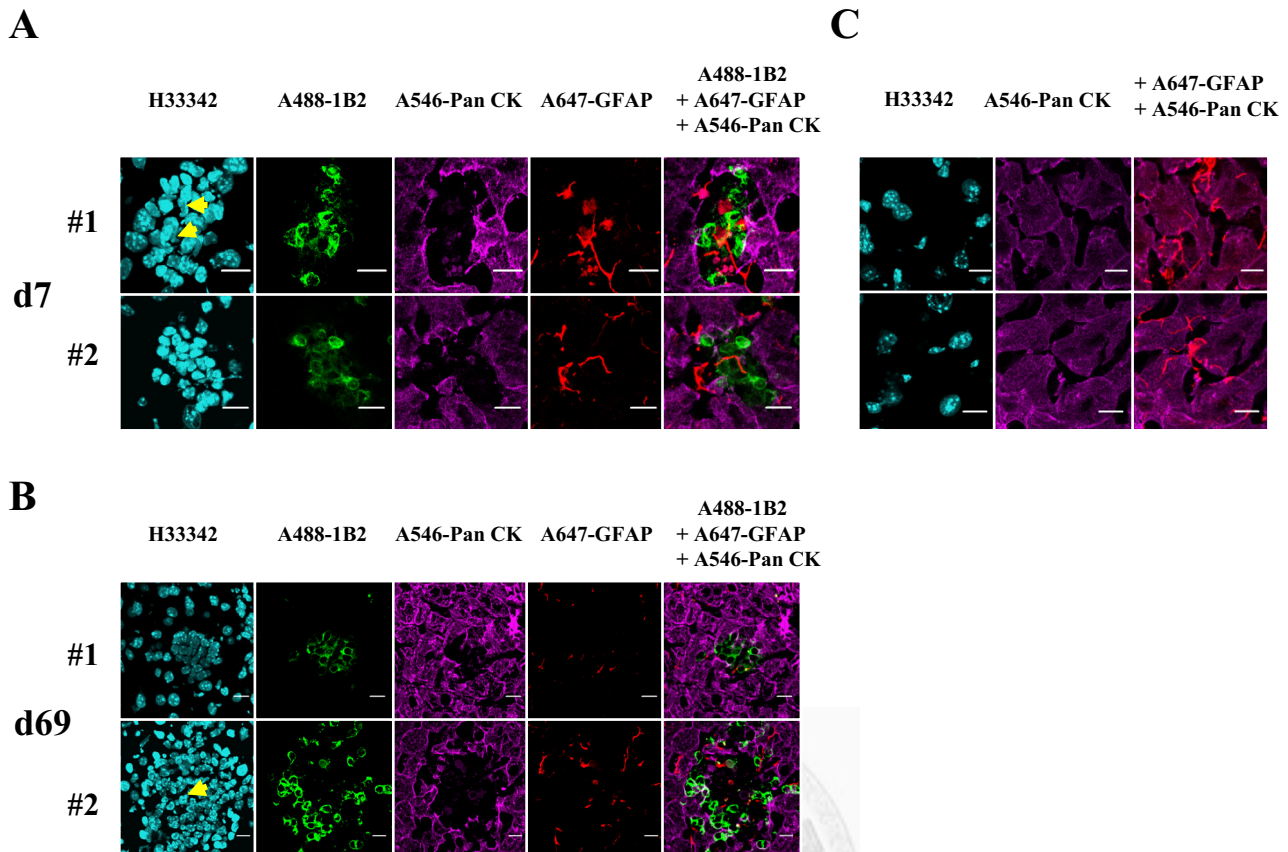
Figure 21. Close physical association of hepatic stellate cells with T_{LM} clusters. Liver cryosections (8 µm thickness) from B6 host mice that had received Ag+IL-4-activated 2C CD8^{+} T cells (1.6×10^7) 7 days (A) and 69 days (B) previously were subjected to immunofluorescent staining. Liver sections were stained with A488-anti-2C TCR (1B2; green), A647-anti-GFAP (red) and A546-anti-pan cytokeratin (pan CK; rose). Confocal images of two representative memory CD8^{+} T cell clusters at each time point clearly are shown (scale bar, 10 µm). In some 1B2^{+} cell clusters, segmental nuclear cells (yellow arrows) are detected, implying involvement of neutrophils. Three repeats per time point were included in each group. C. Two representative images show the distribution of GFAP[+] HSC in the non-cluster fields (scale bar, 10 µm).
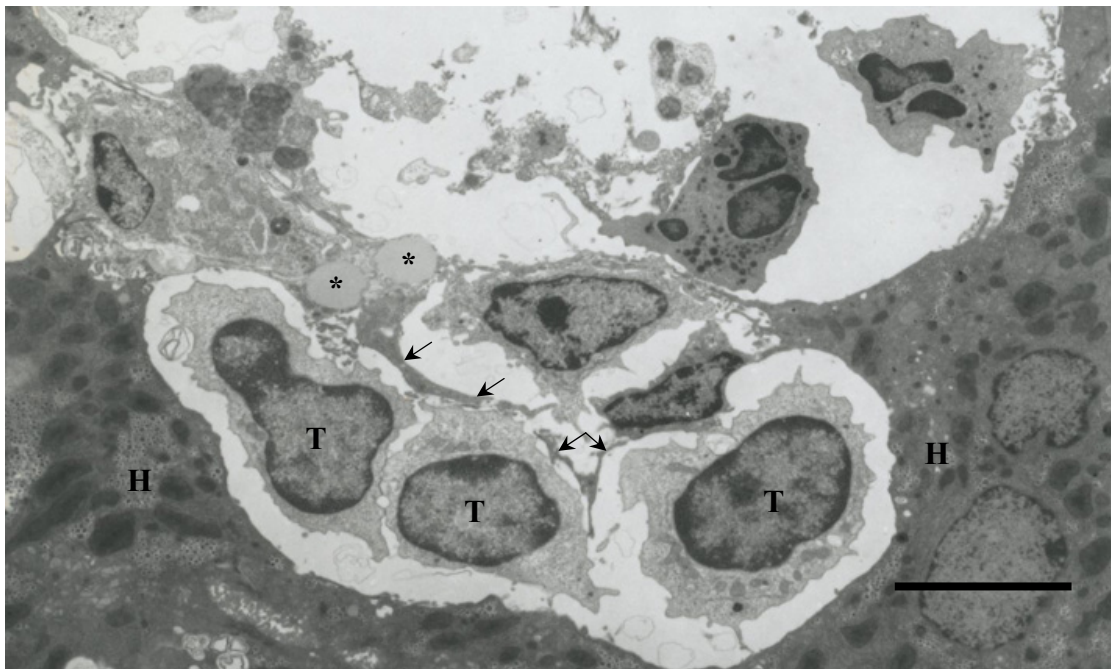
Figure 22. T cell clusters closely contact to the dendrite-like cytoplasmic processes in the space of Disse by ultrastructural observation. Electron micrograph of a lymphocyte cluster in the liver of a B10.*TL* recipients 7 days after receiving 8×10^6 Ag+IL-4-activated 2C CD8$^+$ T cells are shown (scale bar, 5 μm). The identity of cells and organelles are marked as follows: T lymphocytes, "T"; hepatocytes, "H"; lipid droplets, *; dendrite-like cytoplasmic processes, arrows.
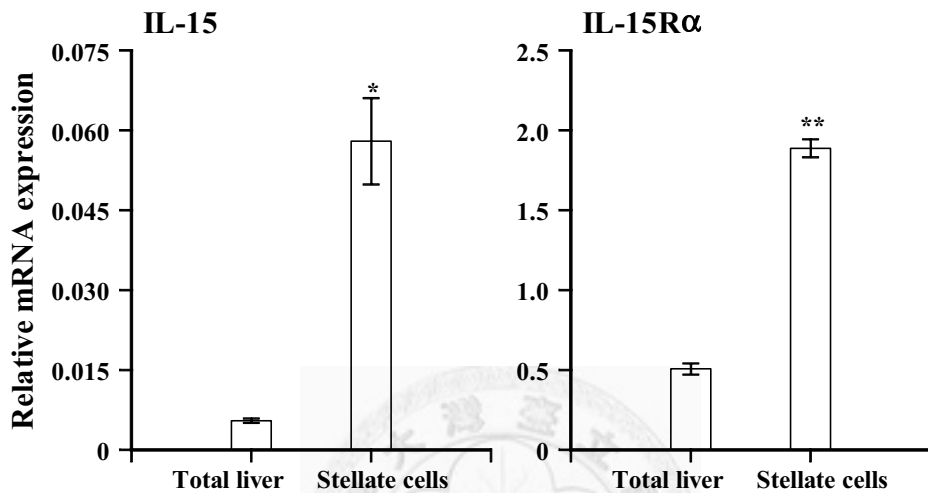
Figure 23. IL-15 and IL-15Rα gene expression by hepatic stellate cells. FSC^{low}SSC^{hi} HSC were sorted from single cell suspensions of naïve B6 mice. RNA samples from total liver and sorted HSC (stellate cells) were analyzed for IL-15 and IL-15Rα gene expression by real-time RT-PCR, and normalized by GAPDH gene expression. *, significant difference between the HSC and total liver (p=0.003). **,very significant difference between the HSC and total liver (p=0.00003). Triplicates were performed for all experimental groups.
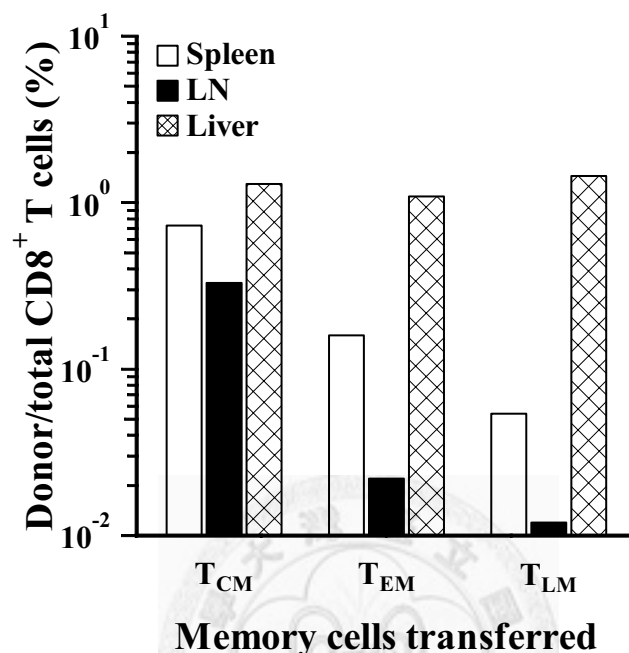
Figure 24.   Homing pattern of T_{LM} cells. 2C memory CD8^{+} T cells were generated by Ag+IL-4-activation and adoptively transferred into B6 hosts (1.6×10^7).   Single cell suspensions from the host spleen and liver were obtained on day 60 after adoptive transfer and stained with FITC-anti-CD62L, Cy5-anti-2C TCR and TR-anti-CD8 mAbs. The donor 2C memory CD8^{+} T cell subsets were then sorted out, and then adoptively transferred to a second set of host mice, B6.*TL* (3×10^5 /mouse).   These host mice were sacrificed 14 days post-adoptive re-transfer. Single cell suspensions from indicated organs were obtained and stained with FITC-anti-CD62L, A405-anti-CD8, and Cy5-anti-Thy-1.2 mAbs.   The ratios of donor cells to total CD8^{+} T cells from the host spleen (blank), mesenteric LN (black), and liver (cross) were estimated.   Results of one of two experiments are shown.
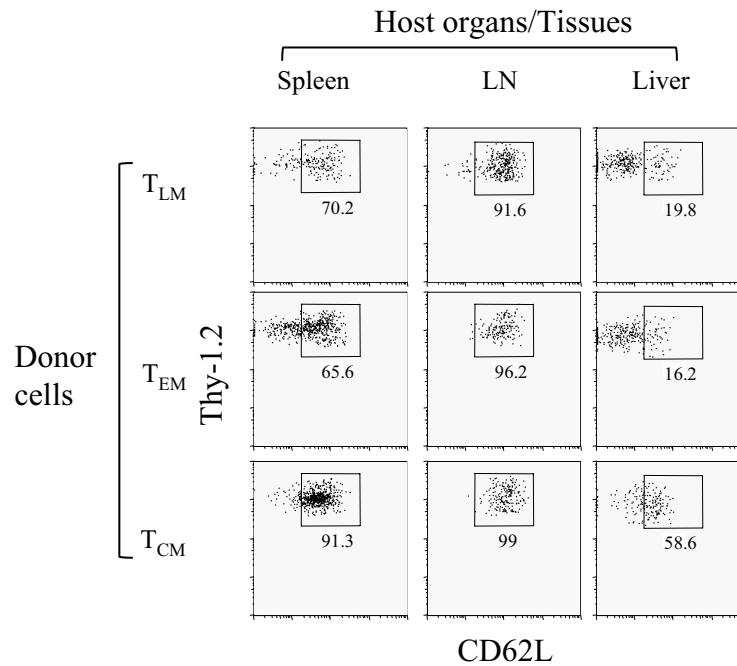
Figure 25. CD62L expression of different subsets of donor memory CD8$^+$ T cells in the liver, spleen and LN. Adoptive transfer of T_{LM}, T_{CM} and T_{EM} cells is as described in Figure 24. Three B6.*TL* hosts were individually transferred with 4.5×10^5 T_{LM}, 5.2×10^5 T_{CM}, and 6×10^5 T_{EM} cells, respectively. The purity of sorted T_{CM} cells and T_{LM} (T_{EM}) cells was always >99% CD62^{low} and CD62L^{hi}, respectively. Single cell suspensions from spleen, LN and liver were obtained and stained with F-anti-CD62L, PE-anti-Thy-1.2, and A405-anti-CD8 mAbs 14 days post re-transfer. The CD62L expression in the indicated organs were analyzed. The frequencies of CD62L^{hi} 2C CD8$^+$ T cells (gated in rectangle) in total donor 2C CD8$^+$ T cells were determined. To facilitate visualization of the relatively small numbers of donor cells, only cells of donor origin are shown. Results of one of two experiments are shown.
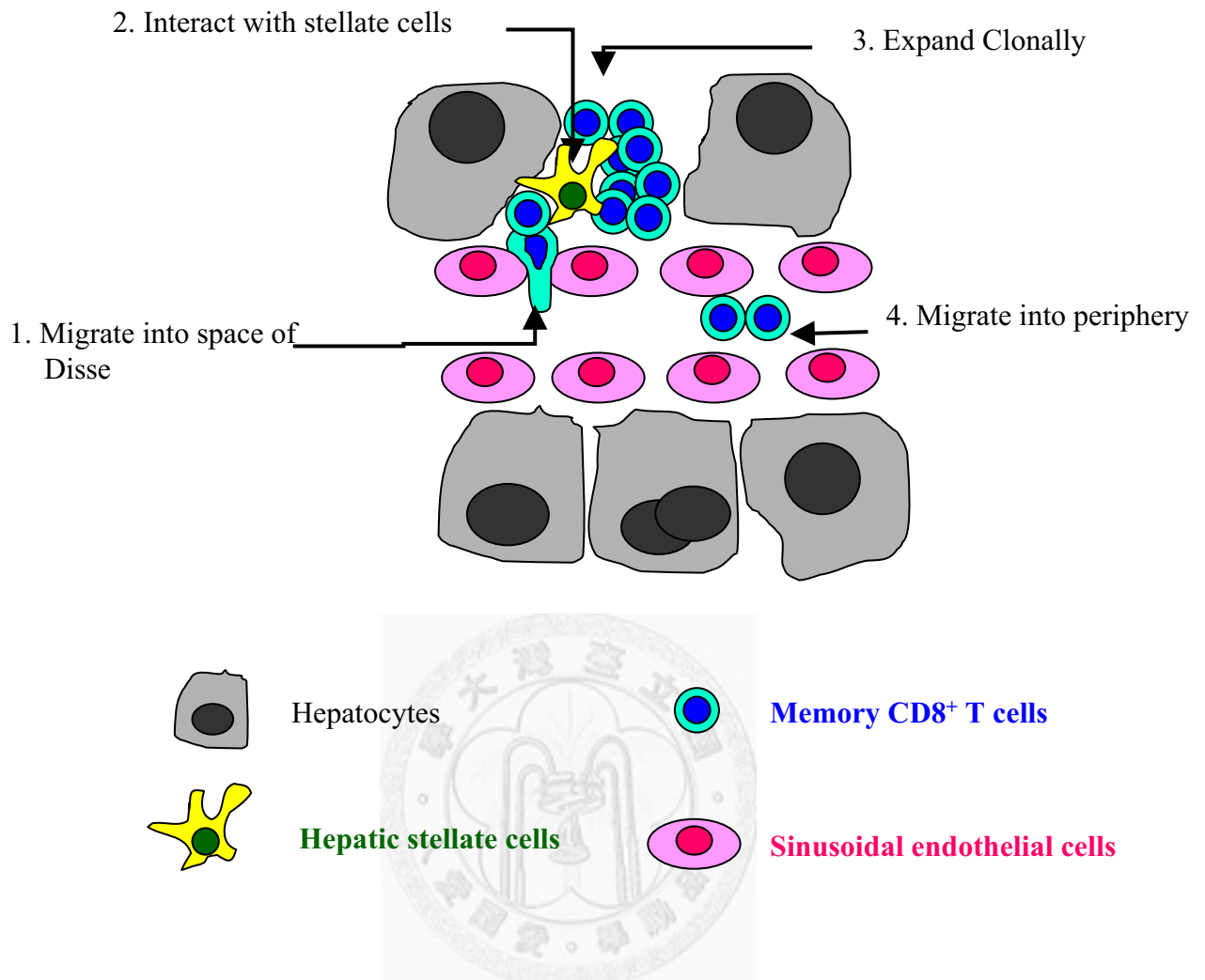
Figure 26. Illustration of liver-induced clonal expansion of memory CD8$^+$ T cells. 1. Single memory CD8$^+$ T cells migrate into hepatic parenchyma *via* by squeezing through sinusoid endothelial cells. 2. Memory CD8$^+$ T cells interact with IL-15Rα^+ stellate cells in the space of Disse, initiates signaling in response to transpresented IL-15 by stellate cells. 3. The memory CD8$^+$ T cells then undergo clonal proliferation and form cell clusters in the liver. 4. After clonal expansion of memory CD8$^+$ T cells, the memory CD8$^+$ T cells migrate back into periphery.

Appendix

THE JOURNAL OF IMMUNOLOGY

Effector Function-Deficient Memory CD8$^+$ T Cells Clonally Expand in the Liver and Give Rise to Peripheral Memory CD8$^+$ T Cells

Yu-Chia Su, Chen-Cheng Lee and John T. Kung

This information is current as of December 9, 2010

Supplementary Data	**http://www.jimmunol.org/content/suppl/2010/11/15/jimmunol.1002606.DC1.html**
References	This article **cites 39 articles**, 18 of which can be accessed free at: http://www.jimmunol.org/content/185/12/7498.full.html#ref-list-1
Subscriptions	Information about subscribing to *The Journal of Immunology* is online at http://www.jimmunol.org/subscriptions
Permissions	Submit copyright permission requests at http://www.aai.org/ji/copyright.html
Email Alerts	Receive free email-alerts when new articles cite this article. Sign up at http://www.jimmunol.org/etoc/subscriptions.shtml/

AMERICAN ASSOCIATION OF IMMUNOLOGISTS · FOUNDED 1913

Effector Function-Deficient Memory CD8+ T Cells Clonally Expand in the Liver and Give Rise to Peripheral Memory CD8+ T Cells

Yu-Chia Su,* Chen-Cheng Lee,* and John T. Kung*,†

Upon adoptive transfer into histocompatible mice, naive CD8+ T cells stimulated ex vivo by TCR+IL-4 turn into long-lived functional memory cells. The liver contains a large number of so formed memory CD8+ T cells, referred to as liver memory T cells (T_{LM}) in the form of cell clusters. The CD62L^{low} expression and nonlymphoid tissue distribution of T_{LM} cells are similar to effector memory (T_{EM}) cells, yet their deficient cytotoxicity and IFN-γ inducibility are unlike T_{EM} cells. Adoptive transfer of admixtures of TCR+IL-4–activated Vβ8+ and Vβ5+ CD8+ T cells into congenic hosts reveals T_{LM} clusters that are composed of all Vβ5+ or Vβ8+, not mixed Vβ5+/Vβ8+ cells, indicating that T_{LM} clusters are formed by clonal expansion. Clonally expanded CD8+ T cell clusters are also seen in the liver of *Listeria monocytogenes*-immune mice. T_{LM} clusters closely associate with hepatic stellate cells and their formation is IL-15/IL-15R–dependent. CD62L^{low} T_{LM} cells can home to the liver and secondary lymphoid tissues, remain CD62L^{low}, or acquire central memory (T_{CM})-characteristic CD62L^{hi} expression. Our findings show the liver as a major site of CD8+ memory T cell growth and that T_{LM} cells contribute to the pool of peripheral memory cells. These previously unappreciated T_{LM} characteristics indicate the inadequacy of the current T_{EM}/T_{CM} classification scheme and help ongoing efforts aimed at establishing a unifying memory T cell development pathway. Lastly, our finding of T_{LM} clusters suggests caution against interpreting focal lymphocyte infiltration in clinical settings as pathology and not normal physiology.   *The Journal of Immunology*, 2010, 185: 7498–7506.

Antigen-specific memory T cells that develop in response to Ag stimulation have been classified as CD62L^{hi}CCR7+ central memory T (T_{CM}) cells or CD62L^{low}CCR7− effector memory T (T_{EM}) cells, with T_{CM} and T_{EM} cells homing to lymphoid tissues and nonlymphoid tissues, respectively (1). Although significant advances have been made in the functional characterization of memory T cell subsets, a unifying development pathway has not emerged. As such, linear differentiation, bifurcative differentiation, and self-renewing effector models have been proposed (2). The process of memory T cell development and maintenance is now known to be influenced by cytokines, Ag-specific T cell frequency, and anatomic locations (3–6) and is thus characterized by considerable complexity.

Because memory CD8+ T cells can be maintained in the absence of secondary lymphoid organs (7, 8), nonlymphoid tissues and organs are expected to play critical roles in their maintenance. Bone marrow has been reported to be the preferred site for homeostatic proliferation of memory CD8+ T cells (9, 10), a process that is dependent on IL-15 and IL-15Rα (11, 12). Whether the expression of IL-15 and IL-15Rα by the many nonlymphoid tissues and organs, such as the liver (13, 14), also contribute to the homeostasis of memory CD8+ T cells is largely unknown.

We have reported previously that adoptive transfer of Ag+IL-4–activated naive CD8+ T cells into histocompatible hosts resulted in potent development of long-lived functional memory cells (5, 15). Using this highly efficient CD8+ memory T cell generation system, we show in this study that the liver, the largest organ of the body, is a site of CD8+ memory T cell growth through the process of clonal expansion. We also describe cells that may participate in this clonal expansion process. Our results are also discussed in the context of memory development pathways.

Materials and Methods

Mice

H2-L^d–restricted 2C TCR transgenic mice (16) were bred onto C57BL/10ScN (B10) and C57BL/6J (B6) backgrounds (5, 17). B6.*TL* and B10.*TL* are B6- and B10-histocompatible *Thy1^{a}CD8^a* congenic strains, respectively. IL-15Rα knockout breeders (18) were purchased (The Jackson Laboratory, Bar Harbor, ME). All mice were bred in the animal facility of the Institute of Molecular Biology under specific pathogen-free conditions and used between 6 and 12 wk of age unless otherwise indicated. All experimental procedures were performed in accordance to active protocols approved by Institutional Animal Care and Utilization Committee of Academia Sinica.

Generating and monitoring memory CD8+ T cells

CD8+ T cells were purified by panning (19). Purified 2C CD8+ T cells were activated by antigenic peptide in the presence of IL-4 for 3 d, cultured for 2 d in IL-2–supplemented medium, and adoptively transferred into indicated hosts as described previously (5). Vβ5+ and Vβ8+ CD8+ T cells were obtained by cell sorting of wild type (WT) CD8+ T cells stained with F–anti-Vβ5, Cy5–anti-TCR Vβ8, and PE–anti-CD8. WT CD8+ T cells were activated in vitro by anti-CD3/CD28 presented by LPS-activated B blasts (20). Indicated numbers of donor CD8+ T cells were transferred i.v. into indicated hosts. The presence of donor CD8+ T cells in host mice was

*Graduate Institute of Immunology, College of Medicine, National Taiwan University; and †Institute of Molecular Biology, Academia Sinica, Taipei, Taiwan

Address correspondence and reprint requests to Dr. John T. Kung, #128, 2nd Sec., Yen-Joiu-Yuan Road, Nankang District, Taipei 11529, Taiwan. E-mail address: mbkung@ccvax.sinica.edu.tw

The online version of this article contains supplemental material.

Abbreviations used in this paper: BM, bone marrow; E, endothelial cells; H, hepatocytes; HSC, hepatic stellate cell; IHL, intrahepatic lymphocyte; L, mononuclear lymphoid cells; LN, lymph node; N, neutrophils; PAT, postadoptive transfer; R, RBCs; T, T lymphocytes; T_{CM}, central memory T cells; T_{EM}, effector memory T cells; T_{LM}, liver memory T cells; WT, wild type.

monitored by flow cytometry and expressed as the ratio of donor to total CD8$^+$ T cells (5).

Isolation of liver lymphocytes

Intrahepatic lymphocytes (IHLs) were isolated by a modification described previously (21). The liver was perfused, excised, homogenized by Cell Strainer (BD Falcon, Franklin Lakes, NJ), and digested (HBSS containing 0.02% collagenase IV [Sigma-Aldrich, St. Louis, MO], 0.002% DNase I [Roche, Basel, Switzerland], and 5% FCS, at 37°C for 45 min). IHLs were enriched by gradient centrifugation (24% HistoDenz [Sigma-Aldrich], 20 min, $1580 \times g$, 4°C). Spleen CD8$^+$ T cells obtained using the IHL isolation procedure proliferated similarly to anti-CD3/CD28 stimulation as those isolated by our routine CD8$^+$ panning procedure (Supplemental Fig. 1), indicating that the IHL isolation procedure did not cause any damage to CD8$^+$ T cells.

Examination of liver memory CD8$^+$ T cells

H&E staining of paraffin-embedded liver sections was performed according to standard procedures. OCT-embedded liver sections (5 μm thick) were fixed in acetone, stained with indicated Abs (4°C, 8 h), and observed by confocal microscopy (Zeiss LSM 510, Oberkochen, Germany). Fluorochrome-conjugated mAbs used include: AlexaFluor488 (A488)-1B2 anti-2C TCR idiotype (22), A488- and PE-conjugated anti–Thy-1.2 (23), A488–anti-Vβ5 (24), PE–anti-CD8 (23), A647–anti-Vβ8 (25), A647–anti-GFAP (BD Pharmingen, San Diego, CA), A546–anti-pan cytokeratin (Sigma-Aldrich). All images were collected by LSM510 (Zeiss). For CD8 IHC staining, liver sections were incubated with 53-6.7 rat anti-mouse CD8 (4°C, 16 h), followed by HRP-goat anti-rat IgG (Jackson ImmunoResearch Laboratories, West Grove, PA; 4°C, 6 h), ImmPACT DAB (Vector Laboratories, Burlingame, CA), counterstained with Mayer's hematoxylin (Sigma-Aldrich). For IL-15, Thy-1.2, and IL-15Rα IHC staining, three serial liver sections were individually stained with rat anti-Thy-1.2 (clone: 30H12), goat anti-mIL-15 (R&D), and goat anti-mIL-15Rα (Santa Cruz Biotechnology, Santa Cruz, CA) primary Abs, followed by staining with appropriate HRP–anti-rat or HRP–anti-goat secondary Ab. DAB precipitation and hematoxylin counterstain were then performed. All images were collected by AxioImager Z1 with Axiovision software (Zeiss).

For electron microscopy, the liver was perfused with 4% paraformaldehyde, fixed for 4 h, made into cubes [∼1 mm^3], postfixed with 2.5% glutaraldehyde plus 4% paraformaldehyde (overnight, 4°C) and then 1% OsO$_4$ (2 h, 4°C), washed, dehydrated, embedded in Spurr resin, sectioned with a diamond knife (Ultracut, Reichert-Jung, Vienna, Austria) and examined by electron microscopy (Tecnai G2 Spirit TWIN, FEI Company, Hillsboro, OR).

In vitro proliferation assay

Sorted memory CD8$^+$ T cell subsets were stimulated (2×10^4 cells/well per 0.2 ml) in wells that had been coated previously with 10 μg/ml each of anti-CD3$^+$ anti-CD28 for 24 h. Proliferation by memory 2C CD8$^+$ T cells was accessed by a 6-h, 0.5-μCi [^{3}H]thymidine pulse.

CTL assay

Ag-specific cytolytic activity by 2C memory CD8$^+$ T cells was determined by the JAM assay (26). L^d-bearing P815 target cells were [^{3}H]thymidine labeled (6-h pulse, 10 μCi/ml) and used at indicated effector/target ratios.

Scoring of CD8$^+$ T cell clusters found in the liver

A cluster is defined as six or more closely situated CD8$^+$ T cells. Vβ8$^+$ clusters are defined as CD8$^+$ clusters containing >80% Vβ8$^+$ cells and no Vβ5$^+$ cells, or CD8$^+$ clusters containing >80% Vβ5$^+$ cells and no Vβ8$^+$ cells.

Listeria monocytogenes immunization

Listeria monocytogenes 5334, a clinical isolate from the National Taiwan University Hospital, was injected i.v. at a sublethal dose (6×10^3 CFU per mouse).

Statistical analysis

The association of T$_{LM}$ clusters with hepatic stellate cells (HSCs), neutrophils, and IL-15$^+$ and IL-15R$^+$ cells was analyzed by Fisher's exact probability test, in which the frequencies of test cells found within the confines of T$_{LM}$ clusters were compared against the frequencies of test cells found in areas away from T$_{LM}$ clusters; $p < 0.05$ is considered statistically significant.

Results

Memory CD8$^+$ T cells are found in large numbers in the liver

Naive 2C CD8$^+$ T cells activated ex vivo by Ag in the presence of added IL-4 become long-lived functional memory cells after adoptive transfer into congenic histocompatible hosts (5, 15). Using this high-efficiency CD8$^+$ T cell memory generation system, we examined for the presence of donor-derived memory T cells in different host tissues and organs (Fig. 1A). Donor CD8$^+$ memory T cells were found most frequently in the liver, followed by bone marrow (BM), spleen, and lastly the lymph node (Fig. 1A). Absolute counts of donor CD8$^+$ T cells were the highest for the spleen, then the liver, followed by BM, and lastly the lymph node (LN) (Fig. 1B).

CD8$^+$ T$_{LM}$ cells express T$_{EM}$-like and T$_{EM}$-unlike properties

Memory CD8$^+$ T cells are divided into CD62L^{hi}CCR7$^+$ T$_{CM}$ and CD62L^{low}CCR7$^-$ T$_{EM}$ subsets that reside in lymphoid and nonlymphoid organs or tissues, respectively (1). The current thinking is that T$_{EM}$ but not T$_{CM}$ CD8$^+$ memory cells possess the genetic programming required for entry into nonlymphoid organs or tissues. Because T$_{LM}$ cells are found in the liver, a nonlymphoid organ, they are expected to be similar to CD8$^+$ T$_{EM}$ cells. Consistent with this expectation, the vast majority of T$_{LM}$ cells expressed the CD62L^{low}
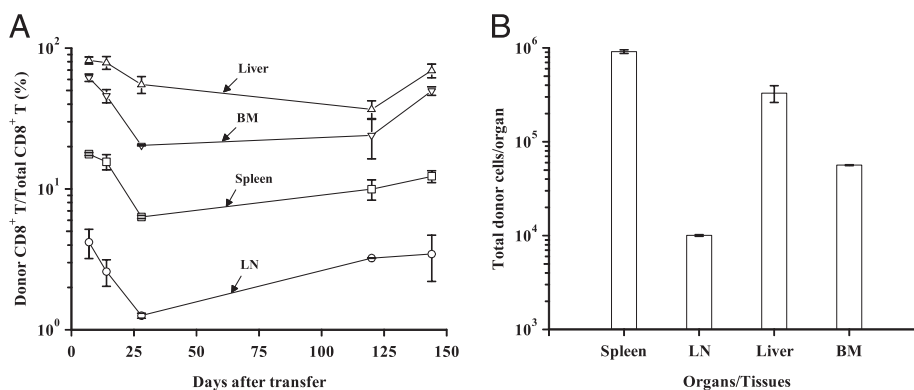
FIGURE 1. High numbers of CD8$^+$ memory T cells in the liver. *A*, Ag + IL-4–activated naive CD8$^+$Thy-1.2$^+$ T cells (8×10^6) from 2C TCR transgenic mice were adoptively transferred into a group of 10 congenic B10.*TL* (Thy-1.2$^-$) hosts. On the indicated days PAT, single-cell suspensions from the spleen, liver, LN, and BM from two hosts were stained with PE–anti-CD8 and Cy5-anti–Thy-1.2 mAbs, and ratios (means ± SEM) of donor to total CD8$^+$ T cells are shown. *B*, On day 28 PAT, single-cell suspensions from the indicated organs of two host mice were stained as in *A*, and the total numbers of donor cells were also determined. Because BM and LN cells were recovered from two femurs and mesenteric LN, respectively, they constituted part of all BM and LN cells and are therefore under estimates of total BM and LN cells in the entire host.
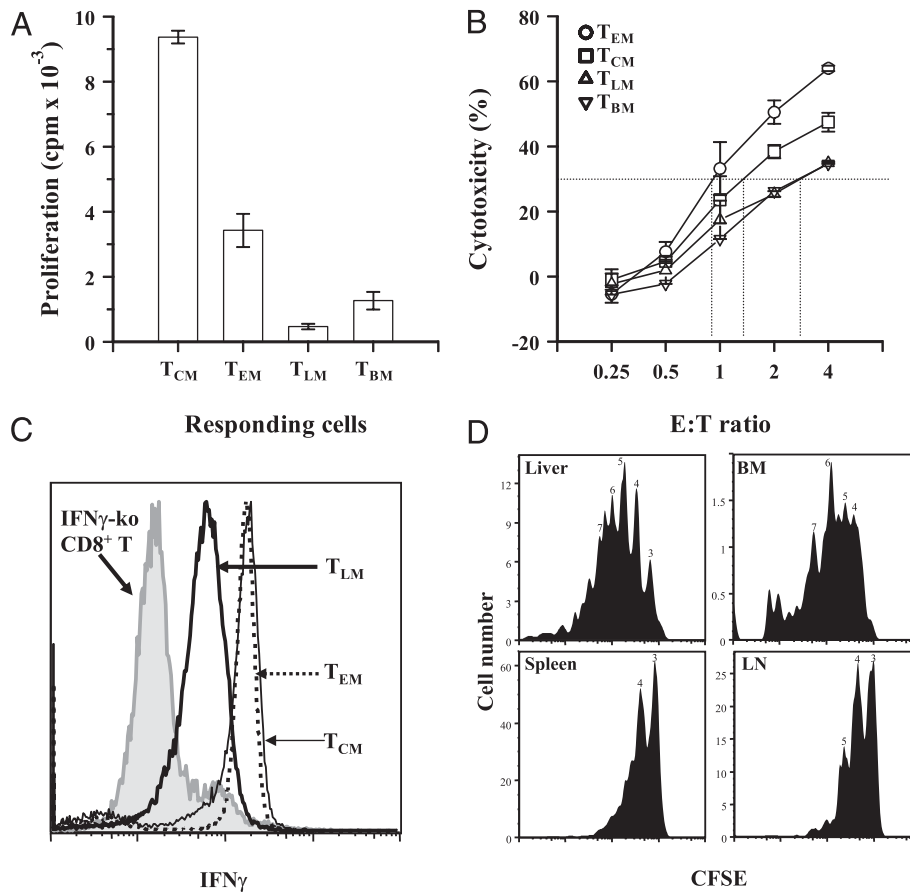
FIGURE 2. Characterization of liver memory CD8+ T cells. *A*, Ag+IL-4-activated 2C CD8+ T cells (16×10^6) were adoptively transferred into each of six B6.*TL* hosts to allow their development into memory T cells. On d70 PAT, single cell suspensions from indicated organs of two host mice were stained with FITC–anti-CD62L, Cy5-anti–Thy-1.2, and TR–anti-CD8. Indicated memory 2C CD8+ T cell subsets, spleen CD62L^hi Thy-1.2+ CD8+ T_{CM} cells, spleen Thy-1.2+ CD62L^low CD8+ T_{EM} cells, liver Thy-1.2+ CD62L^low CD8+ T_{LM} cells, and BM Thy-1.2+ CD62L^low CD8+ T_{BM} cells were isolated by cell sorting. Sorted memory CD8+ T cell subsets were activated in wells coated with anti-CD3+ anti-CD28 for 24 h. Typical results from one of two experiments are shown. *B*, Subsets of 2C memory CD8+ T cells as indicated were obtained from two host mice by cell sorting as in *A* and assayed for Ag-specific cytolytic activity at indicated effector/target cell ratios against L^d-bearing P815 target cells. Typical results from one of two experiments are shown. *C*, On day 60 PAT, subsets of CD8+ memory T cell subsets were obtained from two host mice as in *A*, naive CD8+ T cells (CD8+ CD44^low) were isolated from the spleen of IFN-γ knockout mice by cell sorting. Indicated memory subsets and naive CD8+ T cells were activated in anti-CD3+ anti-CD28–coated wells for 9 h, followed by intracellular staining with Cy5-anti–IFN-γ. Intracellular IFN-γ staining histograms are: naive IFN-γ knockout CD8+ T cells, gray-filled; liver T_{LM}, thick line; spleen T_{CM}, thin line; spleen T_{EM}, dashed line. Typical results from one of three experiments are shown. *D*, This experiment involved two adoptive transfers performed sequentially. For the first adoptive transfer, each of two B10.*TL* hosts received (8×10^6) Ag+IL-4–activated 2C CD8+ T cells. On day 7 PAT, total spleen CD8+ T cells from these B10.*TL* hosts were obtained and CFSE-labeled (2 μM, 37˚C, 15 min). CFSE-labeled CD8+ T cells that contained the 5×10^5 cell equivalent of 2C CD8+ T cells were adoptively transferred into a second B10.*TL* host. On day 28 PAT, single-cell suspensions from the indicated organs were stained with PE-anti–Thy-1.2, Cy5-anti-2C TCR (1B2), and A680–anti-CD8 mAbs; CFSE distribution was analyzed for cells of donor origin (1B2+ Thy-1.2+ CD8+). The number of cell divisions is shown on the top of the histogram. Typical results from one of three experiments are shown.

phenotype (Supplemental Fig. 2). To more comprehensively characterize T_{LM} cells, effector functions were studied (Fig. 2*A*). Whereas spleen T_{CM} cells mounted a strong TCR-stimulated proliferative response, T_{LM} cells were replication incompetent. Spleen T_{EM} cells showed much stronger proliferation than T_{LM} cells, although the magnitude was significantly less than that of T_{CM} cells. T_{LM} cells expressed Ag-specific cytolytic activity at a level that was one third and half those of spleen T_{EM} and T_{CM} cells, respectively (Fig. 2*B*). Similar to T_{LM} cells, CD8+ memory T cells from the BM were also replication incompetent and expressed poor cytotoxicity in comparison with spleen T_{EM}. IFN-γ production by T_{LM} cells was much weaker than those of T_{EM} and T_{CM} cells upon anti-CD3/CD28 stimulation (Fig. 2*C*). Memory CD8+ T cells from the spleen were CFSE-labeled and transferred into a histocompatible host. On day 28 postadoptive transfer (PAT), CFSE fluorescence patterns of donor cells in various host organs were examined. The majority of

memory CD8+ T cell from the liver and BM divided four to six times, and the majority population of memory CD8+ T cell from the spleen and LN divided for three or four times (Fig. 2*D*). In sum, T_{LM} cells display T_{EM}-like and T_{EM}-unlike properties.

Ag+IL-4–activated CD8+ T cells are found in the liver in clusters

H&E-stained liver sections from host mice that were adoptively transferred with Ag+IL-4-activated CD8+ donor cells revealed T_{LM} clusters made up of mostly lymphocytes (Figure 3A). Occasional neutrophils were also found in some cell clusters. T_{LM} clusters bordered hepatocytes and sinusoids and no hepatocytes were found within the confines of these cell clusters. Thy-1.2 expression by constituent cells of T_{LM} clusters in a *Thy-1^a* congenic host clearly indicate that T_{LM} clusters are composed of CD8+ T cells of donor origin (Fig. 3*B*). On day 120 PAT, liver sections from host
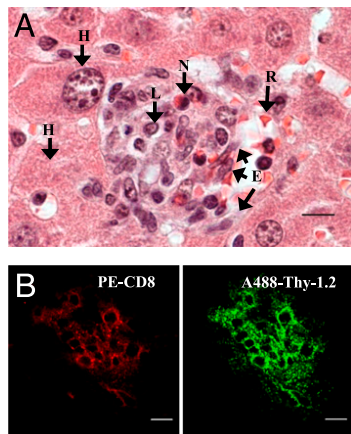
FIGURE 3. Clusters of Ag+IL-4–activated CD8^{+} T cells are found in the liver. Ag+IL-4–activated 2C CD8^{+} T cells (8 × 10^{6}) were adoptively transferred into each of three B10.*TL* hosts. A, On day 7 PAT, all three hosts were sacrificed and H&E staining of a liver paraffin section was performed. A representative cell cluster is shown (scale bar, 10 μm; original magnification ×1000). Mononuclear lymphoid cells, neutrophils, hepatocytes, RBCs, and sinusoids outlined by endothelial cells are marked. *B*, On day 7 PAT, three hosts were sacrificed and liver frozen section was stained with A488-anti-Thy-1.2 and PE–anti-CD8. Fluorescence image of one representative donor cell cluster, showing colocalization of CD8^{+} and Thy-1.2^{+} cells, is displayed. Scale bar, 10 μm. Original magnification ×630. E, endothelial cells; H, hepatocytes; L, mononuclear lymphoid cells; N, neutrophils; R, RBCs.

mice were analyzed by CD8 immunohistochemical staining. Distribution of the Ag+IL-4-activated CD8^{+} T cell clusters in the host liver was estimated (Supplemental Fig. 3*A*). T_{LM} clusters in periportal and midzonal regions were 3.5- and 6-fold more frequently found, respectively, than those in centrilobular regions, with the size of clusters being similar for all regions (Supplemental Fig. 3*B*). Normal levels of serum AST and ALT and the lack of apoptotic cells in the immediate vicinity of T_{LM} clusters indicate that no pathology is associated with the presence of T_{LM} clusters in the liver (Supplemental Fig. 4).

T_{LM} clusters form through the process of clonal expansion

Purified Vβ5^{+} and Vβ8^{+} CD8^{+} T cells were activated in separate cultures by anti–CD3+IL-4, mixed in equal proportions, and adoptively transferred into histocompatible congenic hosts. At the population level, similar proportions of Vβ5^{+} and Vβ8^{+} memory CD8^{+} T cells were found, indicating no biased maintenance (Supplemental Fig. 5). Confocal analysis of 13 T_{LM} clusters of day 7 PAT host liver sections revealed six (46%) that contained exclusively Vβ5[+] and no Vβ8^{+} cells, and six (46%) that contained exclusively Vβ8[+] and no Vβ5^{+} cells (Fig. 4). Similarly, of the 20 T_{LM} clusters identified in day 60 PAT host liver sections, 10 (50%) contained exclusively Vβ5^{+} and no Vβ8^{+} cells, and the other 10 (50%) contained exclusively Vβ8^{+} and no Vβ5^{+} cells. These results indicate that liver CD8^{+} T cells arise through in situ clonal expansion of single cells.

Clonal nature of CD8^{+} T cell clusters in the liver of L. monocytogenes-immune mice

To examine whether mice subjected to live infectious agents also develop CD8^{+} T cell clusters in the liver, WT mice were given a sublethal dose of *L. monocytogenes*. Single-cell suspension recovered from the liver of *L. monocytogenes*-immune hosts contained CD8^{+} T cells that were 64% Vβ8^{+} cells, which is much higher than the ∼25% Vβ8^{+} cells within T cells of nonimmunized mice (Fig. 5*A*). This finding of highly enriched Vβ8^{+} cells is consistent
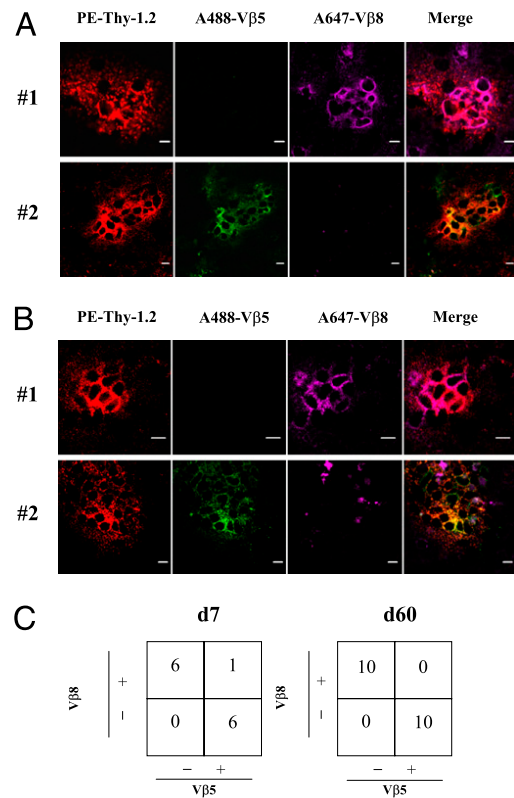

FIGURE 4. Clonal expansion of in vitro TCR+IL-4–activated CD8^{+} T cells in the liver. Equal numbers (4 × 10^{6} each) of the TCR+IL-4–activated Vβ5^{+} and Vβ8^{+} CD8^{+} T cells were mixed and adoptively transferred into each of two B10.*TL* host mice. On days 7 and 60 PAT, one of the two hosts were sacrificed, and liver frozen sections were made, stained with A488-anti–Vβ5, PE-anti–Thy-1.2 and A647-anti-Vβ8, and examined by confocal microscopy. Confocal images of two representative clones (labeled #1 and #2) from day 7 PAT (*A*) and day 60 PAT (*B*) liver sections are shown. These clones contained cells that were either all Vβ8[+] or all Vβ5^{+} cells, with no mixed Vβ5[+]/Vβ8^{+} cells (scale bar, 5 μm; original magnification ×630). *C*, Of the total of 13 donor clusters found in day 7 PAT host liver sections, six contained Vβ8[+] but no Vβ5^{+} cells, and six contained Vβ5[+] but no Vβ8^{+} cells, whereas one contained mixed Vβ8[+] and Vβ5^{+} cells. Of the 20 donor clusters found in day 60 PAT host liver sections, 10 contained Vβ8[+] but no Vβ5^{+} cells, and 10 contained Vβ5^{+} but no Vβ8^{+} cells.

with biased expansion of Vβ8^{+} T cells in some individual mice responding to *L. monocytogenes* infection (27). If liver CD8^{+} T cells were generated elsewhere and homed to microniches that support the survival of memory CD8^{+} T cells, then each CD8^{+} T cell cluster would be expected to contain ∼60% Vβ8^{+} cells. A total of 40 randomly chosen liver sections from three *L. monocytogenes*-immune mice were examined for the presence of CD8^{+} T cell clusters. Scanning of all the 40 liver sections yielded a total of 12 CD8^{+} clusters, six of which contained either no or very few Vβ8^{+} cells (a representative cluster is shown in Fig. 5*B*, *lower row*). For the other six CD8^{+} T cell clusters, Vβ8^{+} cells were readily detectable and constituted 80–100% of Thy-1.2^{+}CD8^{+} cells in the clusters (a representative cluster is shown in Fig. 5*B*, *upper row*). The nonrandom nature of nearly all or no Vβ8^{+} T cell presence in all 12 clusters examined indicates that these clusters were clonal descendents of single cells and that specialized niches exist in the liver that provide the necessary microenvironment for single CD8^{+} T cells to undergo clonal expansion. By considering the thickness of liver sections and the total area scanned, the 12 CD8^{+} T cells clusters found in 40 sections translates to ∼5.8 × 10^{3} CD8^{+} T cell clusters per entire liver of an *L. monocytogenes*-immune mouse. Liver sections from age-matched naive mice that had not been exposed to
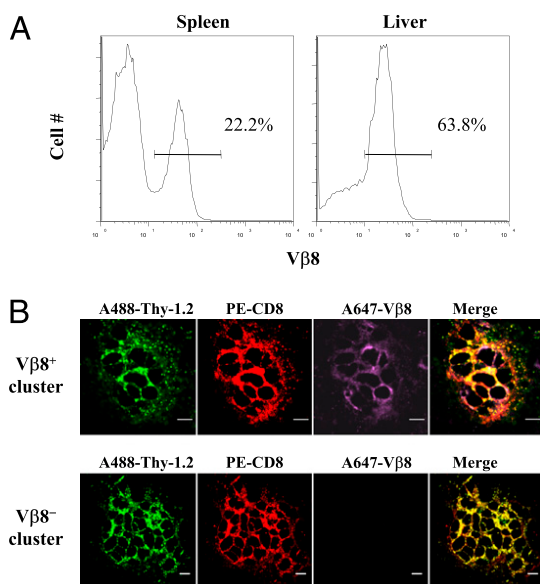
FIGURE 5. Clonal CD8$^+$ T cell expansion in the livers of *L. monocytogenes*-infected mice. B6 mice were given a sublethal dose of *L. monocytogenes* i.v. *A*, Spleen cells and intrahepatic lymphocytes were obtained from B6 mice that had been infected with *L. monocytogenes* 60 days previously and stained with PE–anti-CD8 and Cy5–anti-Vβ8. Histograms of Vβ8 expression, with the percentages of Vβ8$^+$ cells indicated, are shown. *B*, A total of 40 randomly chosen liver sections from three day 60 post *L. monocytogenes*-infected mice were stained with A488-anti–Thy-1.2, PE–anti–CD8, and A647-anti–Vβ8, and subjected to confocal microscopy examination. A total of 12 CD8$^+$ clusters were identified. Of these 12 CD8$^+$ clusters, six were Vβ8$^+$ and six were Vβ8$^-$. One representative each of Vβ8$^+$ (*top row*) and Vβ8$^-$ (*lower row*) clusters are shown (scale bar, 5 μm; original magnification ×630). A total of 45 liver sections from three age-matched naive mice that had not been exposed to *L. monocytogenes* were stained under conditions to *L. monocytogenes*-immune liver sections. From these 45 naive liver sections, only one Vβ8$^-$ cluster was identified. The sum of scanned areas of the 40 *L. monocytogenes*-immune liver sections is similar to the sum of the scanned area of the 45 naive liver sections.

L. monocytogenes were stained under conditions identical to the *L. monocytogenes*-immune liver sections. Examination of naive liver sections comprising an area similar to that of *L. monocytogenes*-immune liver sections revealed only one Vβ8$^-$ cluster as opposed to the 12 clusters found for *L. monocytogenes*-immune livers. Because the frequency of CD8$^+$ T cell clusters we observed in the livers of *L. monocytogenes*-immune mice was >10-fold higher than that of naive livers, the vast majority of CD8$^+$ T cell clusters seen in the liver of *L. monocytogenes*-immune mice must therefore have been formed as a result of *L. monocytogenes* infection.

IL-15R requirement for CD8$^+$ T$_{LM}$ cluster formation

Because IL-15 plays a critical role in the homeostasis of memory CD8$^+$ T cells, we examined whether IL-15 and IL-15R immunoreactive signals can be detected in the vicinity of memory CD8$^+$ T$_{LM}$ clusters (Fig. 6). Using serial liver sections, IL-15 and IL-15R immunoreactive signals in the form of dendrite-like processes were found (Fig. 6*B*, 6*C*). Of the 13 total T$_{LM}$ clusters analyzed, all contained IL-15$^+$ and IL-15R$^+$ dendrite-like processes. Statistical analysis of T$_{LM}$-associated IL-15$^+$ and IL-15R$^+$ signals against those in areas away from T$_{LM}$ clusters showed differences that were highly significant (for IL-15, $p = 0.02$; for IL-15R, $p = 0.0002$). To further study the IL-15R role in T$_{LM}$ cluster formation in the liver, we adoptively transferred Ag+IL-4–activated CD8$^+$ T cells into IL-15R knockout hosts. Whereas 8 T$_{LM}$ clusters were found in nine entire liver sections of WT hosts, none were found in 54 entire liver sections of IL-15R knockout hosts (Fig. 6*D*).
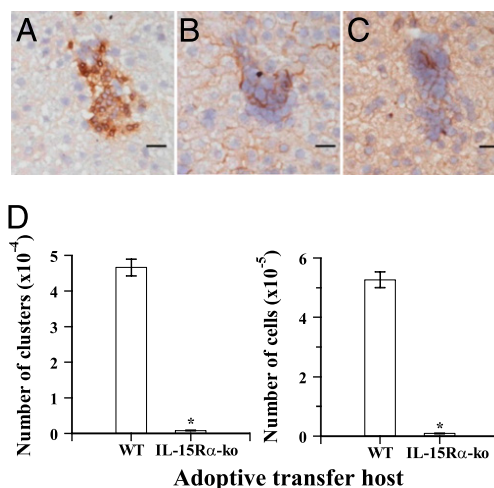

FIGURE 6. IL-15Rα is required for the formation memory CD8$^+$ T cell clusters in the liver. *A*, Ag+IL-4–activated 2C CD8$^+$ T cells (1.6×10^7) were adoptively transferred into three B6.*TL* hosts. On day 7 PAT, 8-μm-thick liver serial sections were subjected to immunohistochemical staining to detect Thy-1.2 (*A*), IL-15 (*B*), and IL-15R (*C*). Images of serial sections of one representative CD8$^+$ T cell cluster are shown (scale bar, 20 μm; original magnification ×200). The cluster is composed of round-shaped Thy-1.2$^+$ donor CD8$^+$ T cells (*A*). Within the confines of the cluster, IL-15$^+$ and IL-15R$^+$ signals in the form of dendrite-like processes can be seen. *D*, Ag+IL-4–activated 2C CD8$^+$ T cells (8×10^6) were adoptively transferred into each of three WT and three IL-15Rα knockout hosts. Liver sections from day 120 PAT hosts were incubated with anti-CD8 mAb, followed by HRP–anti-rat IgG Ab, then DAB precipitation. A cluster is defined as six or more CD8$^+$ T cells in close proximity to each other. The number of donor cell clusters was determined by scanning a defined volume (area of observation × section thickness of 5 μm). The average liver volume of 1.56 cm^3 was derived from volume determinations of five mice at 8–12 wk old. Total CD8$^+$ T cell clusters for the entire liver were estimated by the number of clusters per cubic millimeter multiplied by 1560 (estimated liver volume) and shown in the form of a bar plot (mean ± SEM). The average donor cell numbers calculated from 31 randomly chosen clusters was 11.3. The total CD8$^+$ T cell number for the entire liver was estimated by multiplying the number of clusters by 11.3. Not a single cell cluster was found in all examined IL-15Rα knockout livers (total volume 5.8 mm^3 from 54 liver sections obtained from three whole livers), which corresponds to <0.52 cell clusters/mm^3, <8.1 × 10^2 total cell clusters, or <9.2 × 10^3 total CD8$^+$ T cells per liver.

Considering the area and thickness of the liver sections examined, these numbers can be converted, respectively, for WT and IL-15R knockout hosts to 28.4 and <0.52 T$_{LM}$ clusters/mm^3, a total of 4.4×10^4 and <8.1 × 10^2 T$_{LM}$ clusters per entire liver, 5×10^5 and <9.2 × 10^3 total donor CD8$^+$ T cells per entire liver. Flow cytometric analysis of liver cells of WT and IL-15Rα knockout mice that had previously received adoptively transferred Ag+IL-4–activated CD8$^+$ T cells also showed a highly reduced number of donor 2C CD8$^+$ T cells in IL-15R knockout hosts when compared with WT hosts (Supplemental Fig. 6).

CD8$^+$ T$_{LM}$ clusters are closely associated with HSCs

The clonal nature of liver memory CD8$^+$ T cells is most consistent with the existence of specialized niches in the liver that provide the microenvironment required for clonal expansion of single memory CD8$^+$ T cells. Because HSCs possess dendrite-like processes that are similar in structure to IL-15$^+$ and IL-15R$^+$ signals associated with T$_{LM}$ clusters, we examined for possible HSC presence near T$_{LM}$ clusters, using 1B2 mAb, GFAP, and pancytokeratin to mark donor 2C CD8$^+$ T cells, HSCs, and hepatocytes, respectively. GFAP$^+$
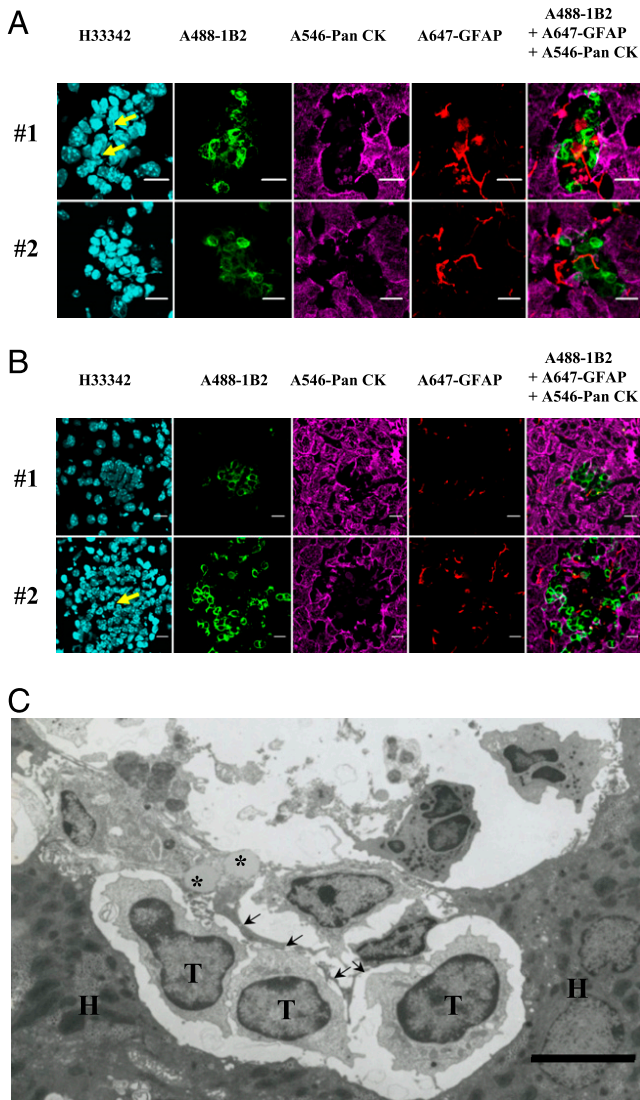
FIGURE 7. CD8^{+} T$_{LM}$ clusters are intimately associated with HSCs. Frozen liver sections (8 μm thick) from three each of day 7 and day 69 PAT B6 host mice that had received Ag+IL-4–activated 2C CD8^{+} T cells (1.6 × 10^{7} per host) previously were stained with A488–anti-2C TCR (1B2; green) to detect donor CD8^{+} T cells, A647–anti-GFAP (red) to detect stellate cells, and A546–anti-pan cytokeratin (pan CK; rose) to mark hepatocytes (scale bar, 10 μm; original magnification ×630). Confocal images of two representative memory CD8^{+} T cell clusters from day 7 (*A*) and day 69 (*B*) PAT hosts show intimate association between donor CD8^{+} T cells and HSCs, with the clusters surrounded by pan-CK^{+} hepatocytes. In some T$_{LM}$ clusters, segmental nuclear cells (yellow arrow) characteristic of neutrophils can be seen. *C*, Electron micrograph of a lymphocyte cluster in the liver of one day 7 PAT B10.*TL* host that had previously received 8 × 10^{6} Ag+IL-4–activated 2C CD8^{+} T cells (scale bar, 5 μm; original magnification ×11,000). The identity of cells and organelles are marked as follows: *, lipid droplets; arrows, dendrite-like cytoplasmic processes; H, hepatocytes; T, T lymphocytes.

HSCs were detected in all the 11 and 14 T$_{LM}$ clusters found, respectively, for day 7 and day 69 PAT hosts (Fig. 7A, 7B). Statistical analysis of GFAP[+] signals that were associated with and away from T$_{LM}$ clusters revealed significant differences (day 7 PAT, $p = 0.045$; day 69 PAT, $p = 0.02$).

Neutrophils with characteristic segmental nuclei and autofluorescence (28) were seen in a significant proportion of CD8^{+} T$_{LM}$ clusters. In day 7 and day 69 PAT liver sections, 6 of 11 and 10 of 14 T$_{LM}$ clusters contained neutrophils. No neutrophils were found in random fields away from T$_{LM}$ clusters, and statistical analysis revealed highly significant differences for neutrophils for areas associated and away from T$_{LM}$ clusters (day 7, $p = 0.006$; day 69, $p < 0.001$).

Our finding demonstrates that colocalization of the GFAP^{+} HSCs and neutrophils are highly specific for CD8^{+} T cell clusters. Because HSCs reside in the space of Disse, which in its normal state is too thin to be observed by conventional light microscopy, electron microscopy was used to reveal ultrastructural details of the spatial relationship among memory CD8^{+} T cells of T$_{LM}$ clusters, hepatocytes, and endothelial cells. Three T cells with characteristic scanty cytoplasm are shown on the lower half of the electron micrograph (Fig. 7C). An HSC, with two clearly visible and characteristic lipid droplets, situated over the leftmost T cell. The dendrite-like cytoplasmic processes of the HSC were seen to form close contact with each of the three T cells, indicating their intimate association.

T$_{LM}$ cells can convert to T$_{CM}$ in lymphoid tissues

Ag+IL-4 activated 2C CD8^{+} T cells were adoptively transferred into B6 hosts to allow their development into memory T cells. On day 60 PAT, host T$_{CM}$ and T$_{EM}$ cells from the spleen and T$_{LM}$ cells were sorted out and retransferred into a second set of hosts. When T$_{LM}$ cells were adoptively transferred, 0.05, 0.01, and 1.44% of donor CD8^{+} T cells among total CD8^{+} T cells were found in the spleen, lymph node, and liver, respectively (Fig. 8). Clearly, T$_{LM}$ cells homed to the liver preferentially as the relative liver/spleen and liver/LN ratios were 29 (1.44 ÷ 0.05) and 144 (1.44 ÷ 0.01), respectively. When T$_{EM}$ cells were adoptively transferred, 0.16, 0.02, and 1.09% of donor CD8^{+} T cells among total CD8^{+} T cells were found in the spleen, lymph node, and liver, respectively. Relative tissue abundance for transferred T$_{EM}$ cells was 6.8 (1.09 ÷ 0.16) and 55 (1.09 ÷ 0.02) for liver-to-spleen and liver-to-LN, respectively. For transferred T$_{CM}$ cells, 0.73, 0.33, and 1.29% of donor CD8^{+} T cells among total CD8^{+} T cells were found in the spleen, lymph node, and liver, respectively. The relative tissue abundances for transferred T$_{CM}$ cells were 1.8 (1.29 ÷ 0.73) and 3.9 (1.29 ÷ 0.33) for liver-to-spleen and liver-to-LN, respectively. Based on these results, T$_{CM}$ cells home to the spleen and LN with the highest efficiency, followed by T$_{EM}$ cells, with T$_{LM}$ cells being the poorest. All T$_{EM}$, T$_{CM}$, and T$_{LM}$ cells, in contrast, homed to the liver with similar efficiency. Adoptively transferred CD62L^{low} T$_{EM}$ and T$_{LM}$ cells that had been sorted to >99% purity showed highly significant conversion to CD62L^{hi} phenotype in host spleen and LN, but remained mostly CD62L^{low} in the liver. Adoptively transferred CD62L^{hi} T$_{CM}$ cells that had been sorted to >99% purity remained unchanged in the LN, with a minor subset changing to CD62L^{low} in the spleen, and significant loss of CD62L expression for the entire population (with 41% falling within the CD62L^{low} region) in the liver. These results indicate that the CD62L states of all T$_{CM}$, T$_{EM}$, and T$_{LM}$ cells can either change or remain the same depending on the anatomic locations in which they are found.

Discussion

The primary finding in this study is that CD8^{+} memory T cells grow in the liver through the process of clonal expansion. Clonal growth in tissues can be visualized only when the rate of cell division exceeds the rate at which daughter cells die or migrate away. The microenvironment that surrounds T$_{LM}$ clusters presumably plays critical roles by providing general and unique requirements for T$_{LM}$ clonal expansion. The formation of T$_{LM}$ clusters in the liver provides a unique and advantageous opportunity for gaining detailed mechanistic understanding at cellular and molecular levels. Following this reasoning, we looked for non-T cells that are intimately associated with T$_{LM}$ clusters. We found
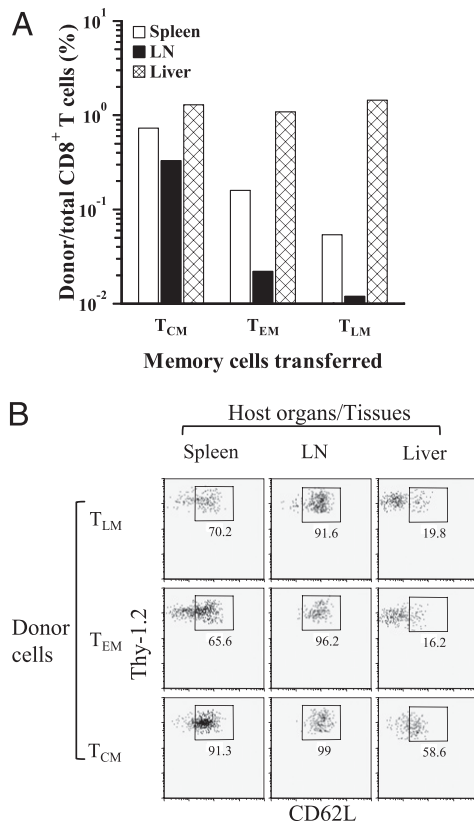
FIGURE 8. Transferred T_{LM} cells remain CD62L^{low} in the host liver, but become CD62L^{low} T_{CM}-like cells in the spleen and LN. *A*, CD8$^+$ T_{LM} cells, spleen T_{CM} cells, and spleen T_{EM} cells were obtained by cell sorting from one day 60 PAT B6 host that had been adoptively transferred with 16×10^6 Ag+IL-4–activated 2C CD8$^+$ T cells previously. Three B6.*TL* hosts were individually transferred with 3×10^5 each of T_{LM}, T_{EM}, and T_{CM} cells, respectively. On day 14 PAT, cells from indicated organs were obtained and stained with FITC–anti-CD62L, A405–anti-CD8, and Cy5-anti–Thy-1.2, and ratios of donor CD8$^+$ T cells to total CD8$^+$ T cells for indicated tissues determined. *B*, CD8$^+$ T_{LM} cells, spleen T_{CM} cells, and spleen T_{EM} cells were obtained as in *A*. Three B6.*TL* hosts were individually transferred with 4.5×10^5 T_{LM}, 5.2×10^5 T_{CM}, and 6×10^5 T_{EM} cells, respectively. To facilitate visualization of the relatively small numbers of donor cells, only cells of donor origin are shown. Types of CD8$^+$ memory T cells and host tissues are as indicated. The purity of sorted T_{CM} cells and T_{LM} (T_{EM}) cells was always >99% CD62^{low} and CD62L^{hi}, respectively. CD62L^{hi} cells are boxed, and the percentages of donor cells that are CD62L^{hi} given. Typical results from one of two experiments are shown.

that all T_{LM} clusters were closely associated with IL-15$^+$ and IL-15R$^+$ cells with dendrite-like processes. The failure to form T_{LM} clusters in the liver of IL-15R knockout hosts is consistent with a significant role played by HSCs in the formation and maintenance of T_{LM} clusters, most likely through IL-15 transpresentation (29). The finding of enriched IL-15 and IL-15Rα mRNA expression in isolated HSCs (Supplemental Fig. 7) is also consistent with a role played by HSC in T_{LM} generation and maintenance, although more experimentation is required to definitively establish this point. T_{LM} clusters also showed close association with neutrophils, which may have been attracted there as a result of chemokine production by T_{LM} cells. Alternatively, memory T cells may stimulate HSCs to produce chemokines that attract neutrophils. In this connection, transformed HSCs have been shown to produce neutrophil-attracting chemokines (30). In contrast, neutrophils can stimulate collagen synthesis in HSCs (31) and possibly other substances that may be required for T_{LM} clonal growth.

The mostly CD62L^{low} phenotype of T_{LM} cells found in the liver is expected, because memory CD8$^+$ T cells in tissues are classified as CD62L^{low} T_{EM} cells (1). If T_{LM} cells belong to T_{EM} cells that do not undergo significant homeostatic expansion (2), how can our finding that T_{LM} cells are undergoing clonal expansion be reconciled? We show that CD62L^{low} T_{EM} cells obtained from the spleen possess different functional attributes (e.g., ability to mount TCR-stimulated proliferation, IFN-γ production, and cytotoxicity) from T_{LM} cells obtained from the liver. A simple explanation is that T_{EM} cells are capable of location- or organ-specific homeostatic expansion. Thus, the microenvironment in the liver but not the spleen meets all the requirements for homeostatic expansion of T_{EM} cells. Alternatively, when peripheral T_{EM} cells gain access to the liver, they undergo specific changes, possibly through their close association with HSCs and neutrophils (e.g., to enable their homeostatic expansion). An additional noteworthy point is concerned with our finding of T_{EM}-similar and T_{EM}-dissimilar properties of T_{LM} cells. The current T_{CM} and T_{EM} classification scheme for memory T cell subsets (1) may work well for commonly studied memory T cells, but it appears to be inadequate for memory cells that have not been studied extensively, such as the T_{LM} cells reported in this study. Development of new markers, along with CD62L and CCR7, will be required for a comprehensive classification scheme of all CD8$^+$ memory T cell subsets.

Although T_{LM} cells are similar to T_{EM} cells in regard to CD62L^{low} expression and the ability to gain access to tissues, they are nevertheless much poorer than T_{EM} cells at expressing IFN-γ inducibility and cytolytic activities. The deficient functional attributes of T_{LM} cells may be caused by their engagement in cell cycle progression, a state that may be incompatible with high-function capabilities. Deficient functional activities may also be the consequence of active homeostatic expansion. To express potent functional properties, memory cells must not have been engaged recently in cell cycle progression. The findings that T_{LM} cells undergo clonal growth in the liver and yet fail to proliferate in response to TCR stimulation appear paradoxical, but could be explained by the mutually exclusive genetic programs for cytokine-mediated homeostatic expansion and TCR-stimulated expansion.

CD8$^+$ memory cells undergo homeostatic expansion by dividing once every 2 wk or more (32). Thus, at any given time, a small fraction of the memory pool is engaged in cell cycle progression. T cell activation is known to be associated with loss of CD62L expression (33). If CD62L loss also occurs when CD62L^{hi} T_{CM} cells are engaged in cell cycle progression, then two issues arise. First, the small fraction of T_{CM} cells engaged in cell cycle progression may be mistakenly classified as CD62L^{low} T_{EM} cells. Second, when there is a cell division-associated loss of CD62L expression, it is not clear how long it will take to regain CD62L^{hi} expression after cell cycle progression ceases.

Adoptively transferred CD62L^{low} T_{LM} cells become CD62L^{hi} cells in host spleen and LN; this is consistent with the $T_{EM} \rightarrow T_{CM}$ linear development model (2, 34). However, the transferred CD62L^{low} T_{LM} cells remained mostly CD62L^{low} in the liver, which supports the idea of the liver as a continuing source of memory T cells. When inside the liver, CD62L^{low} T_{LM} cells remain CD62L^{low} and become CD62L^{hi} T_{CM} cells only after their departure from the liver. If so, the liver is a site in which T_{EM}-like T_{LM} cells undergo clonal expansion, which is consistent with the self-renewing model of memory T cell development (2, 35).

Adoptively transferred T_{CM} cells were found in the liver. If T_{CM} cells can convert to CD62L^{low} T_{EM} cells, then they would be expected to gain access to nonlymphoid tissues. Adoptively transferred T_{CM} cells recovered from host spleen and LN showed no decrease in the level of CD62L expression. However, there was

a significant decrease in CD62L expression at the population level for T_{CM} donor cells recovered from host liver, such that more than 40% were scored as CD62L^{low}. One possible interpretation of this result is that T_{CM} cells could turn into T_{EM} (T_{LM}) cells either before or after gaining entry into the liver. This possibility contradicts the linear development model (2, 34), but is consistent with the reported $T_{CM} \rightarrow T_{EM}$ conversion (36). Alternatively, whereas it may be true that all T_{CM} cells are CD62L^{hi}, the converse that all CD62L^{hi} cells are T_{CM} cells is not true. If so, a small subset of T_{EM} cells exists within CD62L^{hi} T_{CM} cells, and it is these CD62L^{hi} T_{CM} cells that have homed to the liver. There is a third possibility that the liver environment is incompatible with CD62L^{hi} expression, and that when CD62L^{hi} cells enter the liver, they lose CD62L expression either by shedding or by downregulation of CD62L gene expression. Although our system of generating memory CD8$^+$ T cells is highly efficient, the generated memory T cells might not be entirely identical to those generated as a result of natural infection. Given that significant heterogeneity exists within the known memory subsets, activation of highly purified naive CD8$^+$ T cells in vitro under controlled Ag+IL-4 stimulation will likely yield memory T cells characterized by a more uniform differentiation state and functionality. Natural infection, although highly relevant to human disease, is rather complex because tissue tropism and many types of APCs may be involved, and it is likely to generate memory T cells characterized by considerable heterogeneity. Our finding of clonally expanded CD8$^+$ T cell clusters in *L. monocytogenes*-infected mice nevertheless provides an example that the formation of CD8$^+$ clusters can be seen in real infections. In this connection, it has been reported that the number of dividing Ag-specific CD8$^+$ T cells in mice immune to lymphocytic choriomeningitis virus is most numerous in the bone marrow, and few are found in the liver (9), thus raising the possibility that Ag-specific CD8$^+$ T cell clonal growth in the liver may be different for different infectious agents and the conditions under which the immune response is initiated. Clearly, more studies are needed to address this issue. All these possibilities point to the importance of development of new markers that can comprehensively and unambiguously define memory T cells in the context of subsets, tissue location, their activation and homeostatic expansion history.

Bone marrow has been shown to be an important homeostatic proliferation site for memory CD8$^+$ T cells (9). We show in this study that the liver, the largest organ of the body, is also a site of CD8$^+$ memory T cell growth. Having two anatomical locations that allow homeostatic expansion is consistent with its critically important nature, and when normal physiology of the liver or bone marrow is temporarily interrupted, homeostatic expansion can still take place. Alternatively, the liver and the bone marrow are responsible for homeostatic expansion of nonoverlapping memory T cell subsets, or that renewed memory T cells from the liver and bone marrow may be functionally distinct. Reports contrasting the long-held view that the liver is a graveyard for activated T cells have been published (37–39). CD8$^+$ memory T cells do more than gain entry and survive in the liver, our results show that they actually grow in the liver. Why and how the liver promotes memory CD8$^+$ T cell renewal and the cause death of other activated T cells is a question of fundamental importance that is worthy of further research. Caution should be exercised in interpreting clinical findings of focal lymphocyte infiltration in patient liver biopsy specimens because focal lymphocyte growth may represent normal physiology and not necessarily pathology.

References

1. Sallusto, F., D. Lenig, R. Förster, M. Lipp, and A. Lanzavecchia. 1999. Two subsets of memory T lymphocytes with distinct homing potentials and effector functions. *Nature* 401: 708–712.
2. Ahmed, R., M. J. Bevan, S. L. Reiner, and D. T. Fearon. 2009. The precursors of memory: models and controversies. *Nat. Rev. Immunol.* 9: 662–668.
3. Marzo, A. L., K. D. Klonowski, A. Le Bon, P. Borrow, D. F. Tough, and L. Lefrançois. 2005. Initial T cell frequency dictates memory CD8$^+$ T cell lineage commitment. *Nat. Immunol.* 6: 793–799.
4. Obar, J. J., K. M. Khanna, and L. Lefrançois. 2008. Endogenous naive CD8$^+$ T cell precursor frequency regulates primary and memory responses to infection. *Immunity* 28: 859–869.
5. Huang, L. R., F. L. Chen, Y. T. Chen, Y. M. Lin, and J. T. Kung. 2000. Potent induction of long-term CD8$^+$ T cell memory by short-term IL-4 exposure during T cell receptor stimulation. *Proc. Natl. Acad. Sci. USA* 97: 3406–3411.
6. Masopust, D., V. Vezys, E. J. Wherry, D. L. Barber, and R. Ahmed. 2006. Cutting edge: gut microenvironment promotes differentiation of a unique memory CD8 T cell population. *J. Immunol.* 176: 2079–2083.
7. Moyron-Quiroz, J. E., J. Rangel-Moreno, L. Hartson, K. Kusser, M. P. Tighe, K. D. Klonowski, L. Lefrançois, L. S. Cauley, A. G. Harmsen, F. E. Lund, and T. D. Randall. 2006. Persistence and responsiveness of immunologic memory in the absence of secondary lymphoid organs. *Immunity* 25: 643–654.
8. Obhrai, J. S., M. H. Oberbarnscheidt, T. W. Hand, L. Diggs, G. Chalasani, and F. G. Lakkis. 2006. Effector T cell differentiation and memory T cell maintenance outside secondary lymphoid organs. *J. Immunol.* 176: 4051–4058.
9. Becker, T. C., S. M. Coley, E. J. Wherry, and R. Ahmed. 2005. Bone marrow is a preferred site for homeostatic proliferation of memory CD8 T cells. *J. Immunol.* 174: 1269–1273.
10. Mazo, I. B., M. Honczarenko, H. Leung, L. L. Cavanagh, R. Bonasio, W. Weninger, K. Engelke, L. Xia, R. P. McEver, P. A. Koni, et al. 2005. Bone marrow is a major reservoir and site of recruitment for central memory CD8$^+$ T cells. *Immunity* 22: 259–270.
11. Becker, T. C., E. J. Wherry, D. Boone, K. Murali-Krishna, R. Antia, A. Ma, and R. Ahmed. 2002. Interleukin 15 is required for proliferative renewal of virus-specific memory CD8 T cells. *J. Exp. Med.* 195: 1541–1548.
12. Judge, A. D., X. Zhang, H. Fujii, C. D. Surh, and J. Sprent. 2002. Interleukin 15 controls both proliferation and survival of a subset of memory-phenotype CD8(+) T cells. *J. Exp. Med.* 196: 935–946.
13. Grabstein, K. H., J. Eisenman, K. Shanebeck, C. Rauch, S. Srinivasan, V. Fung, C. Beers, J. Richardson, M. A. Schoenborn, M. Ahdieh, et al. 1994. Cloning of a T cell growth factor that interacts with the beta chain of the interleukin-2 receptor. *Science* 264: 965–968.
14. Giri, J. G., S. Kumaki, M. Ahdieh, D. J. Friend, A. Loomis, K. Shanebeck, R. DuBose, D. Cosman, L. S. Park, and D. M. Anderson. 1995. Identification and cloning of a novel IL-15 binding protein that is structurally related to the alpha chain of the IL-2 receptor. *EMBO J.* 14: 3654–3663.
15. Chang, M. L., Y. T. Chen, Y. C. Su, and J. T. Kung. 2003. Cytotoxic T lymphocytes generated by short-term in vitro TCR stimulation in the presence of IL-4 are therapeutically effective against B16 melanoma. *J. Biomed. Sci.* 10: 644–650.
16. Sha, W. C., C. A. Nelson, R. D. Newberry, D. M. Kranz, J. H. Russell, and D. Y. Loh. 1988. Selective expression of an antigen receptor on CD8-bearing T lymphocytes in transgenic mice. *Nature* 335: 271–274.
17. Chang, J. F., C. A. Thomas, III, and J. T. Kung. 1991. Induction of high level IL-2 production in CD4$^-$8$^-$ helper lymphocytes requires post-thymic development. *J. Immunol.* 147: 851–859.
18. Lodolce, J. P., D. L. Boone, S. Chai, R. E. Swain, T. Dassopoulos, S. Trettin, and A. Ma. 1998. IL-15 receptor maintains lymphoid homeostasis by supporting lymphocyte homing and proliferation. *Immunity* 9: 669–676.
19. Fichtner, A. T., S. Anderson, M. G. Mage, S. O. Sharrow, C. A. Thomas, III, and J. T. Kung. 1987. Subpopulations of mouse Lyt-2$^+$ T cells defined by the expression of an Ly-6-linked antigen, B4B2. *J. Immunol.* 138: 2024–2033.
20. Chen, Y. T., and J. T. Kung. 2005. CD1d-independent developmental acquisition of prompt IL-4 gene inducibility in thymus CD161(NK1)$^-$CD44^{low}CD4$^+$CD8$^-$ T cells is associated with complementarity determining region 3-diverse and biased Vbeta2/Vbeta7/Vbeta8/Valpha3.2 T cell receptor usage. *J. Immunol.* 175: 6537–6550.
21. Mehal, W. Z., F. Azzaroli, and I. N. Crispe. 2001. Immunology of the healthy liver: old questions and new insights. *Gastroenterology* 120: 250–260.
22. Kranz, D. M., D. H. Sherman, M. V. Sitkovsky, M. S. Pasternack, and H. N. Eisen. 1984. Immunoprecipitation of cell surface structures of cloned cytotoxic T lymphocytes by clone-specific antisera. *Proc. Natl. Acad. Sci. USA* 81: 573–577.
23. Ledbetter, J. A., and L. A. Herzenberg. 1979. Xenogeneic monoclonal antibodies to mouse lymphoid differentiation antigens. *Immunol. Rev.* 47: 63–90.
24. Bill, J., O. Kanagawa, D. Linten, Y. Utsunomiya, and E. Palmer. 1990. Class I and class II MHC gene products differentially affect the fate of V beta 5 bearing thymocytes. *J. Mol. Cell. Immunol.* 4: 269–279, discussion 279–280.
25. Staerz, U. D., H. G. Rammensee, J. D. Benedetto, and M. J. Bevan. 1985. Characterization of a murine monoclonal antibody specific for an allotypic determinant on T cell antigen receptor. *J. Immunol.* 134: 3994–4000.

26. Matzinger, P. 1991. The JAM test. A simple assay for DNA fragmentation and cell death. *J. Immunol. Methods* 145: 185–192.

27. Huleatt, J. W., I. Pilip, K. Kerksiek, and E. G. Pamer. 2001. Intestinal and splenic T cell responses to enteric *Listeria monocytogenes* infection: distinct repertoires of responding CD8 T lymphocytes. *J. Immunol.* 166: 4065–4073.

28. Heintzelman, D. L., R. Lotan, and R. R. Richards-Kortum. 2000. Characterization of the autofluorescence of polymorphonuclear leukocytes, mononuclear leukocytes and cervical epithelial cancer cells for improved spectroscopic discrimination of inflammation from dysplasia. *Photochem. Photobiol.* 71: 327–332.

29. Sandau, M. M., K. S. Schluns, L. Lefrancois, and S. C. Jameson. 2004. Cutting edge: transpresentation of IL-15 by bone marrow-derived cells necessitates expression of IL-15 and IL-15R alpha by the same cells. *J. Immunol.* 173: 6537–6541.

30. Sprenger, H., A. Kaufmann, H. Garn, B. Lahme, D. Gemsa, and A. M. Gressner. 1997. Induction of neutrophil-attracting chemokines in transforming rat hepatic stellate cells. *Gastroenterology* 113: 277–285.

31. Casini, A., E. Ceni, R. Salzano, P. Biondi, M. Parola, A. Galli, M. Foschi, A. Caligiuri, M. Pinzani, and C. Surrenti. 1997. Neutrophil-derived superoxide anion induces lipid peroxidation and stimulates collagen synthesis in human hepatic stellate cells: role of nitric oxide. *Hepatology* 25: 361–367.

32. Tough, D. F., S. Sun, X. Zhang, and J. Sprent. 2000. Stimulation of memory T cells by cytokines. *Vaccine* 18: 1642–1648.

33. Jung, T. M., W. M. Gallatin, I. L. Weissman, and M. O. Dailey. 1988. Down-regulation of homing receptors after T cell activation. *J. Immunol.* 141: 4110–4117.

34. Wherry, E. J., V. Teichgräber, T. C. Becker, D. Masopust, S. M. Kaech, R. Antia, U. H. von Andrian, and R. Ahmed. 2003. Lineage relationship and protective immunity of memory CD8 T cell subsets. *Nat. Immunol.* 4: 225–234.

35. Bannard, O., M. Kraman, and D. T. Fearon. 2009. Secondary replicative function of CD8^{+} T cells that had developed an effector phenotype. *Science* 323: 505–509.

36. Marzo, A. L., H. Yagita, and L. Lefrançois. 2007. Cutting edge: migration to nonlymphoid tissues results in functional conversion of central to effector memory CD8 T cells. *J. Immunol.* 179: 36–40.

37. Crispe, I. N., T. Dao, K. Klugewitz, W. Z. Mehal, and D. P. Metz. 2000. The liver as a site of T-cell apoptosis: graveyard, or killing field? *Immunol. Rev.* 174: 47–62.

38. Dikopoulos, N., I. Jomantaite, R. Schirmbeck, and J. Reimann. 2003. Specific, functional effector/memory CD8+ T cells are found in the liver post-vaccination. *J. Hepatol.* 39: 910–917.

39. Keating, R., W. Yue, J. A. Rutigliano, J. So, E. Olivas, P. G. Thomas, and P. C. Doherty. 2007. Virus-specific CD8^{+} T cells in the liver: armed and ready to kill. *J. Immunol.* 178: 2737–2745.